

**DESIGN AND SIMULATION OF CAPACITIVE MEMS  
MICROPHONE FOR FULLY IMPLANTABLE COCHLEAR  
IMPLANTS**

**SOMANAATHAN MUTHUSAMY**

**FACULTY OF ENGINEERING  
UNIVERSITY OF MALAYA  
KUALA LUMPUR**

**2018**

**DESIGN AND SIMULATION OF CAPACITIVE MEMS  
MICROPHONE FOR FULLY IMPLANTABLE COCHLEAR  
IMPLANTS**

**SOMANAATHAN MUTHUSAMY**

**THESIS SUBMITTED IN FULFILMENT OF THE  
REQUIRMENTS FOR THE DEGREE OF MASTER OF  
MECHATRONIC ENGINEERING**

**FACULTY OF ENGINEERING  
UNIVERSITY OF MALAYA  
KUALA LUMPUR**

**2018**

## ORIGINAL LITERACY WORK DECLARATION

Name of Candidate: Somanaathan Muthusamy

(I.C/Passport No: Matric No: KGF160010

Name of Degree: Master of Mechatronic Engineering

Title of Thesis: Design and simulation of capacitive mems microphone for fully implantable cochlear implants

Field of Study: BIOMEMS

**I do solemnly and sincerely declare that:**

- 1) I am the sole author/writer of this Work;
- 2) This Work is original;
- 3) Any use of any work in which copyright exists was done by way of fair dealing and for permitted purposes and any excerpt or extract from, or reference to or reproduction of any copyright work has been disclosed expressly and sufficiently and the title of the Work and its authorship have been acknowledged in this Work;
- 4) I do not have any actual knowledge nor do I ought reasonably to know that the making of this work constitutes an infringement of any copyright work;
- 5) I hereby assign all and every right in the copyright to this Work to the University of Malaya ("UM"), who henceforth shall be owner of the copyright in this Work and that any reproduction or use in any form or by any means whatsoever is prohibited without the written consent of UM having been first had and obtained;
- 6) I am fully aware that if in the course of making this Work I have infringed any copyright whether intentionally or otherwise, I may be subject to legal action or any other action as may be determined by UM.

Candidate's Signature

Date:

Subscribed and solemnly declared before,

Witness's Signature

Date:

Name:

Designation

## ABSTRACT

In this work we present the design, Taguchi optimization and simulation of an acoustic sensors array for detecting specific frequencies in a range and allowing their identification from a complex audio signal to develop an application for cochlear implants. The technological development of cochlear implants has enabled patients affected by severe to intense hearing loss to hear sounds and recognize speech in various degree. The sensitivity is obtained when a membrane resonates when stimulated by acoustic wave. In this research sensitivity and linearity of membrane has been improved to overcome the disability of hearing soft and loud sound. The different gap size between the membrane and backplates generates a capacitance change that can pass to an electronic circuit for output signal. The frequency of membrane increases when the spring constant of each membrane increase.

In this study, several structures have been studied to optimize the sensitivity and linearity. Based on the results, shortlisted the best performance structures for the Taguchi optimization and Eigen frequency analysis for designated number of arrays. Each array again simulated for identify the sensitivity, linearity and dimension. The best design is being verified from this methodology. This design produces high sensitivity  $0.18\text{pF/Pa}$ , linearity  $0.0011\text{pF}/\mu\text{m}$  and mechanical sensitivity  $35.6\mu\text{m/Pa}$  compares to existing design. This innovative design can improve current commercial cochlear implant by hearing soft and loud sound without adjusting manually. The life quality of cochlear implant patient is improved by new high sensitive capacitive microphone.



## ABSTRAK

Dalam karya ini, kami membentangkan reka bentuk, pengoptimuman dan simulasi Taguchi dan simulasi pelbagai sensor akustik untuk mengesan frekuensi tertentu dalam pelbagai dan membolehkan pengenalan mereka dari isyarat audio kompleks untuk membangunkan aplikasi untuk implan koklea. Perkembangan teknologi implan koklea telah membolehkan pesakit terjejas oleh pendengaran yang teruk dan kuat untuk mendengar suara dan mengiktiraf ucapan dalam pelbagai peringkat. Kepekaan diperoleh apabila membran bergema ketika dirangsang oleh gelombang akustik. Dalam kepekaan kajian dan linieriti membran telah diperbaiki untuk mengatasi kecacatan mendengar bunyi lembut dan kuat. Saiz jurang yang berlainan di antara membran dan backplate menghasilkan perubahan kapasitif yang boleh lulus ke litar elektronik untuk isyarat keluaran.

Dalam kajian ini, beberapa struktur telah dikaji untuk mengoptimumkan kepekaan dan linier. Berdasarkan hasilnya, disenarai pendek struktur kinerja terbaik untuk pengoptimalan Taguchi dan analisis kekerapan Eigen untuk bilangan baris yang ditetapkan. Setiap array sekali lagi disimulasikan untuk mengenal pasti kepekaan, linearity dan dimensi. Reka bentuk terbaik sedang disahkan dari metodologi ini. Reka bentuk ini menghasilkan kepekaan tinggi  $0.18\text{pF} / \text{Pa}$ , linearity  $0.0011\text{pF} / \mu\text{m}$  dan kepekaan mekanik  $35.6\mu\text{m} / \text{Pa}$  berbanding dengan reka bentuk yang sedia ada. Reka bentuk yang inovatif ini dapat meningkatkan implan koklea komersial semasa dengan mendengar bunyi lembut dan kuat tanpa menyesuaikan secara manual. Kualiti hidup pesakit implan koklea diperbaiki oleh mikrofon kapasitif tinggi yang baru.

## ACKNOWLEDGEMENT

First, I would like to express gratitude to my advisor, Prof Norhayati Soin. I have been amazingly fortunate to have a supervisor who has given me the freedom to explore things on my own, and with her patient guidance whenever my steps are faltering.

Throughout this journey of research, she has shared tremendous knowledge in the area Mems application. Her kindness and support have helped me a lot to overcome many critical situations throughout my project. It has been a magnificent pleasure to work under her as one of his research project students.

A special thanks to my family members for sharing their understandings and helping me in terms of my finance in my study. Their passionate belief in the education has encourage me to excel academically. Their strong values have formed who I am today and will continue to do so. I'm dedicating this success to my lovely Father and Mother Mr & Mrs Muthusamy Sarasuwathy for their continuous encouragements and motivation. I'm taking this opportunity to thank all my family members for their effort to make my dream comes true.

Lastly, I would like to thank to those who has helped me in research project directly or indirectly.

## TABLE OF CONTENT

Abstract .....	III
Abstrak .....	IV
Acknowledgement .....	V
Table of content .....	VI
List of Figures .....	IX
List of Tables .....	XIII
List of Symbols And Abbreviation .....	XIV
List of Appendices .....	XV
<b>CHAPTER 1 INTRODUCTION .....</b>	<b>1</b>
1.1 Overview .....	1
1.2 Objective of thesis .....	2
1.3 Scope of work .....	3
1.4 Organization of thesis .....	3
<b>CHAPTER 2 LITERATURE REVIEW .....</b>	<b>4</b>
2.1 Introduction to mems microphones. ....	4
2.2 Previous study of cochlear implanted mems microphone .....	6
2.3 Study of capacitive mems microphone .....	9
2.3.1 Overview of mems capacitive microphone .....	9
2.3.2 Previous study of capacitive mems microphone for hearing aid .....	10

2.4 Summary .....	16
<b>CHAPTER 3 RESEARCH METHODOLOGY .....</b>	<b>18</b>
3.1 Introduction .....	18
3.2 Project methodology .....	18
3.3 Overall project flow chart .....	19
3.3.1 Identify the design specification .....	20
3.3.2 Structure selection and basic dimension of structure .....	21
3.3.3 Comsol multiphysics 4.3a.....	22
3.3.4 Taguchi optimization method using minitab .....	28
3.3.5 Determination of suitable structure .....	32
3.3.6 Analysis of sensitivity and linearity .....	32
3.3.7 Analysis of eigenfrequency of each array.....	35
3.3.8 Determination of suitable dimension of arrays .....	38
<b>CHAPTER 4 RESULTS AND DISCUSSION .....</b>	<b>39</b>
4.1 Analysis of sensitivity and linearity of structures.....	39
4.1.1 Mems microphone structure 1.....	39
4.1.2 Mems microphone structure 2.....	44
4.1.3 Mems microphone structure 3.....	49
4.1.4 Mems microphone structure 4.....	54
4.1.5 Mems microphone proposed structure .....	59
4.2 Determination of suitable structure ci.....	63
4.3 Analysis eigenfrequency of each array .....	65
4.3.1 Introduction.....	65
4.3.2 Taguchi method of array for geometric analysis.....	65
4.3.3 Eigen frequency analysis of each arrays.....	67
4.4 Analysis of sensitivity and linearity of each array.....	75

4.5 Determination of suitable dimension of arrays.....	88
4.6 Summary capacitive microphone final design .....	89
<b>CHAPTER 5 CONCLUSION AND FUTURE WORKS.....</b>	<b>91</b>
5.1 Conclusion.....	91
5.2 Future works.....	92
<b>REFERENCES .....</b>	<b>93</b>
<b>APPENDIXES.....</b>	<b>95</b>
Appendix A: Table of calculation .....	95
Appendix B: Overall dimension of array.....	97
Appendix C: Reference journals .....	98

## LIST OF FIGURES

Figure 2. 1 Classification of implantable sensor .....	5
Figure 2. 2 Proposed system for the sensing sound (Koyuncuoğlu et al., 2017) .....	6
Figure 2. 3 Diagram show the Top View arrangement of Microphone array. ....	7
Figure 2. 4 Cross sectional view of microphone .....	7
Figure 2. 5 Different behaviors on membranes when stimulated by a mechanical force, (a) 8	
First oscillating mode, (b) third oscillating mode and (c) sixth oscillating mode. ....	8
Figure 2. 6 Cross section view of corrugated membranes .....	10
Figure 2. 7 3D Detail view of corrugated microphone design .....	11
Figure 2. 8 Central deflection of corrugated and flat diaphragm with $N=2, 5, 8$ .....	11
Figure 2. 9 Top and front view of the structure.....	12
Figure 2. 10 Maximum displacement curves with variable diameter.....	13
Figure 2. 11 Top view diaphragm layout mask (b) cross section view of the microphone .	15
Figure 2. 12 Center deflection versus sound pressure of a flat and spring supported	
diaphragm.....	15
Figure 3. 1 Overall project flow chart.....	19
Figure 3. 2 Show basic dimension of structures.....	21
Figure 3. 3 2D sketches from the Autodesk inventor 2017 .....	22
Figure 3. 4 Selection of geometric parameter to the COMSOL model .....	23
Figure 3. 5 COMSOL live link interfaces.....	23
Figure 3. 6 Selection of material .....	24
Figure 3. 7 Boundary load condition .....	25
Figure 3. 8 Generating meshing .....	25
Figure 3. 9 Generating or computing the simulation.....	26

Figure 3. 10 Von Mises stress diagram.....	26
Figure 3. 11 Surface displacement y component field .....	27
Figure 3. 12 Generating new file .....	28
Figure 3. 13 Selection of level of design and the number of factors.....	28
Figure 3. 14 Select number of factors in available design tab .....	29
Figure 3. 15 Selecting the available design.....	29
Figure 3. 16 Modify the parameter and name accordingly .....	30
Figure 3. 17 Graph of Main effects Plots for means .....	31
Figure 4. 1 Structure of a central-post MEMS microphone.(Yang, 2010) .....	39
Figure 4. 2 Main effects plot for diameter and thickness .....	40
Figure 4. 3 Show the y displacement component of the structure.....	41
Figure 4. 4 Graph of Mechanical sensitivity vs Pressure.....	42
Figure 4. 5 Graph of capacitance vs pressure of optimized and non-optimized parameter. 42	
Figure 4. 6 Graph of Capacitance Vs Displacement for Non-Optimized membrane.....	43
Figure 4. 7 Graph of Capacitance Vs Displacement for Optimized membrane.....	43
Figure 4. 8 Main effect plot for means of significant parameter of corrugated diaphragm. 44	
Figure 4. 9 Show the y displacement corrugated membrane .....	45
Figure 4. 10 Graph of Mechanical sensitivity vs Pressure.....	46
Figure 4. 11 Graph of Capacitance Vs Displacement for Non-Optimized membrane.....	47
Figure 4. 12 Graph of Capacitance Vs Displacement for Optimized membrane.....	47
Figure 4. 13 Graph of Capacitance Vs Pressure of Optimized and Non Optimized membrane.....	48
Figure 4. 14 Main effects plot for means for spring supported microphone .....	49
Figure 4. 15 Show the z displacement spring supported membrane .....	50
Figure 4. 16 Graph of Mechanical sensitivity vs Pressure.....	51

Figure 4. 17 Graph of capacitance vs displacement for non-optimized parameter .....	52
Figure 4. 18 Graph of capacitance vs displacement for optimized parameter .....	52
Figure 4. 19 Graph of Capacitance vs Pressure of Non-optimized structure.....	53
Figure 4. 20 Graph of Capacitance vs Pressure of Non-Optimized structure.....	53
Figure 4. 21 Main effects plot for means for spring condenser microphone .....	55
Figure 4. 22 shows y displacement of spring supported membranes .....	56
Figure 4. 23 show Graph of Mechanical sensitivity vs Pressure.....	57
Figure 4. 24 Graph of capacitance vs displacement for non-optimized and optimized structure.....	57
Figure 4. 25 Graph of capacitance vs pressure of non-optimized and optimized structure.	58
Figure 4. 26 Proposed structure design dimension.....	59
Figure 4. 27 Main effects plot for means for proposed design .....	59
Figure 4. 28 shows y displacement of proposed design .....	60
Figure 4. 29 show the graph of mechanical sensitivity vs pressure .....	61
Figure 4. 30 Shows the graph of capacitance vs displacement .....	62
Figure 4. 31 Main effects plot for means of proposed design Eigen frequency .....	66
Figure 4. 32 Microphone array 1 Eigenfrequency @635Hz.....	68
Figure 4. 33 Microphone array 2 eigenfrequency @1000Hz.....	68
Figure 4. 34 Microphone array 3 eigenfrequency @1500Hz.....	69
Figure 4. 35 Microphone array 4 eigenfrequency @2000Hz.....	69
Figure 4. 36 Microphone array 5 eigenfrequency @2500Hz.....	70
Figure 4. 37 Microphone array 6 eigenfrequency @3000Hz.....	70
Figure 4. 38 Microphone array 7 eigenfrequency @3500Hz.....	71
Figure 4. 39 Microphone array 8 eigenfrequency @4000Hz.....	71
Figure 4. 40 Microphone array 9 eigenfrequency @4500Hz.....	72



Figure 4. 41 Microphone array 10 eigenfrequency @5030Hz.....	72
Figure 4. 42 Histogram of internal stress vs frequency .....	73
Figure 4. 43 The graph of spring constant vs frequency.....	74
Figure 4. 44 Shows y displacement of Array 1 .....	76
Figure 4. 45 Shows y displacement of Array 2 .....	76
Figure 4. 46 Shows y displacement of Array 3 .....	77
Figure 4. 47 Shows y displacement of Array 4 .....	77
Figure 4. 48 Shows y displacement of Array 5 .....	78
Figure 4. 49 Shows y displacement of Array 6 .....	78
Figure 4. 50 Shows y displacement of Array 7 .....	79
Figure 4. 51 Shows y displacement of Array 8 .....	79
Figure 4. 52 Shows y displacement of Array 9 .....	80
Figure 4. 53 Shows y displacement of Array 10 .....	80
Figure 4. 54 Graph of Capacitance Vs Displacement of Array 1.....	81
Figure 4. 55 Graph of Capacitance Vs Displacement of Array 2.....	81
Figure 4. 56 Graph of Capacitance Vs Displacement of Array 3.....	82
Figure 4. 57 Graph of Capacitance Vs Displacement of Array 4.....	82
Figure 4. 58 Graph of Capacitance Vs Displacement of Array 5.....	83
Figure 4. 59 Graph of Capacitance Vs Displacement of Array 6.....	83
Figure 4. 60 Graph of Capacitance Vs Displacement of Array 7.....	84
Figure 4. 61 Graph of Capacitance Vs Displacement of Array 8.....	84
Figure 4. 62 Graph of Capacitance Vs Displacement of Array 9.....	85
Figure 4. 63 Graph of Capacitance Vs Displacement of Array 10.....	85
Figure 4. 64 Graph of Mechanical Sensitivity Vs Pressure of all arrays.....	86
Figure 4. 65 Graph of Capacitance Vs Pressure of all Arrays .....	86

## LIST OF TABLES

Table 3. 1 Design specification .....	20
Table 4. 1 Numerical value of Optimized Parameter .....	41
Table 4. 2 Show results of sensitivity of optimized and non-optimized parameter .....	41
Table 4. 3 Numerical value of Optimized Parameter .....	45
Table 4. 4 Show results of sensitivity of optimized and non-optimized parameter .....	46
Table 4. 5 Numerical value of optimized parameter .....	50
Table 4. 6 Show results of sensitivity of optimized and non-optimized parameter .....	51
Table 4. 7 Numerical value of optimized parameter .....	56
Table 4. 8 Show results of sensitivity of optimized and non-optimized parameter .....	56
Table 4. 9 Optimized parameter of the proposed Design .....	60
Table 4. 10 shows the results of sensitivity, capacitance and linearity .....	61
Table 4. 11 Table of Comparison .....	63
Table 4. 12 Taguchi optimization array matrix for proposed design .....	66
Table 4. 13 Spring constant value and frequency obtained .....	74
Table 4. 14 Detail technical specification of proposed design cochlear implants .....	88
Table 4. 15 Summary of final design characteristics.....	89
Table 4. 16 characteristics of microphone final design and existing design.....	89

## LIST OF SYMBOLS AND ABBREVIATION

CI Cochlear Implant

HA Hearing Aids

MEI Middle Ear Implant

DOE Degree of Experiment

RF Radio Frequency

$\omega$  angular velocity (rad/s)

m mass of membranes (kg)

f frequency of membrane (Hz)

K is spring constant (N/m)

$\Delta X$  is deflection of membrane (m)

## **LIST OF APPENDICES**

Appendix A: Table of Calculation

Appendix B: Overall dimension of Array

Appendix C: Reference Journals

University of Malaya

## CHAPTER 1 INTRODUCTION

### 1.1 OVERVIEW

The cochlea is a key organ in the inner ear, which converts the mechanical waves of the incoming sound into electrical signals to the auditory nerves. Any damage in cochlea would result problems with the sensorineural connections in the inner ear and cause severe hearing loss. There are nearly 360 million people living with disabling hearing loss greater than 40 dB SPL (sound pressure level) as of 2015 (Koyuncuoğlu et al., 2017).

The technological development of cochlear implants has enabled patients affected by severe to intense hearing loss to hear sounds and recognize speech in various degrees. The inconsistency of hearing results in subjects with post-lingual deafness has been significant, and the most crucial causes predict a good outcome are a fleeting period of pre-implant hearing deprivation and some residual hearing.

This is the reason for cochlear implants prolonged to contribute to a larger population (Bittencourt et al., 2012). It has been concluded that cochlear implants give an improved performance in post-lingual deaf patients when compared to conventional hearing aids as verified by audiological tests. The silicon microphones were designed based on the principles of the piezoelectric, piezoresistive, and capacitive. These types of microphones had been successfully fabricated using silicon micromachining techniques. However, the capacitive microphones have been studied by many researchers due to its superior performances such as high sensitivity, low power consumption, low noise level, and high stability.

The frequency response of the microphone elaborates how the sensitivity varies with frequency, similarly, the linearity of the microphone describes how the magnitude of the microphone output varies with the amplitude of the incident pressure.

The dual back plate microphone has several advantages over the single-back plate structure. It has the potential for up to twice the sensitivity, a higher bias voltage further increasing the sensitivity, and increased linearity assuming comparable materials and geometry to a corresponding single-back plate microphone. In capacitive microphones, the vent resistance has the potential to dominate the low frequency noise, especially in high-sensitivity devices (Glucomentor, 2012). Noise contributions from the interface circuit also depend on the type of interface circuit chosen.

According to United States FDA (Food and Drug Administration) Medical devices reported disadvantage of hearing less soft and loud sound without changing sensitivity of cochlear implant. U.S. Department of Health and Human Services. U.S Food and Drug administration.[<https://www.fda.gov/MedicalDevices/ProductsandMedicalProcedures/ImplantsandProsthetics/CochlearImplants/ucm062843.htm>]. Accessed 15 March 2018.

## **1.2 OBJECTIVE OF THESIS**

The objective of this thesis is to improve sensitivity and linearity Capacitive MEMS microphone for fully implantable Cochlear Implants. The objective of this thesis in details is below.

- I. Improve the mechanical sensitivity of the capacitive mems microphone of each microphone by higher than  $0.007\mu\text{m}/\text{Pa}$
- II. Improve capacitive sensitivity of mems microphone of each structure of arrays by higher than  $0.17\text{ pF}/\text{Pa}$
- III. improve linearity of the capacitive mems microphone of each structure of arrays by higher than  $0.003\text{ pF}/\mu\text{m}$

### **1.3 SCOPE OF WORK**

The scope of this thesis to improve sensitivity and linearity Capacitive MEMS microphone for fully implantable Cochlear Implants is outlined as follows;

- I. Design and develop capacitive MEMS microphone to for fully implantable cochlear implants
- II. Conduct Taguchi optimization on existing hearing aids microphone without changing the diaphragm membrane features.
- III. Conduct structural simulation studies through COMSOL Simulation software on existing hearing aid's microphone without changing the diaphragm membrane features.
- IV. Perform the Eigen frequency analysis to structure for each arrays

### **1.4 ORGANIZATION OF THESIS**

This thesis is organized in five chapters. In Chapter 1, the explanation for the project, which will be given in a general term, problem statements and objective of this project will be elaborated followed by the scopes of the project will be covered in this project.

Chapter 2 describes the fundamental of the cochlear implants and various capacitive microphones for hearing aids that can be used for cochlear implants

In Chapter 3, it describes the methodology for development of capacitive mems microphone of fully implanted cochlear implants

As for Chapter 4, the results that are obtained are discussed as well as both discussions and analysis for this project. The strength and weakness of this project are also discussed in this chapter. Finally, in Chapter 5, a conclusion is made for this project and recommendations for future works for this project will be the ending for this thesis.

## CHAPTER 2 LITERATURE REVIEW

The purpose of this chapter is to review literature related to the capacitive mems microphone and shows some of the fundamental aspects of the fully implanted cochlear mems microphone. Further, in this chapter will have the recent development of mems microphones and it's contributing to comparison of structure. This will help to draw design specification of this proposed mems microphone structure.

### 2.1 INTRODUCTION TO MEMS MICROPHONES.

Hearing loss is among the most common disabling conditions in decades and affects about 5.3% of the world population(Lima, Moret, & Tabanez, 2015). Of this quota, 8.9% are children under 10 years of age, with an incidence of congenital hearing loss from 1.5 to 5.95 every 1000 births.

There are few forms of hearing loss can be treated using hearing devices, such as hearing aids (HAs), middle ear implants (MEIs) or cochlear implants (CIs). With few exemptions, these devices use one or more microphones, located in a behind-the-ear device or in the outer ear canal, to capture the sound field, which can be in turn processed and transmitted forward(Calero, Paul, Gesing, Alves, & Cordioli, 2018). In HAs, the sound is processed, amplified and sent into the ear canal using vibration-acoustic systems.

Cochlear implants CI are used by such patients to bypass the damaged hair cells or other components of cochlea and directly stimulate the nerve cells. The current state CI systems has several drawbacks such as frequent battery replacement requirement or risk of external components damage under water(Koyuncuoğlu et al., 2017). Fully implantable CI systems have the potential to eliminate many of the problems, but a reliable internal power source and an implantable acoustic sensor are the main bottlenecks. In these cases, the CI



which uses an electrode array inserted into the cochlea to stimulate the auditory nerve fibers appears as an alternative. In currently available CIs, the sound signal is also picked up by microphones located (Calero et al., 2018). In a behind-the-ear unit and it is then processed and transmitted via radio frequency (RF) to a subcutaneous element surgically implanted on the temporal bone.

The table below shows the implantable sensor. This classification is based, primarily on the sensor positioning and considers the transduction mechanism such as capacitive, electromagnetic, optical, piezo resistive and piezoelectric (Calero et al., 2018). Finally, the classification accounts for the sensor type: microphone, accelerometer, and displacement sensor and force transducer.

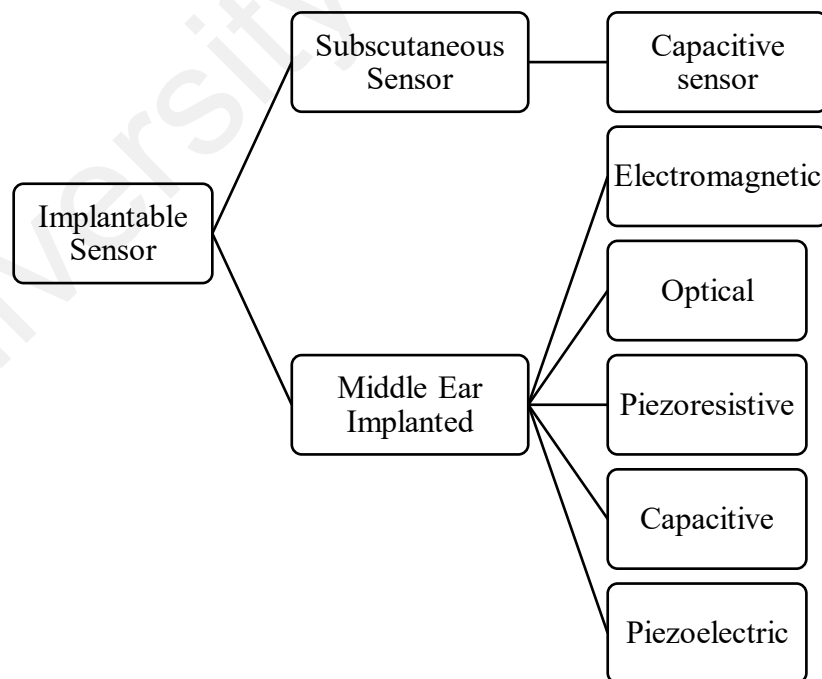


Figure 2. 1 Classification of implantable sensor

## 2.2 PREVIOUS STUDY OF COCHELAR IMPLANTED MEMS MICROPHONE

In the cochlear implant the entire natural hearing mechanism is bypassed, although most parts of the hearing system are operational such as the eardrum and ossicles. An array of piezoelectric cantilever transducers is placed in the eardrum to provide the necessary signal for neural stimulation (Koyuncuoğlu et al., 2017). The author research is based on the Thin Film PZT Acoustic Sensor for Fully Implantable Cochlear Implants. The following Figure 2.2 shows the proposed system from the author.

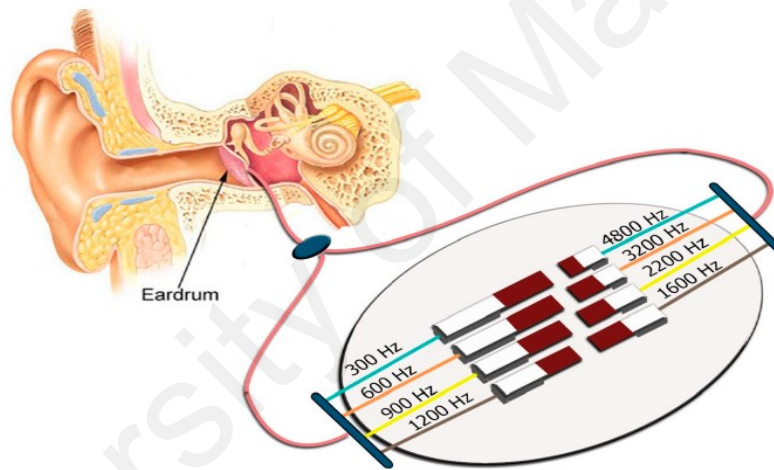


Figure 2. 2 Proposed system for the sensing sound (Koyuncuoğlu et al., 2017)

The system designed in a way when an acoustic sound pressure impinges on the eardrum, the cantilever beam matched with exciting frequency starts to vibrate along with it. It's consist of 8-channel or array of multi-frequency structure, where each cantilever resonates to a selected frequency band in the cochlea. The results show the microphone arrays resonating at a specific frequency within the hearing band from 300Hz to 1600Hz, the transducer senses eardrum vibration and generates the required voltage output for the

stimulating circuitry. The high sensitivity of the microphone sensor, 391.9 mV/Pa @900 Hz. Furthermore, the cantilever beam length varies accordingly to the frequency of resonating. Similarly, according to (Quiroz, Báez H., Mendoza, Alemán M., , & Villa, 2014). Developed acoustic sensors array of specific frequencies in a range and of complex audio signal. Designed an array of 14 microphones, its responding to a specific frequency from a defined range. The analyzed frequency range was selected from 512 Hz to 4.2 kHz where the intelligence information has in it. Figure 2.4 shows the arrangement of microphone arrays according to resonate frequency.

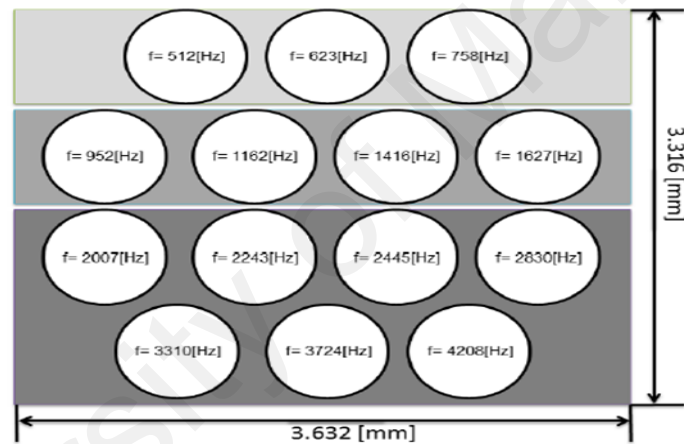


Figure 2. 3 Diagram show the Top View arrangement of Microphone array.

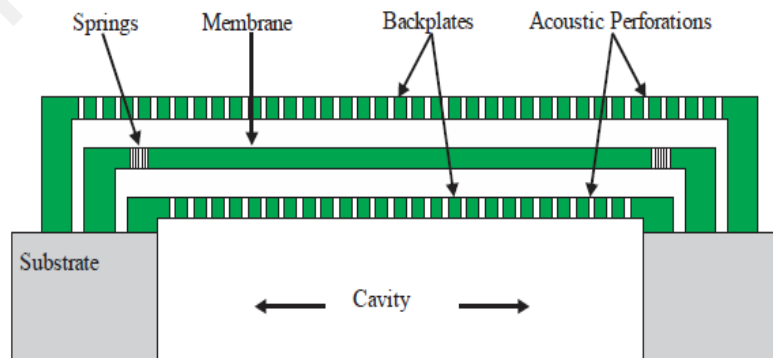


Figure 2. 4 Cross sectional view of microphone

It consists of 14 membranes of the array which having the same diameter, referring to the Figure 2.4, number of springs and its geometrical characteristics are depending on the specific frequency at which each microphone responds when stimulated by a complex audio signal. Figure 2.5 clearly shows the performance of microphone membrane at a different resonating frequency at specified number of spring.

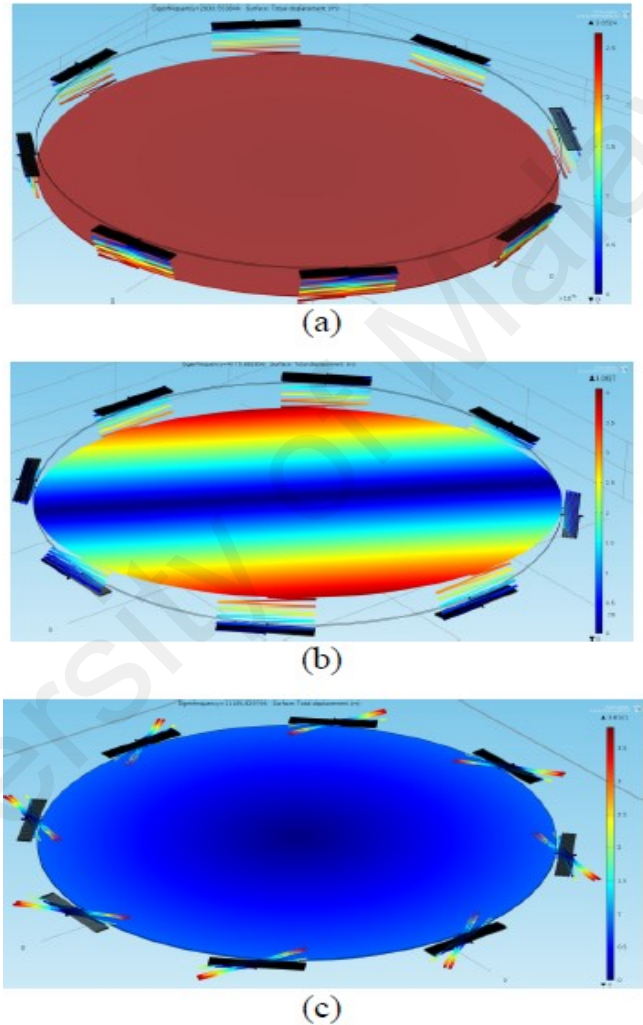


Figure 2. 5 Different behaviors on membranes when stimulated by a mechanical force,  
(a)First oscillating mode, (b) third oscillating mode and (c) sixth oscillating mode.

## **2.3 STUDY OF CAPACITIVE MEMS MICROPHONE**

The literature review in this section is more focusing on the capacitive mems microphone. Further, in this section several previous studies on the mems capacitive microphone will be reviewed and it's included the comparison structure that's selected for the optimization process in the chapter 4 results and discussion.

### **2.3.1 OVERVIEW OF MEMS CAPACITIVE MICROPHONE**

Historically the first capacitive microphone was introduced in 1983 by Royer et al (Krishnapriya & Baiju, 2014). The MEMS microphone offers low power consumption, good sensitivity and are available in very small. The MEMS capacitive microphones are used in mobile phone applications, laptops and other consumer applications, medical application such as hearing aids, automotive and military applications.

Capacitive mems microphones diaphragm comes with several shapes mostly are in circular, square, rectangle and some other shapes with perforated holes(Chaithra, Nithya, & Nagaraja, 2017). Most of Its come back plates. The capacitive mems microphones diaphragm is generally flat in shape. The most crucial factor of capacitive mems microphone displacement of diaphragm and sensitivity. The sensitivity decreased if the air damping is not reduced. Therefore, the perforation in diaphragm controls the air damping in gap and increases the sensitivity of the microphone

### 2.3.2 PREVIOUS STUDY OF CAPACITIVE MEMS MICROPHONE FOR HEARING AID

There are several microphone structures developed for a capacitive mems microphone for hearing aids. In this section 2.3.1 will elaborate the general finding of each structure and the sensitivity and linearity. The primary important given to these parameters due to achieve objective of the project.

#### i. TYPE OF DIAPHRAGM IN CAPACITIVE

According to analytical study shows that the mechanical sensitivity of diaphragm can be increased using corrugations this is because of reducing the effect of residual stress in corrugated diaphragm (Taybi & Ganji, 2013). Based on the understanding from the paper the mechanical sensitivity means ratio of deflection over pressure  $\mu\text{m}/\text{Pa}$ . As the deflection of the microphone increases the sensitivity of microphone increases.

The following Figure 2.6 below shows the cross section of the corrugated diaphragm proposed by the author. The number of corrugation also plays a key role in the deflection of the microphone membrane.

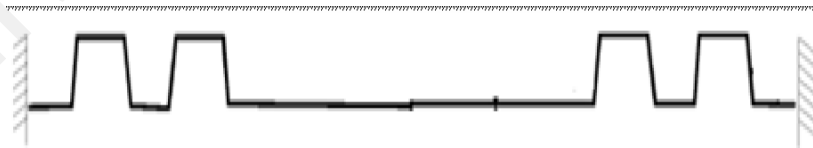


Figure 2. 6 Cross section view of corrugated membranes

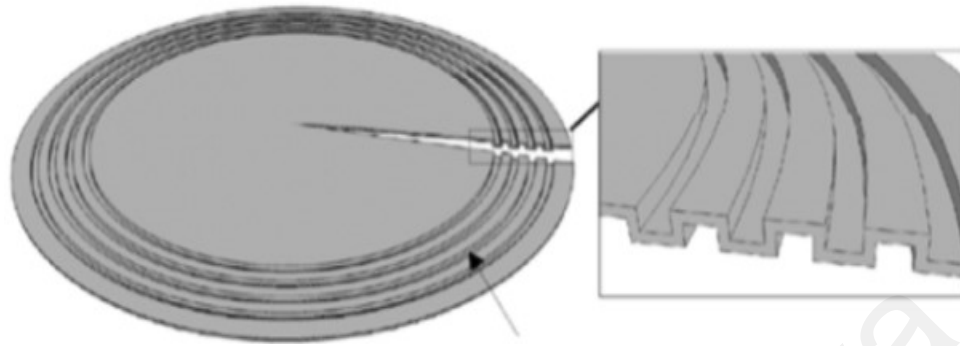


Figure 2. 7 3D Detail view of corrugated microphone design

The Behavior of a corrugated diaphragm is determined by the number of corrugations (N). The number corrugation gives significant effects on the sensitivity. As the number of corrugations increases, the central deflection also increases under the same load. The following Figure 2.8 shows the central deflection of circular corrugated diaphragms versus pressure for different number of corrugations.

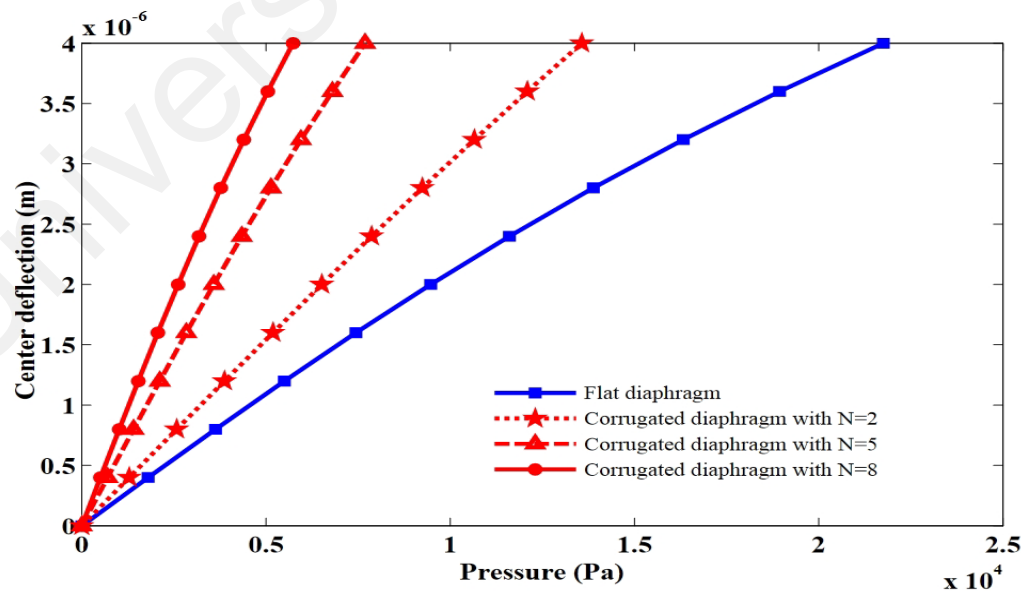


Figure 2. 8 Central deflection of corrugated and flat diaphragm with N=2, 5, 8

Based on the Figure 2.8, comparison between the flat diagram and N=8 corrugated diaphragm the central deflection of the corrugated membrane shows high deflection to pressure under the same load.

Some structure analyses the sensitivity of structural based one thickness of microphone membranes (Yang, 2010). According to the finding the central post of the circular membranes is fixed. The deflection of the membranes is reacting at the circumference of the circle. The following Figure 2.9 shows the top view and front view of structure.

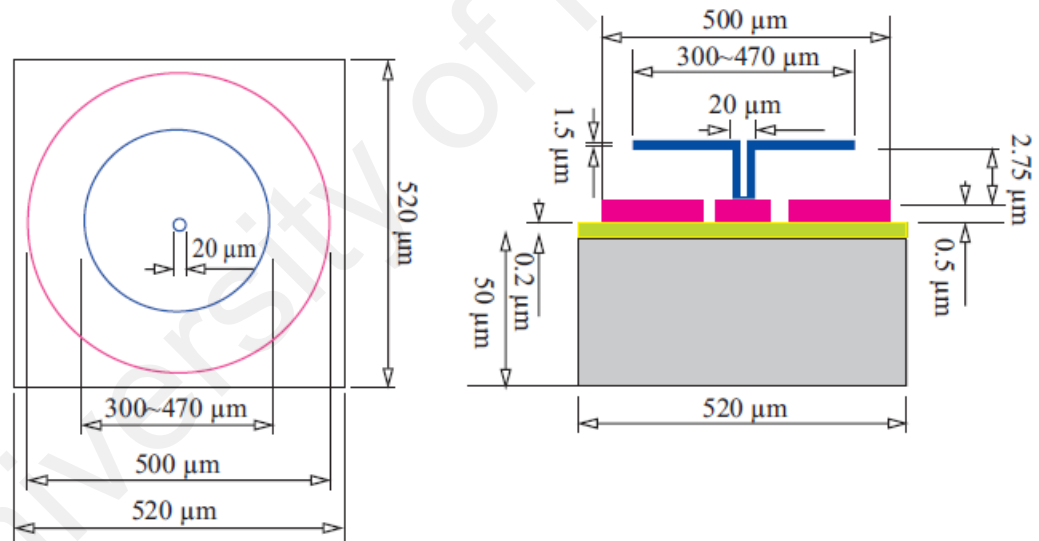


Figure 2. 9 Top and front view of the structure

The central-post novel MEMS microphone with free boundary condition have been designed to reduce the residual stress and improve the sensitivity of the membrane. The shorter release distance design is helpful to avoid the sticking between membrane and under-electrode to increase the process yield.



It has been reported by the author the displacement of the membrane increases with the increasing membrane diameter to enhance sensitivity of the microphone. The membrane cannot be increased without any restriction as it may cause breakdown due to instability when the membrane deflection is 1/3 of the distance between the two electrodes.

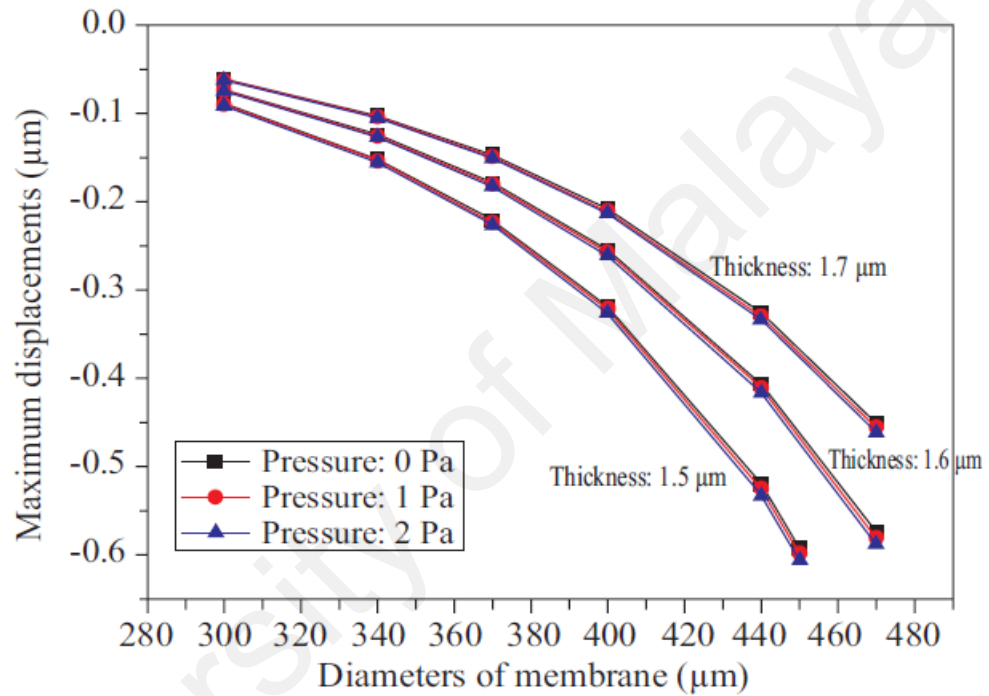


Figure 2. 10 Maximum displacement curves with variable diameter.

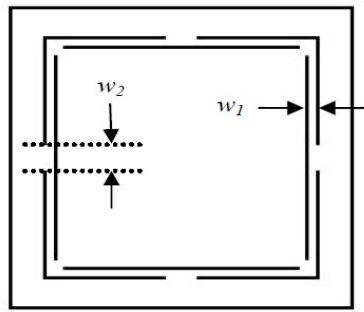
Based on the above graph shown in the Figure 2.10. Its show the maximum displacement is achieve at 1.5μm. This gives clear indication the thickness of microphone membranes plays significant role in achieving the maximum sensitivity. However, the minimum thickness of membranes determined by the yield strength of membranes under boundary condition.

The Early MEMS microphone design utilizes a silicon-type with fully clamped flat diaphragm, so its deflection to the sound pressure is very small (in the order of several nanometers). Since mechanical sensitivity is proportional to the deflection of the diaphragm, a larger diaphragm deflection is highly desirable for a high sensitivity microphone (Mohamad, 2010).

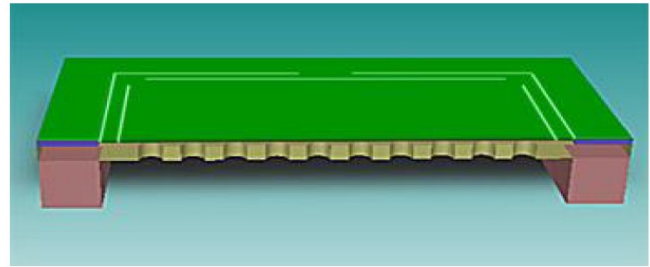
Spring type diaphragm generally are restricting the movement of the top and bottom plate (Chaithra et al., 2017). Mechanical energy is generally stored by the spring. When a spring is compressed or stretched from its resting position, it exerts an opposing force approximately proportional to its change in length.

Based on the proposed structure by (Mohamad, 2010). The structure demonstrated in free moving diaphragm which is supported by a spring mechanism around its corner. The material property is significant in deflection of the diaphragm membrane. Due to that Polysilicon material was proposed to be used as the diaphragm material due to its low stiffness property and to prevent the extra deposition of conductive material on the diaphragm.

The maximum center deflection of a flat and spring supported diaphragm for a sound pressure between 0 dB SPL and 140 dB SPL (dB SPL – decibel about the sound pressure level, 0 dB SPL =  $2 \times 10^{-5}$  Pa). It's reported the spring supported diaphragm deflection is linearly proportional to the sound pressure decibel and its parallel with the flat diaphragm response, the sensitivity has been increased about 100 times. This also indicates that the spring supported diaphragm can be a suitable candidate to replace or enhance the existing flat diaphragm condenser MEMS microphone.



(a) Mask layout showing thin slits



(b) Cross section of diaphragm and perforated back plate

Figure 2. 11 Top view diaphragm layout mask (b) cross section view of the microphone

The above Figure 2.11 it's a proposed design of the author. As a result, the spring supported design in the graph below in Figure 2.12 shows the central deflection of the spring supported diaphragm greater than the flat diaphragm. Further to that the flat diaphragm response has a higher resonance frequency (about 109 kHz) due to the greater diaphragm stiffness compared to about 9.75 kHz resonance frequency of a spring supported diaphragm.

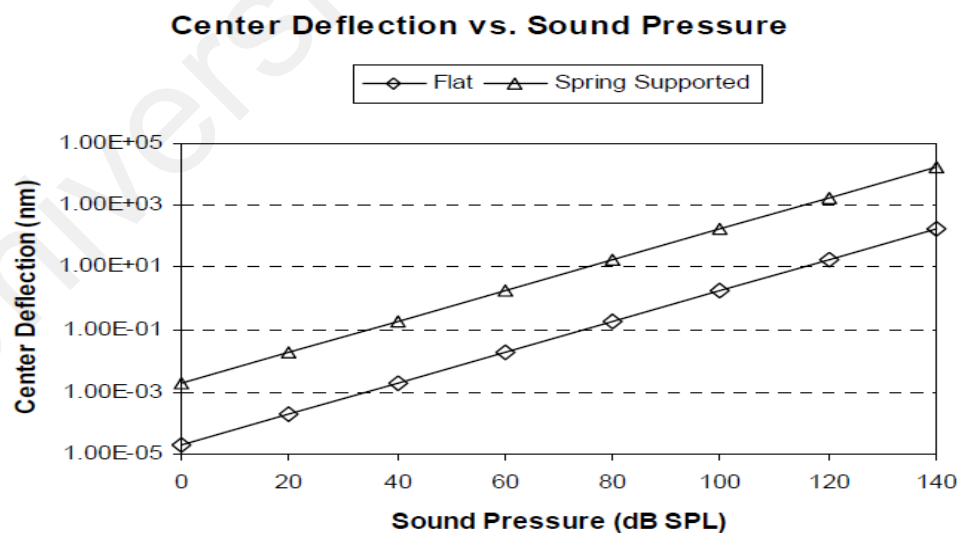

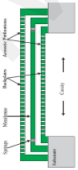
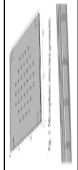

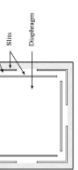
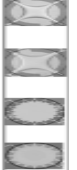
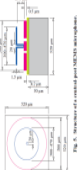
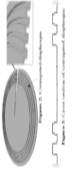

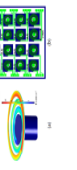
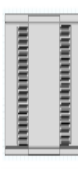


Figure 2. 12 Center deflection versus sound pressure of a flat and spring supported diaphragm

## 2.4 SUMMARY

Several type capacitive diaphragm is reviewed for cochlear implants and hearing aids. In cochlear implant microphone few number array has been developed to resonate at frequency from 400Hz to 5000Hz. The sensitivity varies in each arrays fully implantable cochlear implant microphone. The sensitivity decreases when frequency of each array increases. The sensitivity of each microphone array can be increase from the existing design. This will overcome the disadvantage of hearing less soft and loud sound without changing sensitivity of cochlear implant.

TABLE OF PARAMETER COMPARISON FOR MEMS MICROPHONE FROM LITERATURE REVIEW									
NO	PARAMETER JOURNAL ASSOCIATE	STRUCTURE OF MICROPHONE	MECHANISM OF MICROPHONE	DIMENSION OF DIAPHRAGM	DEFLECTION	MICROPHONE MATERIAL	SENSITIVITY & LINEARITY	FREQUENCY	COMMENTS AND FINDINGS
1	Thin Film PZT Acoustic Sensor for Fully Implantable Cochlear Implants		CANTILEVER SUPPORTED BEAM	BEAM LENGTH 0.8mm-3.4mm WIDTH 1mm PZT THK 1µm	NOT SPECIFIED	SILICON & PZT	392 mV/Pa @ 900 Hz	300Hz- 4800 Hz	Number of array used is 8. Beam length varies due to the frequency of excitation. Sensitivity varies according to the beam length.
2	Design and simulation of a membranes-based acoustic sensors array for cochlear implant applications		SPRING SUPPORTED	DIAMETER IS 700µm THK 2.25 µm	NOT SPECIFIED	POLYSILICON	0.17 pF/Pa	500Hz- 4200Hz	Number of array used is 14. Layout dimension of array is 3.83mm x 3.83mm. Frequency varies according to number of spring supported.
3	Design and Simulation of MEMS Microphone for Hearing Aid Application		SPRING SUPPORTED	500µm X 500µm X 0.5 µm	0.13µm @ 1Pa	GOLD	17.4 pF/Pa	10 kHz- 43 kHz	Its perforated square hole microphone diaphragm. Flat frequency response from 100Hz to 10 kHz covering the audio frequency range.
4	Design and Multiphysics Analysis of MEMS Capacitive Microphone		CORROGATED DIAPHRAGM	Thickness of 3µm, size of 0.5mm x 0.5mm and air gap of 1µm.	0.7169µm @ 1KPa	ALUMINIUM	7E-10 mV/Pa	NOT SPECIFIED	The corrugation and perforation in diaphragm reduces the residual stress and increases the mechanical sensitivity of diaphragm. Instead of perforated back plate, holes have been made on the diaphragm.
5	Modelling and Optimisation of a Spring-Supported Diaphragm Capacitive MEMS Microphone		SPRING SUPPORTED	4 mm X 4mm X 4µm	NOT SPECIFIED	POLYSILICON	4.67 mV/Pa	10.2kHz	A 1 mm2 spring-supported diaphragm microphone is designed using several optimized performance parameters to give a -3 dB operating bandwidth of 10.2 kHz, a sensitivity of 4.67 mV/Pa
6	Analytical Analysis and Finite Element Simulation of Advanced Membranes for Silicon Microphones		SPRING SUPPORTED	DIAMETER IS 100µm THK 0.4µm	NOT SPECIFIED	SILICON	8.2 mV/Pa/V	78.3kHz	This advantages are particularly valid for few and narrow spring structures and result in higher microphone sensitivity..
7	THE SENSITIVITY ANALYSIS OF A MEMS MICROPHONE WITH DIFFERENT MEMBRANE DIAMETERS		CENTRAL SUPPORT	DIAMETER IS 370µm THK 0.4µm	0.07µm @ 1Pa	POLYSILICON	0.84 Pf	1MHz	Finding the relationship between the sensitivity and dimension of the diameter of the membrane. As the diameter of membrane increase sensitivity increase
8	The Effect of Corrugations on Mechanical Sensitivity of Diaphragm for MEMS Capacitive Microphone		CORRUGATED DESIGN	DIAMETER IS 500µm THK 2µm	3.5µm @ 500Pa	Diaphragm with Poisson's ratio of 0.22. Young's modulus of 160 GPa.	0.007µm/Pa	NOT SPECIFIED	Number of corrugations is taken as 8. Mechanical sensitivity increases as the pressure and number of corrugation increase
9	Design and Fabrication of Fully Implantable MEMS Cochlea		ELECTRODE TYPE	2mm X 2mm TO 0.75mm X 0.75mm	NOT SPECIFIED	SIXNY diaphragm	NOT SPECIFIED	1kHz to 7kHz	The sound is detected by thin SIXNY diaphragm due to resonant frequency and the displacement of the membrane caused by acoustic pressure. The displacement is detected employing piezoresistive electrodes (NIG).
10	Spiral-Shaped Piezoelectric MEMS Cantilever Array for Fully Implantable Hearing Systems		SPIRAL CANTILEVER SUPPORTED MASS	2 mm X 2 mm X 12.5µm.	NOT SPECIFIED	SILICON	NOT SPECIFIED	300Hz-700 Hz	The test array consisting of 16 cantilevers has been fabricated by standard bulk micromachining using a Si-on-insulator (SOI) wafer and aluminum nitride (AlN) as a complementary metal-oxide-semiconductor (CMOS) and biocompatible piezoelectric material.
11	Optimization of MEMS Based Capacitive Accelerometer for Fully Implantable Hearing Aid Application		ACCELEROMETER TYPE	Plate Thickness 25µm. Width of Finger 2µm. Finger overlap width 2µm Finger length 116µm	NOT SPECIFIED	SILICON	2.617E-4 pF/µm	10KHz	Comb drive accelerometer consists of fixed fingers attached to the accelerometer frame and movable fingers fixed to the proof mass and suspended by springs. Any external acceleration causes the proof mass and movable fingers to move along the direction of body force, the fixed comb remains stationary.

## **CHAPTER 3 RESEARCH METHODOLOGY**

### **3.1 INTRODUCTION**

This chapter provides the research plan of this study and describes the necessary steps for the research to achieve the objective. The research method is foundation as it layout approaches and measurement that, make sure the research will handle correctly. This chapter describes the steps in Simulation studies and Taguchi Optimization Method for the capacitive microphone for the fully implantable hearing device.

### **3.2 PROJECT METHODOLOGY**

The main objective of this section is to outline a research method of this capacitive mems microphone. It presents and explains the list of steps taken to carry out this research from data collection through data analysis. This research presents five capacitive mems microphone structure and compared the performance of the microphone such as the sensitivity and linearity. To reduce complexity of the optimization and simulation studies the method has been separated into two parts. In first section the simulation analysis of the selected structures to optimized for maximum sensitivity and linearity.

Then evaluating structure, performance in producing highest sensitivity and linearity. The selected best outcome structure will go forward to the second section of the simulation studies for Eigen frequency analysis for the designated number of arrays. Then further evaluating the structure of each array for Eigen frequency, sensitivity and linearity of the overall cochlear implant structure.

### 3.3 OVERALL PROJECT FLOW CHART

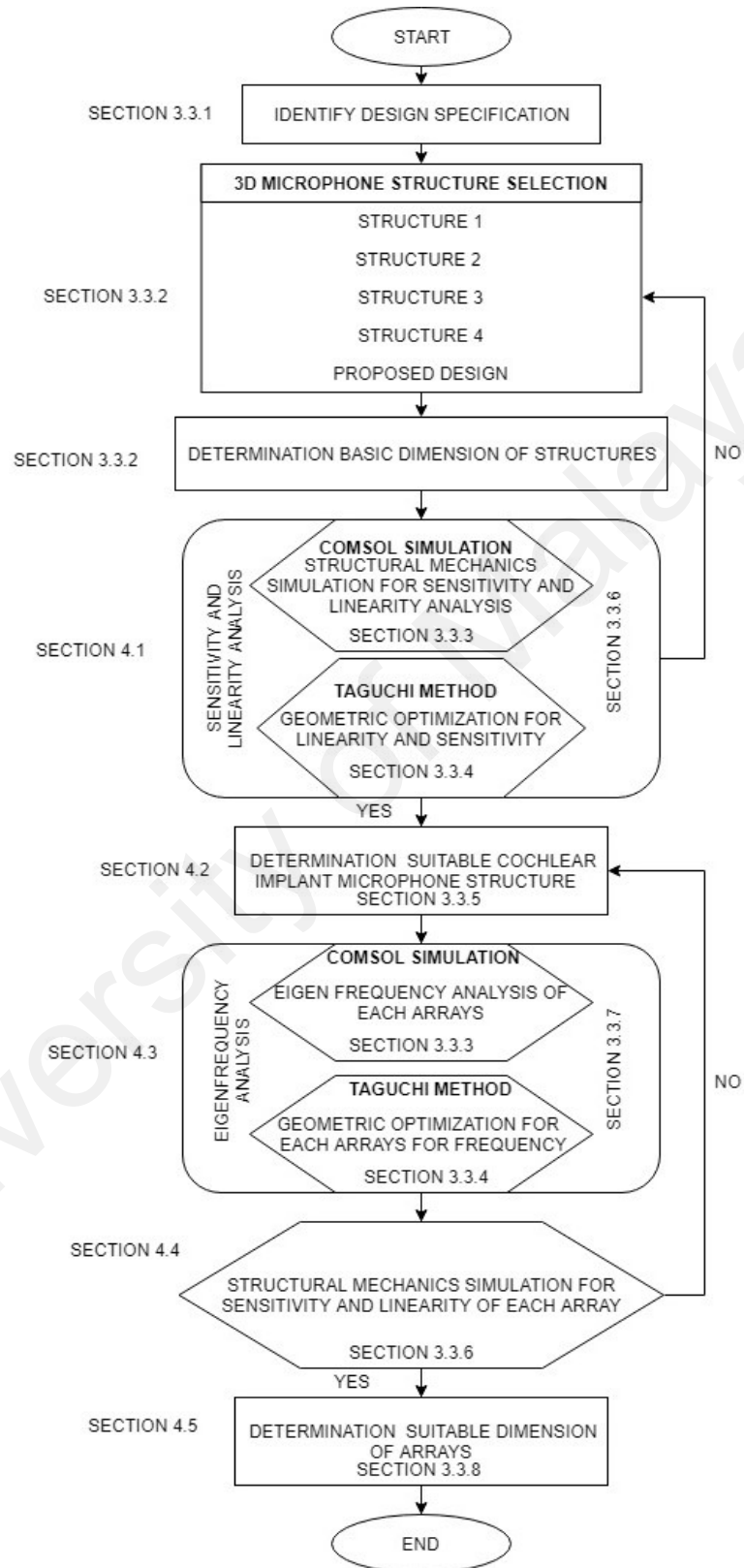


Figure 3. 1 Overall project flow chart

### 3.3.1 IDENTIFY THE DESIGN SPECIFICATION

The Table 3.1 shows the existing design and proposed design specification for this research project. The design specification is derived from the literature review summary after analyzing performance on the sensitivity, linearity and frequency of response of each structure array. The analysis of simulation and optimization is focused to accomplish the proposed design specification.

DESIGN SPECIFICATION			
ITEM	PARAMETERS	EXISTING DESIGN	PROPOSED DESIGN
1	Number of Array	8 (Koyuncuoğlu et al., 2017)	10
2	Overall array Dimension	3.3mm x 3.6mm	3.0mm x 3.0mm
3	Capacitive Sensitivity	0.17 pF/Pa (Quiroz, Báez H., Mendoza, Alemán M., , & Villa, 2014)	>0.17pF/Pa
4	Linearity	0.0002 pF/μm (Apoorva Dwivedi & Khanna, 2016)	>0.0002pF/μm
5	Mechanical Sensitivity	0.007μm/Pa (Taybi & Ganji, 2013)	>0.007μm/Pa
6	Frequency	300Hz - 4800 Hz (Koyuncuoğlu et al., 2017)	300Hz - 5000Hz
7	Material	Polysilicon	Polysilicon

Table 3. 1 Design specification



### 3.3.2 STRUCTURE SELECTION AND BASIC DIMENSION OF STRUCTURE

In this section four structure has been selected from literature review journals and a proposed structure to meet the objective of this thesis. The four structures have been selected randomly from the literature review summary table. The selected structure is from hearing device application. By this implementation of capacitive mems microphone for cochlear implants are feasible to develop. The basic dimension contributes vital part in optimization and the simulation studies for deflection of membrane and frequency analysis.

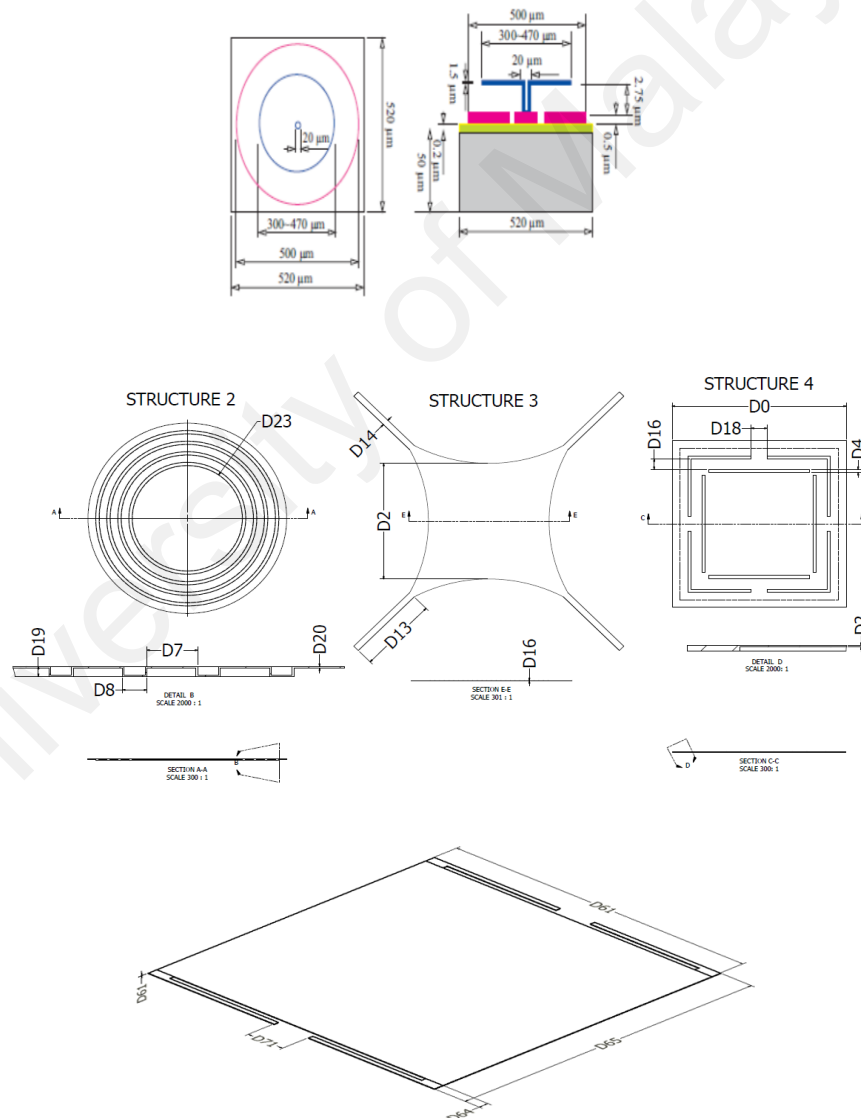


Figure 3. 2 Show basic dimension of structures

### 3.3.3 COMSOL MULTIPHYSICS 4.3a

Following is the simulation steps of COMSOL Multiphysics and optimization of the microphone structure from the author Taybi, M., & Ganji, B. A. (2013). Geometric part has created using Autodesk inventor Professional 2017. Then transfer 3D CAD data using the Livelink feature of COMSOL Multiphysics.

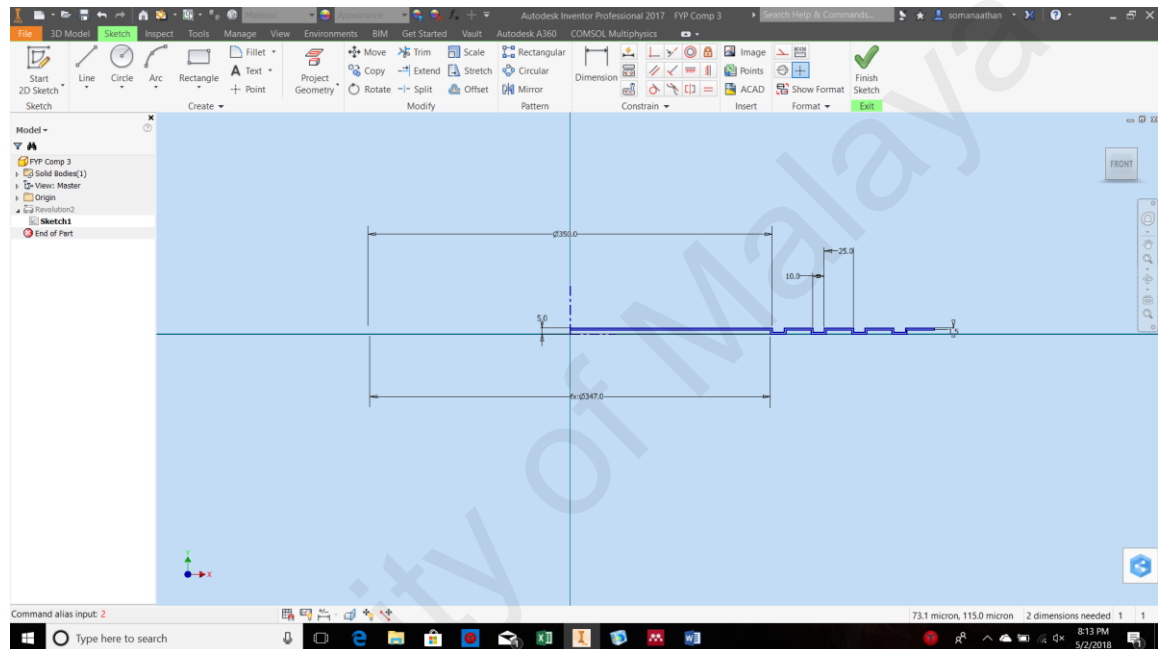


Figure 3. 3 2D sketches from the Autodesk inventor 2017

Before building 2D sketches it's important to verify units in Micrometer  $\mu\text{m}$  in document settings in the Autodesk inventor tool. Create 2D sketch and constraint it accordingly. Use suitable feature such as extrude, revolve, sweep and loaf to create 3D parts. Since above structure is in circular form, revolve feature is used to create the 3D model.

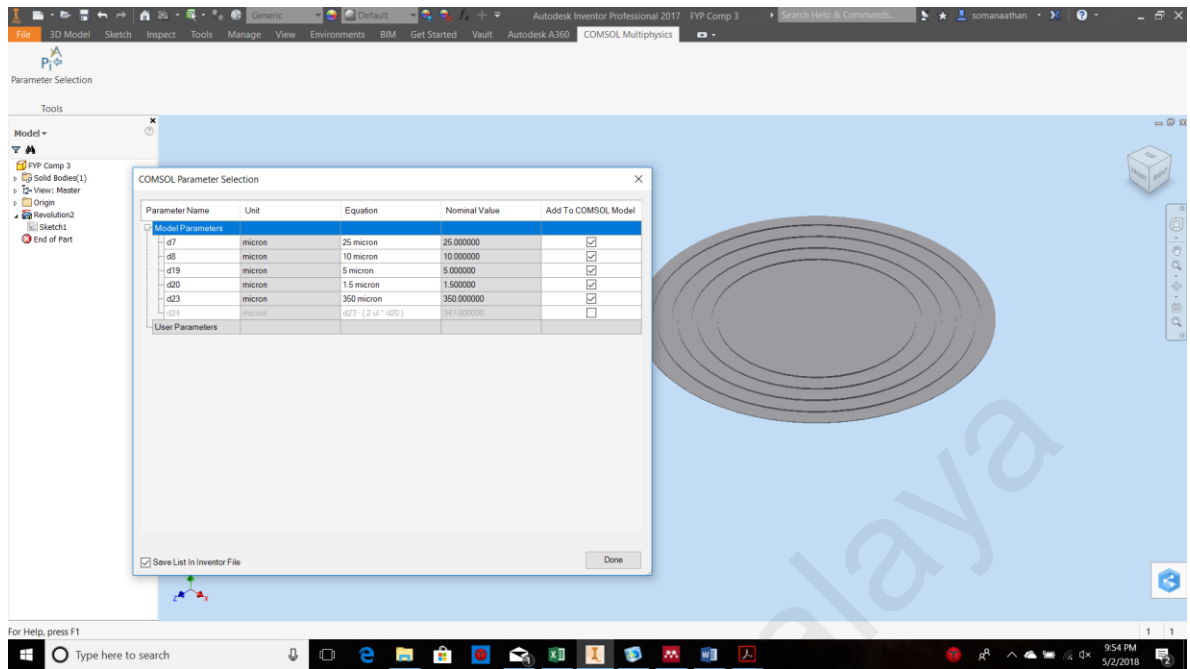


Figure 3. 4 Selection of geometric parameter to the COMSOL model

To transfer the geometric parameter to COMSOL model, select the parameter selection in COMSOL Multiphysics in Autodesk inventor tap.

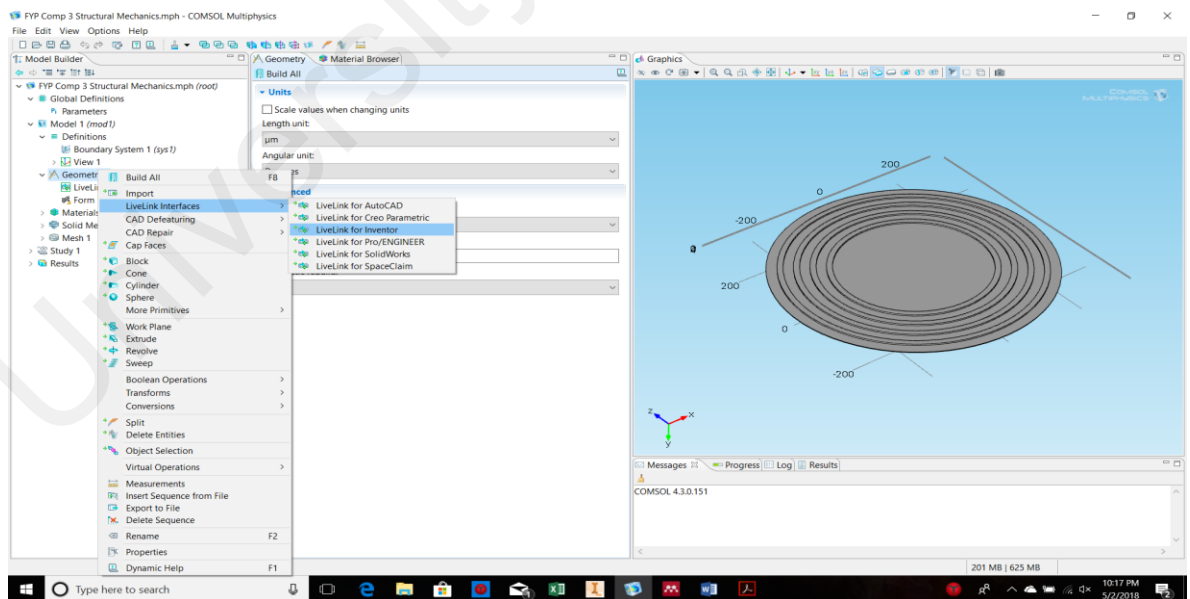


Figure 3. 5 COMSOL live link interfaces

Open new documents in the COMSOL Multiphysics, select solid structural and add physics model. Right click on the geometric model, select the live link for inventor in the live link interfaces.

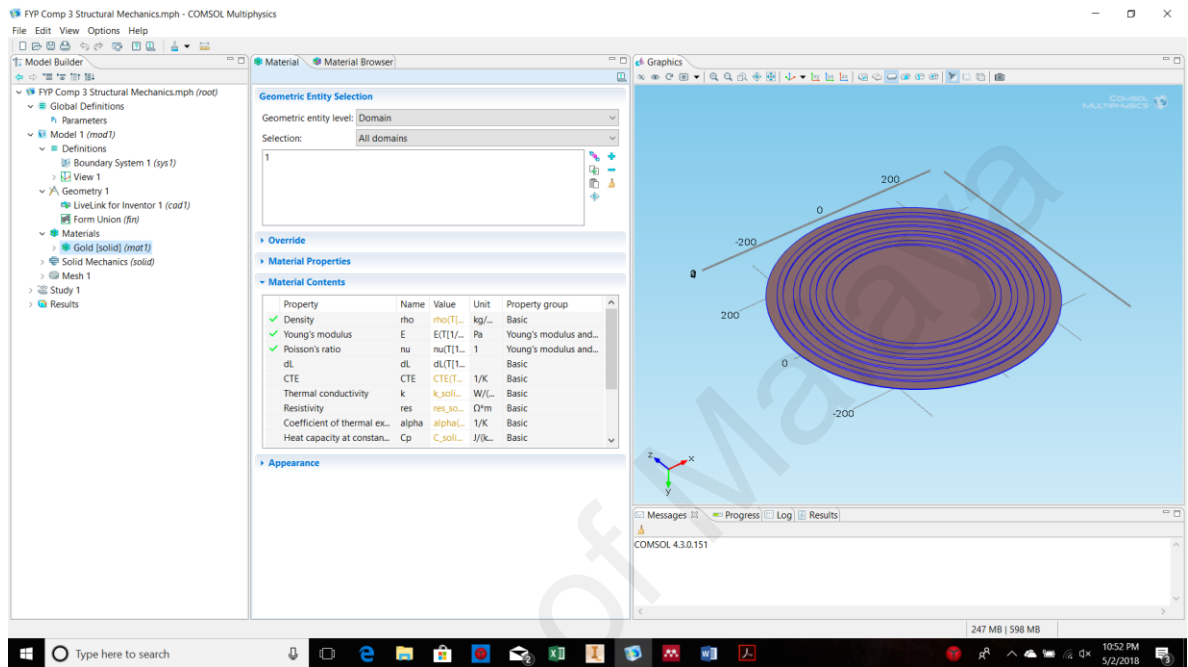


Figure 3. 6 Selection of material

Select the Gold (Au) material from the material browser. COMSOL has already predetermined the material properties for the user.

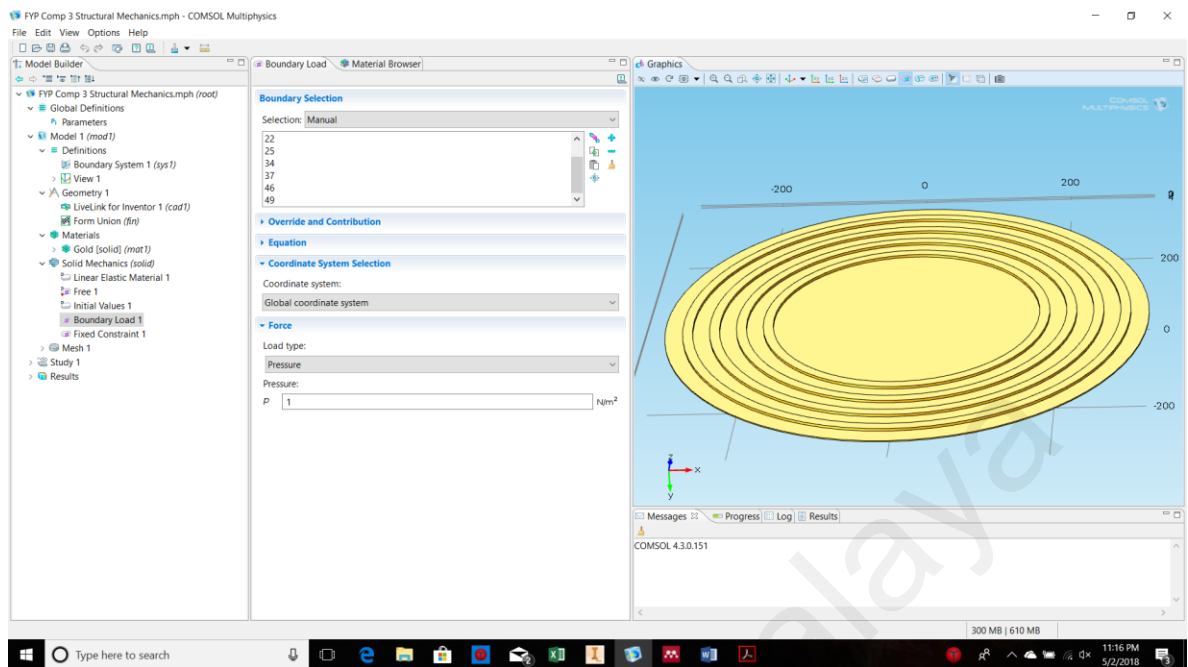


Figure 3. 7 Boundary load condition

Assign the boundary load by changing the load type to Pressure to 1Pa. Select the surface that experiencing pressure. Add fixed constraint and select the corner surface.

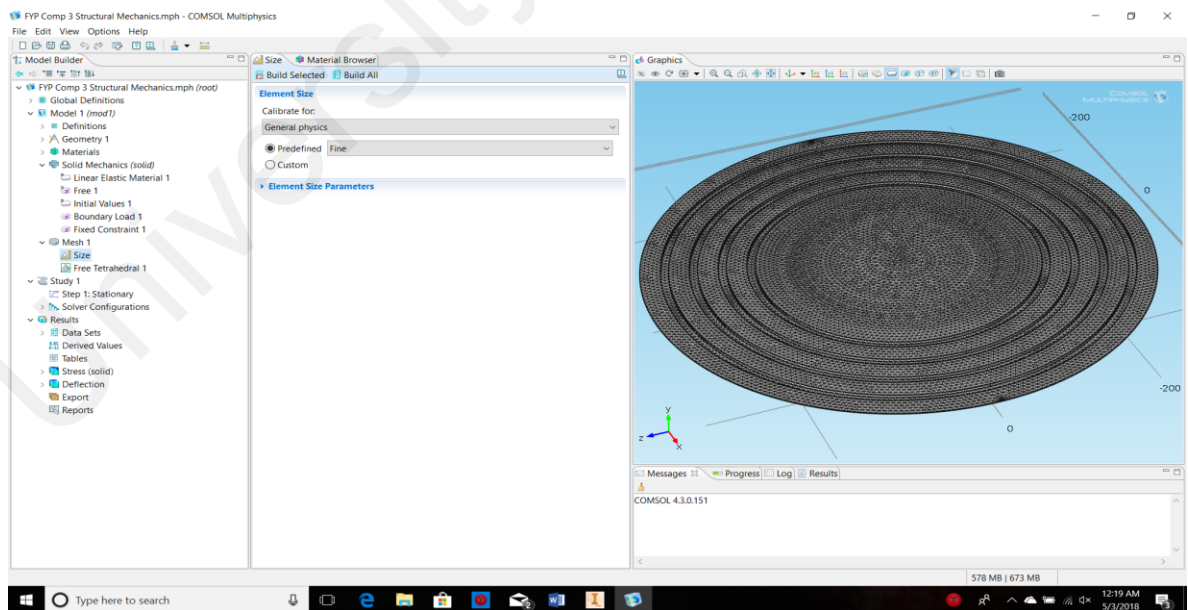


Figure 3. 8 Generating meshing

Select finer mesh size in predefined column.

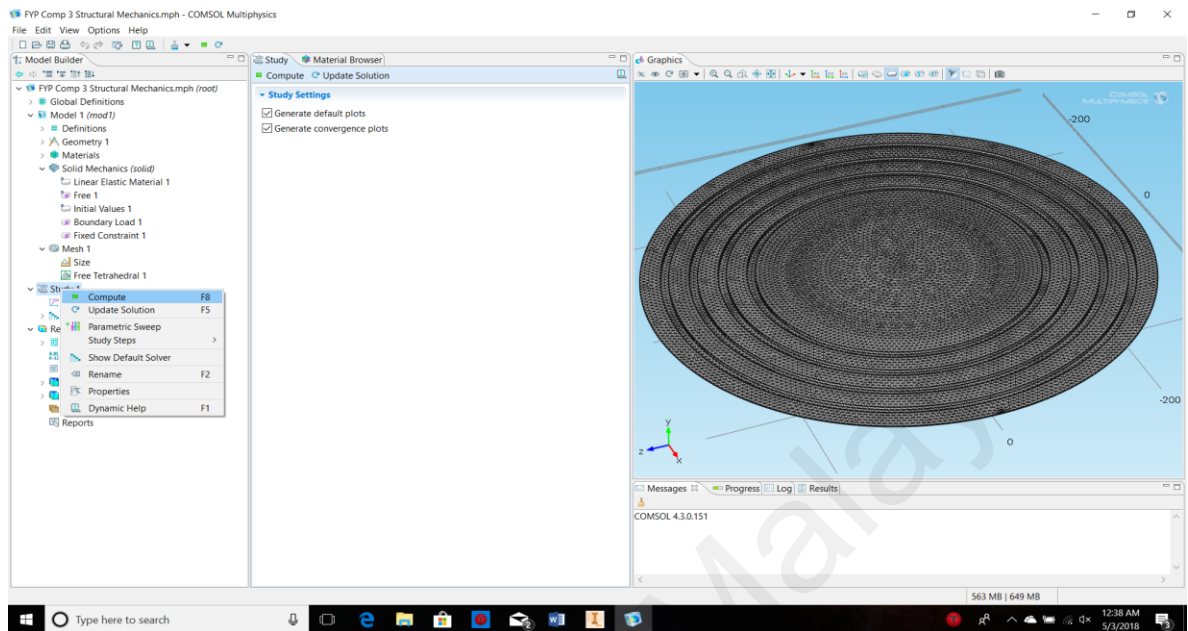


Figure 3. 9 Generating or computing the simulation

Right click on the study pane and compute the simulation

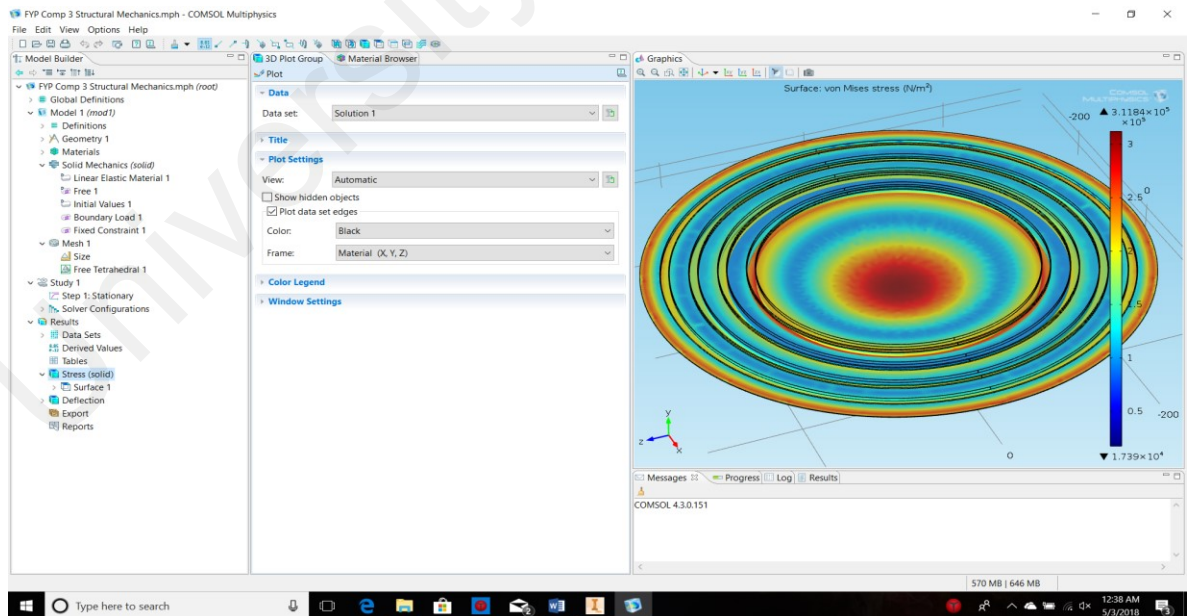


Figure 3. 10 Von Mises stress diagram

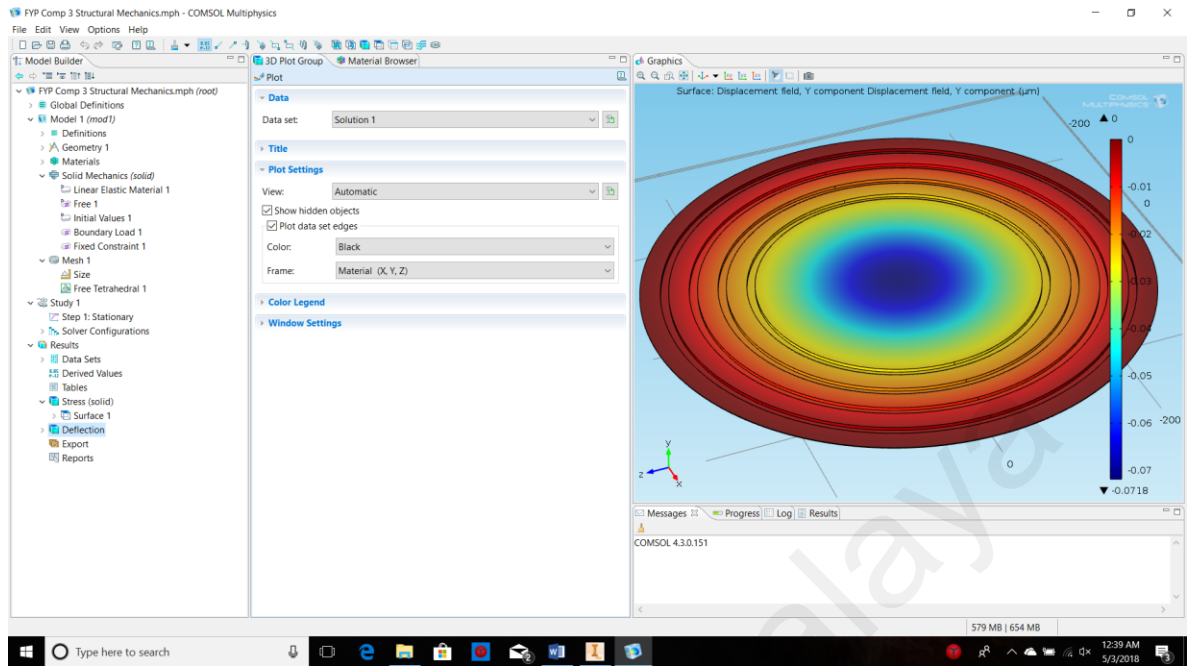


Figure 3. 11 Surface displacement y component field

Based on the simulation results, outcomes in terms of the von Mises stress diagram where it will indicate the maximum yield stress of the structure as shown in Figure 3.10 and also show the maximum deflection of the structure according to the x, y and z axis as its shown in the Figure 3.10.

There will similar steps of simulation studies will be undergoes again for analyzing Eigen frequency of the structure. Shortlisting one most influential structure for deflection and that structure will undergo further frequency analysis for number of arrays specified in design specification for the cochlear implants.



### 3.3.4 TAGUCHI OPTIMIZATION METHOD USING MINITAB

The following optimization method has been done by using the Minitab 18.0 version. This section will elaborate the steps on Taguchi optimization.

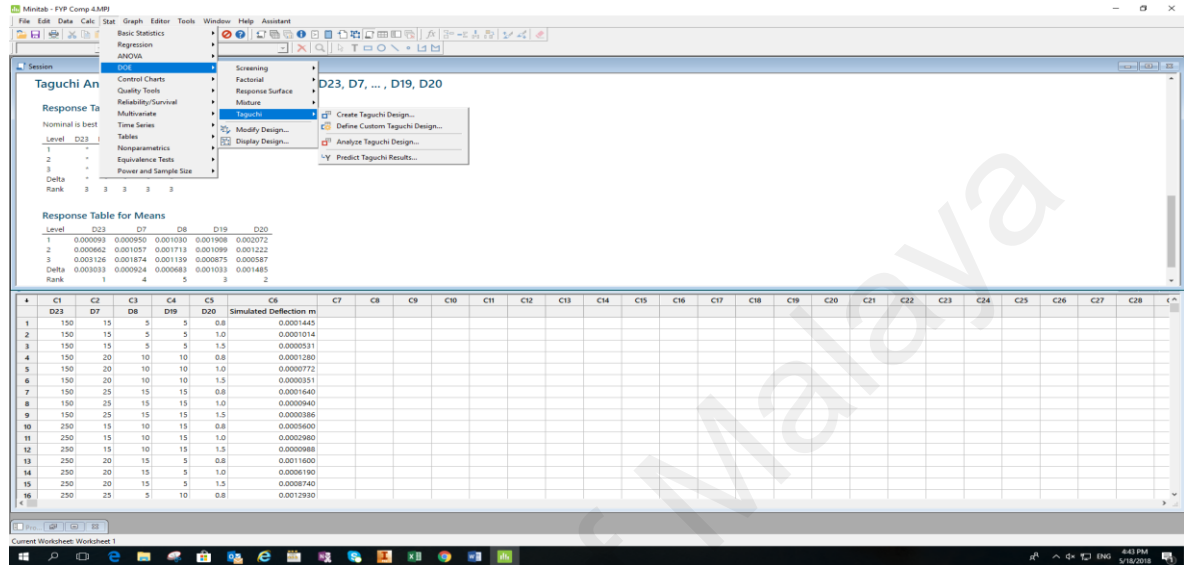


Figure 3. 12 Generating new file

Create new file, click start in the top pane selects the Degree of Experiment (DOE) followed by selecting the Taguchi and create Taguchi designs as shown in the Figure 3.12.

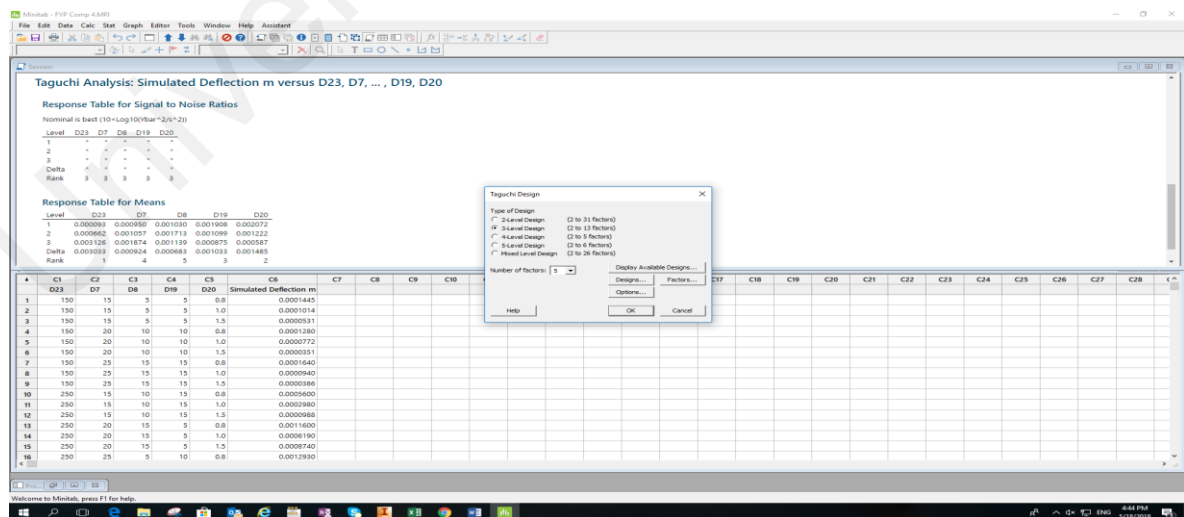


Figure 3. 13 Selection of level of design and the number of factors



The selection of level of design is depending on the number of variable on each factor to be experimented as shown Figure 3.13 Thus, very important in deciding number of factors and the level of design according to the particular membrane parameter to be tested to achieve the objective of optimizing.

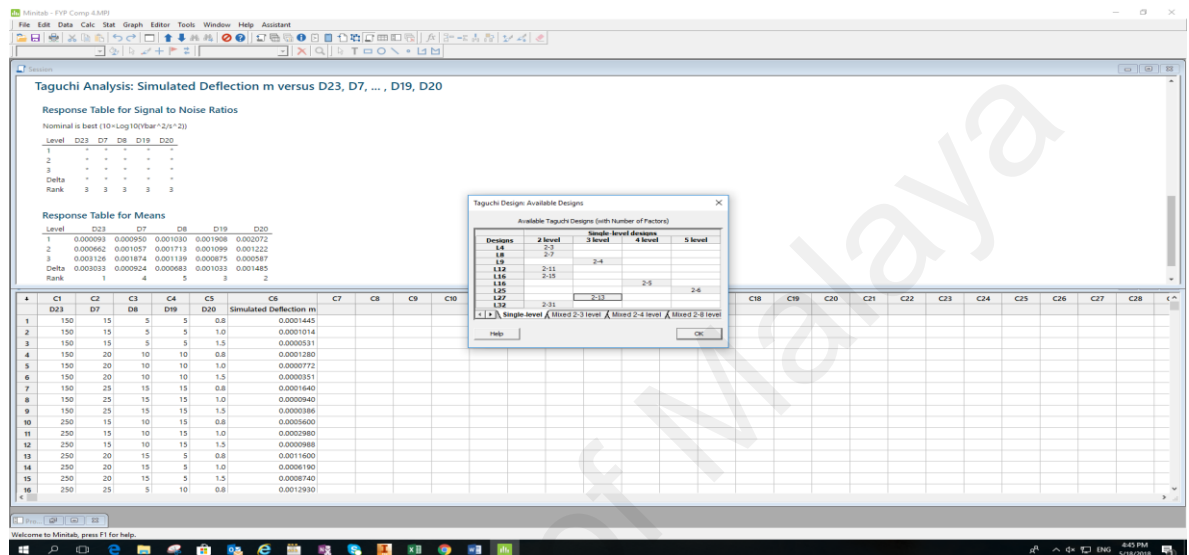


Figure 3. 14 Select number of factors in available design tab

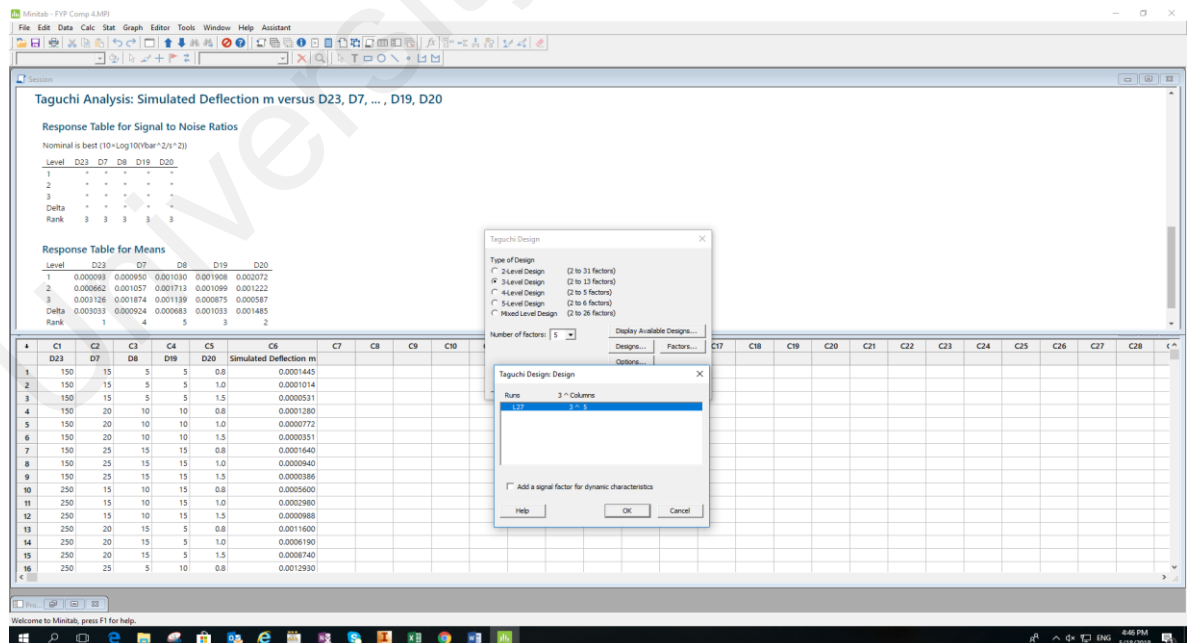


Figure 3. 15 Selecting the available design

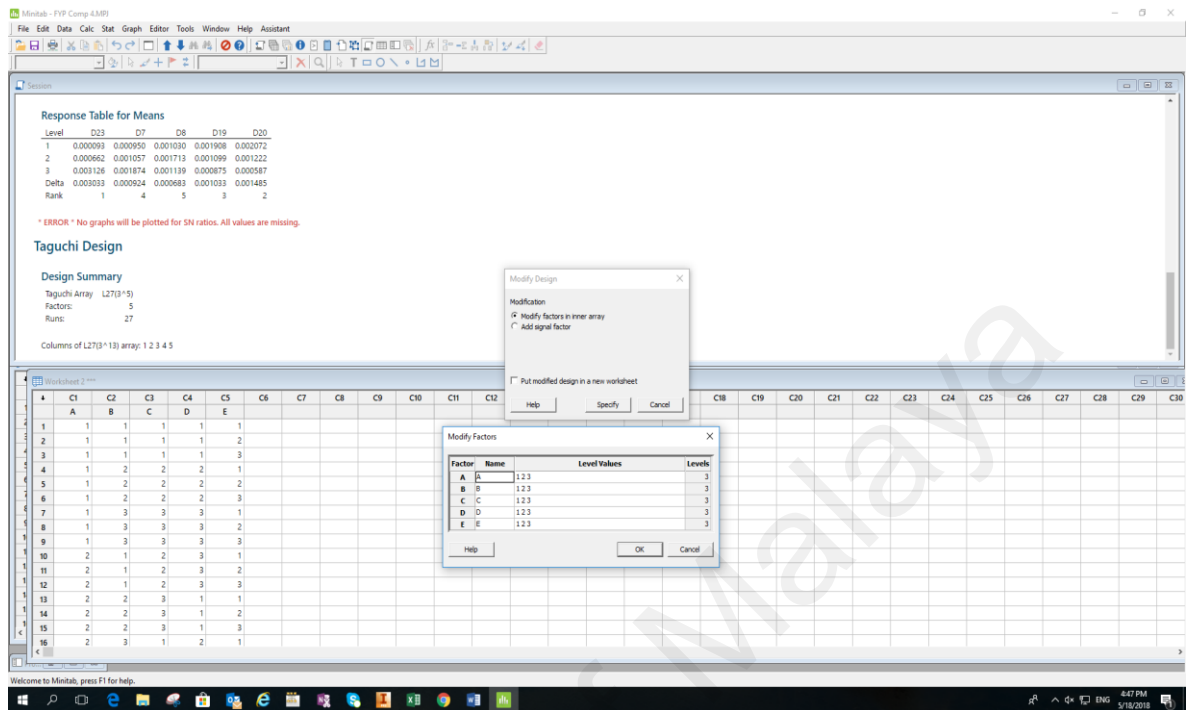


Figure 3. 16 Modify the parameter and name accordingly

After selecting the number of orthogonal arrays according to the requirement as shown in Figure 3.14 and Figure 3.15. Number of orthogonal arrays indicate the number of experiment or runs required for the simulation. To edit or modify factors click on the start and the DOE pane to select modify factors name and level values according to the requirement of the experiment clearly shown in the Figure 3.16. Add deflection or displacement value from the simulation experiment in the column beside the factors manually. For example, in column C6 and name the column as deflection value. These will help us to diagnose result of optimization. The graph of the Main Effect Plot for Means as shown in the Figure 3.17 indicate the effect changes in selected parameters in related to deflection of the structure.

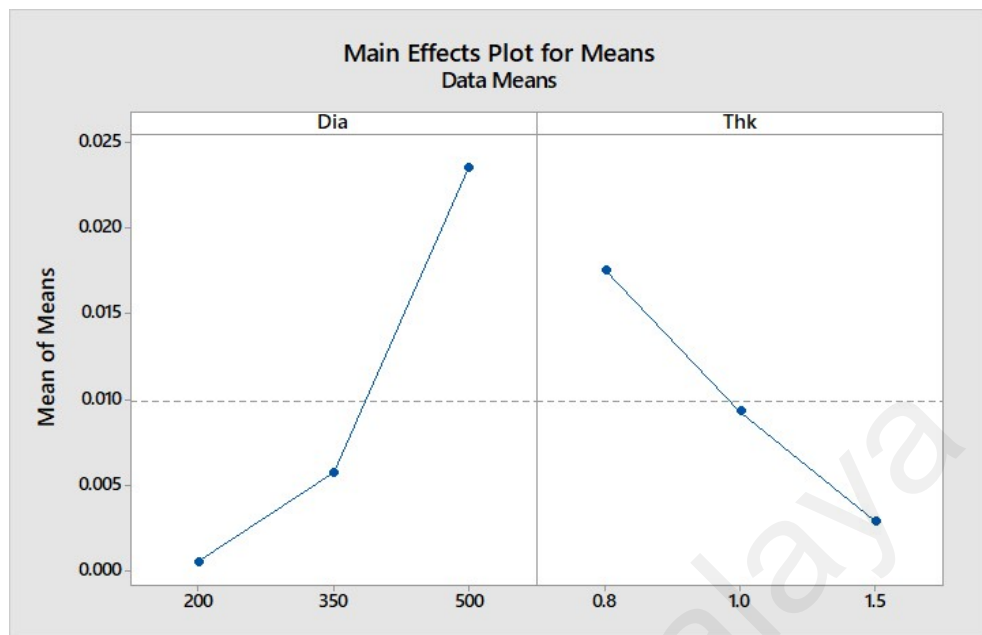


Figure 3. 17 Graph of Main effects Plots for means

The graph of main effect plot shown in Figure 3.17 can be obtained in under analyze Taguchi design tool pane located in DOE section.

As a summary of this section 3.2 its show the steps on COMSOL Simulation and Taguchi optimization using Minitab software. These are the steps being followed through the simulation and optimization process for every comparison structure. However the parameter analyzed will be different according to each structure.

### **3.3.5 DETERMINATION OF SUITABLE STRUCTURE**

In this section the result of four selected structures on the sensitivity, linearity and Dimension of the structure of the optimized and non-optimized results are tabulated for analysis. The tabulation of data is very important to analyze which structure can get higher linearity and sensitivity for further Eigen frequency studies.

Furthermore, the tabulated data will be able to convey the result of an optimized structure in terms of sensitivity and linearity. The selection of structure is mostly relying on the mechanical sensitivity because it has ability to capture the sound far from the source. The highest mechanical sensitive structure will go for Eigen frequency analysis.

### **3.3.6 ANALYSIS OF SENSITIVITY AND LINEARITY**

The analysis of sensitivity and linearity is primary important in this research. This is due to the objective of research is to improve sensitivity and linearity. The method of analysis and the equation of involved will be discussed in this section. This method will be utilized in chapter 4 result and discussion in section 4.1 and 4.4

The sensitivity of microphone is often represented in mechanical sensitivity and capacitive sensitivity. In this research both parameter will be discussed for better understanding of sensitivity. To extent the understanding of capacitive sensitivity. The understanding of capacitance is very important (Chaithra et al., 2017). The capacitance can be classified in static parallel capacitance and dynamic parallel capacitance. The static parallel capacitance will be employs when the membrane doesn't move. However the dynamic parallel capacitance will employs to structure when diaphragm is moving. This research will be more focusing on the dynamic parallel capacitance as the membrane disturbed by acoustic pressure

The capacitance represents as follows:

$$\text{Capacitance (F)} = \frac{\epsilon.A}{d_i - d_f} \quad (3.1)$$

$$\text{Capacitance (F)} = \frac{\epsilon.A}{\Delta d} \quad (3.2)$$

$\epsilon$  is permittivity of the material between the parallel plates (free plate permittivity  $8.85 \times 10^{-12}$  F/m). A plate surface area ( $m^2$ ).  $d_i$  distance between two parallel plate (m).  $d_f$  membrane deflection.

The capacitance sensitivity represents as follows:

$$\text{Capacitive sensitivity (F/Pa)} = \frac{\text{capacitance}}{\text{Pressure}} \quad (3.3)$$

The mechanical sensitivity is focusing on the deflection of membrane. The mechanical sensitivity is defined as how much the deflection changes per sound pressure applying on the diaphragm (Scheeper et al., 1994).

The mechanical sensitivity represents as follows:

$$\text{Mechanical Sensitivity } \left( \frac{m}{Pa} \right) = \frac{\text{deflection of membrane}}{\text{Pressure}} \quad (3.4)$$

The linearity of the microphone can be limited by the microphone, amplifier, or both. Capacitive devices are inherently nonlinear due to the nonlinear relationship between capacitance and gap size. As diaphragm deflection increases, distortion increases so THD at a specific SPL can be decreased by increasing the diaphragm stiffness.

Normally linearity is often discussed through graph of capacitance versus displacement. In this research, similarly it will be represented through the graph capacitance versus displacement.

The measurement of gradient between two consecutive points will able to provide understanding on the linearity. In simple words the slope of capacitance must constant at every displacement.

The linearity can be express as follows:

$$linearity (F/m) = \frac{\Delta Capacitance}{\Delta Displacement} \quad (3.5)$$

### 3.3.7 ANALYSIS OF EIGENFREQUENCY OF EACH ARRAY

This section will be discussed the methodology in obtaining theoretical value of frequency for comparison with simulated value and also discussed limitation of using higher number of arrays. The Number of membranes of the array must be arranged the accordingly with geometric and frequency parameter. Example, as shown in diagram of Figure 2.2.2.

In this research only ten number of linear arrays is processed. All though higher number of arrays can produced a very high quality signal but it has given significant disadvantages on the cost, size of microphone is bulky (Zwyssig, Lincoln, & Renals, 2010) and as the number of signals increases, the complexity of the electronics to acquire and process the data will grow as well(Papež & Vlček, 2015).

Normally the size of membrane will be same in all the arrays but the number of support each structure will be varies in order to achieve the different desired frequency (Quiroz, Báez H., Mendoza, Alemán M., , & Villa, 2014).

However in this research the size of each array membrane will be different in size in order to reduce the space. Similar work has been done from (Koyuncuoğlu et al., 2017) the frequency is been set to resonate at different beam length.

The following is derived expression to obtain theoretical value frequency, assuming each microphone array are producing simple harmonic motion (SHM) when in contact with acoustic wave. According to Hooke's law the determination of spring constant (K N/m) value is important in identifying the frequency of resonance

Determination of spring constant (K) value of membrane.

$$Force = Pressure (acoustic) * Contact Area$$

According Hooke's Law

$$Force = k * \Delta X$$

K is spring constant (N/m)

$\Delta X$  is deflection of membrane (m)

The equation of spring constant can be write in terms:

$$k = \frac{Pressure (acoustic) * Contact Area}{\Delta X} \quad (3.6)$$

To calculate theoretical value of resonance frequency. Simple harmonic motion (SHM) of a single spring system considered

$$\omega = \sqrt{(k/m)} \quad (3.7)$$

$$\omega = 2\pi f \quad (3.8)$$

$$f = \sqrt{\frac{k}{4 * m * \pi^2}} \quad (3.9)$$

$\omega$  angular velocity (rad/s)

m mass of membranes (kg)

f frequency of membrane (Hz)



The following equation is derived for proposed structure. This equation shows relationship of structural parameter to the Eigen frequency and spring constant.

$$\Delta X = \frac{\text{Pressure} \cdot \text{Area} [((D61 - D71))/2]^3}{2 \cdot E \cdot D64 \cdot D69^3} \quad (3.10)$$

$$k = \frac{\text{Pressure (acoustic)} * \text{Contact Area}}{\Delta X}$$

$$k = \frac{\text{Pressure (acoustic)} * \text{Contact Area}}{\frac{\text{Pressure (acoustic)} * \text{Contact Area} [((D61 - D71))/2]^3}{2 * E * D64 * D69^3}} \quad (3.11)$$

$$k = \frac{2 * E * D64 * D69^3}{[((D61 - D71))/2]^3} \quad (3.12)$$

$$f = \sqrt{\frac{k}{4 * m * \pi^2}} \quad (3.13)$$

$$f = \sqrt{\left( \frac{2 * E * D64 * D69^3}{4 * m * \pi^2} \right)} \quad (3.14)$$

### **3.3.8 DETERMINATION OF SUITABLE DIMENSION OF ARRAYS**

This section will finalize result of mechanical sensitivity, capacitance, capacitive sensitivity, spring constant, and linearity of each arrays of cochlear implant. Along with this the key parameter dimension of each array will be tabulated. This section will bring end to this research project.

University of Malaya

## CHAPTER 4 RESULTS AND DISCUSSION

### 4.1 ANALYSIS OF SENSITIVITY AND LINEARITY OF STRUCTURES

This chapter comprises the analysis of the results. The findings of the research as in mechanical sensitivity and linearity is compared with previous findings. The purpose of this chapter is to discuss the performance of each structure by optimizing parameter. There are four structures has chosen to improve the performance by Taguchi method of optimization.

Based on previous chapter, the methodology of the simulation modeling and Taguchi optimization has been explained to achieve the results. The performance of each structure will be discussed in detail as in-terms of mechanical sensitivity, capacitance and linearity.

#### 4.1.1 MEMS MICROPHONE STRUCTURE 1

The first optimized structure in this section is from the (Yang, 2010). In his paper It has been clearly analyzed the effect of sensitivity in various diameter and thickness of microphone membranes. The structure is supported in the central position and the deflection of the membrane is acting on the circumference of the circle.

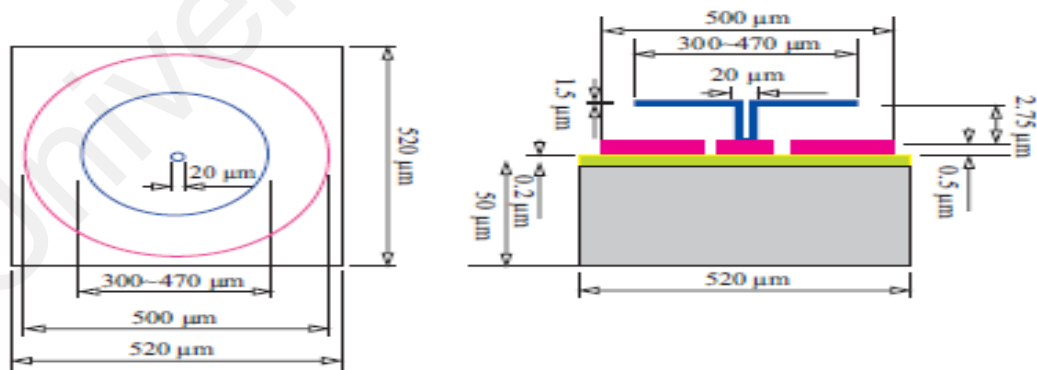


Figure 4. 1 Structure of a central-post MEMS microphone.(Yang, 2010)

The above picture is depicted from the journal article. The journal has analyzed with several membrane thickness from 1.7  $\mu\text{m}$ , 1.6  $\mu\text{m}$ , 1.5  $\mu\text{m}$  with the diameter ranges from 300mm to 450mm. Based on the outcome the highest mechanical sensitivity 0.007  $\mu\text{m}/\text{Pa}$  recorded at 1.5  $\mu\text{m}$  membranes thickness with the diameter of 450mm.

In this research, to improve sensitivity and linearity Taguchi optimization method is used to optimize the parameter such as diameter and thickness. The material used for the membranes is polysilicon. In this optimization material property retains the same. Based on the Taguchi optimization Degree of Experiment (DOE) the mean effect plot of graph shows as below.

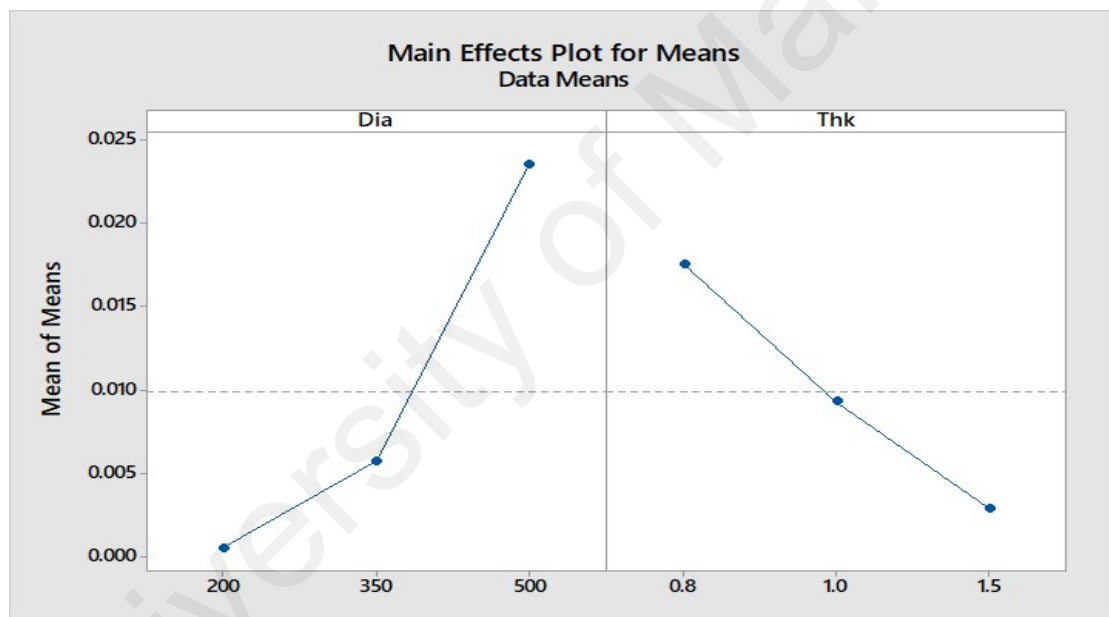


Figure 4. 2 Main effects plot for diameter and thickness

The graph of mean effect plot show that the deflection of microphone membranes greatly influences the diameter at 500mm and thickness of 0.8 $\mu\text{m}$ .

The following discussion are containing of table and graphs for that's shows out come from the optimization process for comparison purpose.

Parameter	Non Optimized	Optimized
Diameter mm	450	500
Thickness $\mu\text{m}$	1.5	0.8

Table 4. 1 Numerical value of Optimized Parameter

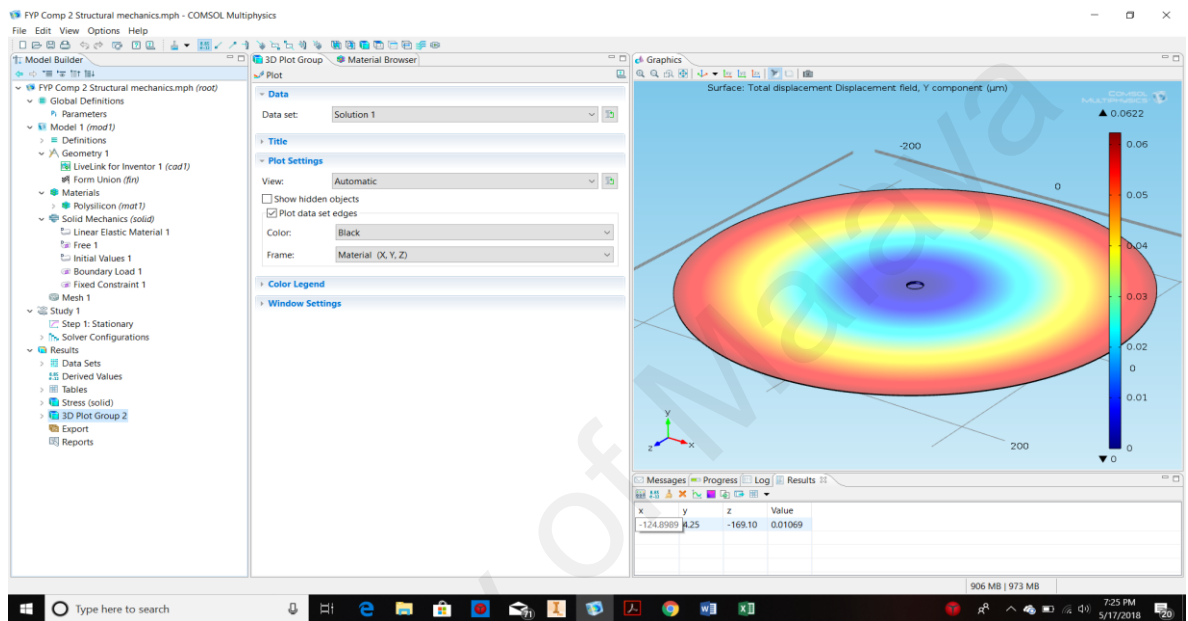


Figure 4. 3 Show the y displacement component of the structure

Pressure	Non-Optimized	Optimized	Non-Optimized	Optimized
	Deflection	Deflection	Sensitivity	Sensitivity
1	0.006	0.066	0.0058	0.066
2	0.012	0.131	0.0058	0.066
3	0.017	0.195	0.0058	0.065
4	0.023	0.258	0.0058	0.065
5	0.029	0.319	0.0058	0.064
6	0.035	0.387	0.0058	0.065
7	0.040	0.453	0.0058	0.065
8	0.046	0.491	0.0058	0.061
9	0.052	0.544	0.0058	0.060
10	0.058	0.593	0.0058	0.059

Table 4. 2 Show results of sensitivity of optimized and non-optimized parameter

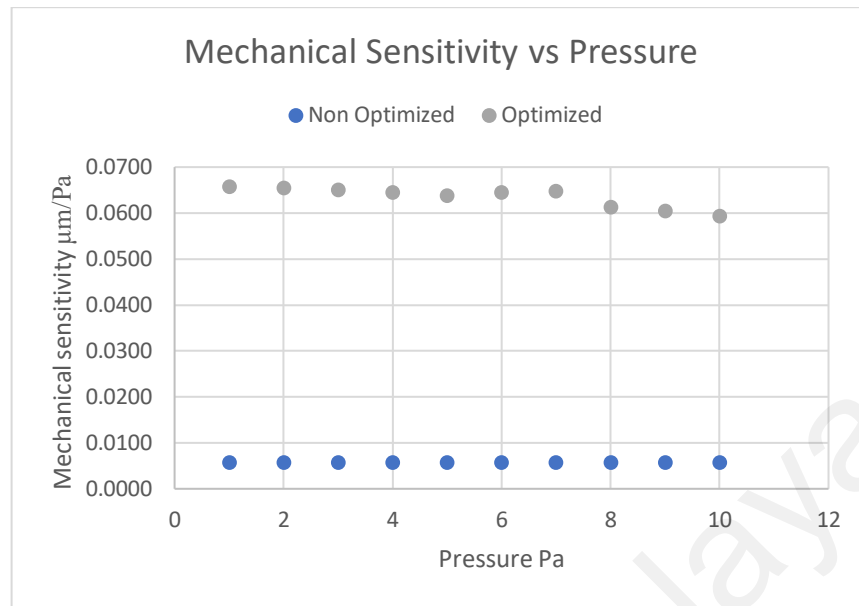


Figure 4. 4 Graph of Mechanical sensitivity vs Pressure

The above the graph shows the sensitivity of structure has been improved by changing the diameter 450mm increased to 500mm and thickness from 1.5 $\mu\text{m}$  reduced to 0.8 $\mu\text{m}$  as a result of the changes the mechanical sensitivity has increased to from 0.0058  $\mu\text{m}/\text{Pa}$  to 0.066  $\mu\text{m}/\text{Pa}$ . The improvement almost to 11.37 times from the Non-optimized parameter.

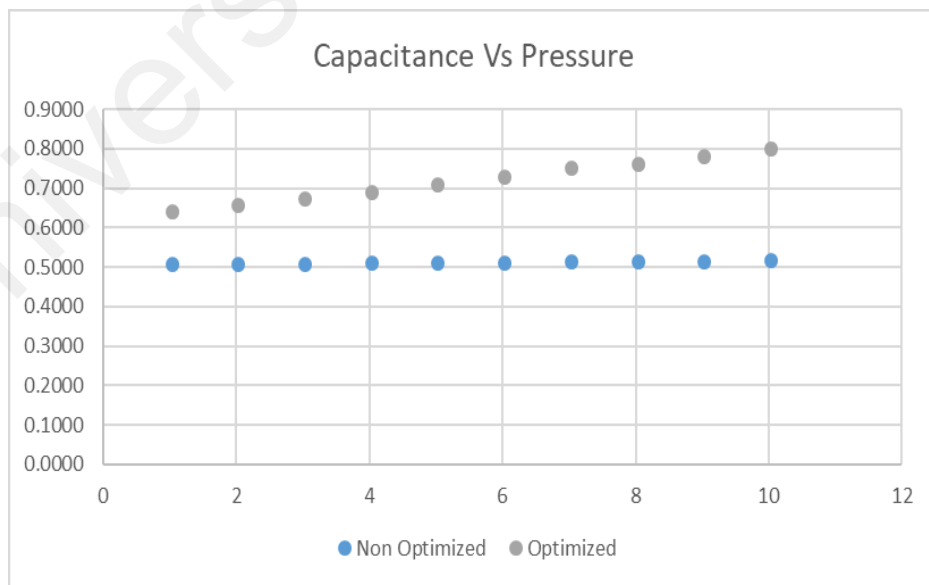


Figure 4. 5 Graph of capacitance vs pressure of optimized and non-optimized parameter

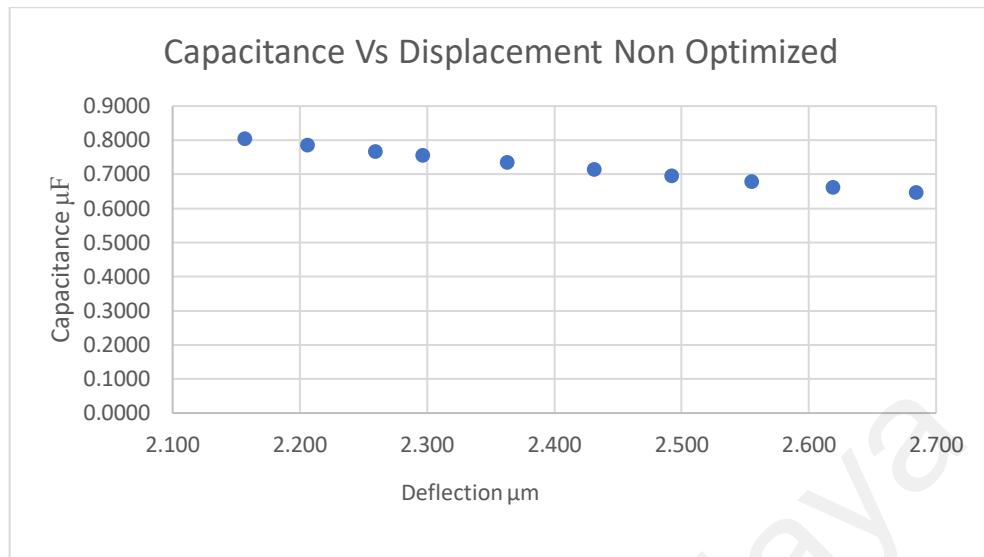


Figure 4. 6 Graph of Capacitance Vs Displacement for Non-Optimized membrane

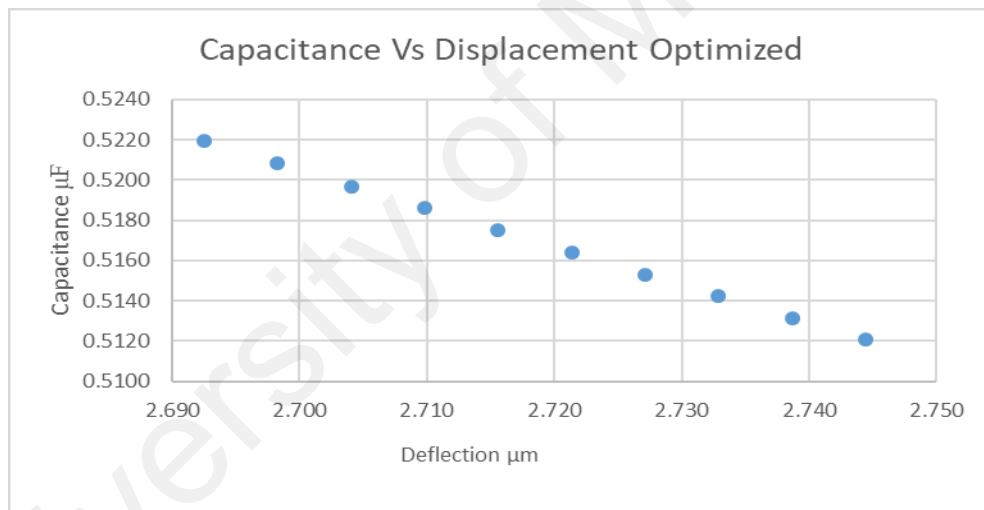


Figure 4. 7 Graph of Capacitance Vs Displacement for Optimized membrane

Based on the above graph the capacitance vs deflection of Non-optimized membranes its show that the maximum value of capacitance is  $0.5122\mu\text{F}$  and the maximum capacitance of the optimized value is  $0.6466\mu\text{F}$ . The capacitance has increased almost 1.26 times of Non-optimized parameter. The graph of capacitance vs displacement clearly indicating the linearity of optimized microphone membranes greatly increased its  $0.3\text{pF}/\mu\text{m}$  compare non optimized structure which is  $0.2\text{pF}/\mu\text{m}$

#### 4.1.2 MEMS MICROPHONE STRUCTURE 2

The second comparison structure that will be discussed in this section is from author (Taybi & Ganji, 2013). Its reported microphone corrugated diaphragm is reduced the effect of residual stress in diaphragm. The mechanical sensitivity of the diaphragm and deflection of corrugated diaphragm have little dependence on residual stress and strongly depend on the number and height of the corrugation. Based on the author diaphragm radius of 0.5mm, diaphragm thickness of  $2\mu\text{m}$  and for corrugated diaphragm. The mechanical sensitivity achieved is for 3 corrugated diaphragms is  $0.002\mu\text{m}/\text{Pa}$ .

In this research, to improve sensitivity and linearity Taguchi optimization method is used to optimize the parameter such as diameter and thickness, height of corrugation and the width of corrugation. The material used for the membranes is polysilicon. In this optimization material property retains the same. Based on the Taguchi optimization Degree of Experiment (DOE) the mean effect plot of graph shows as below.

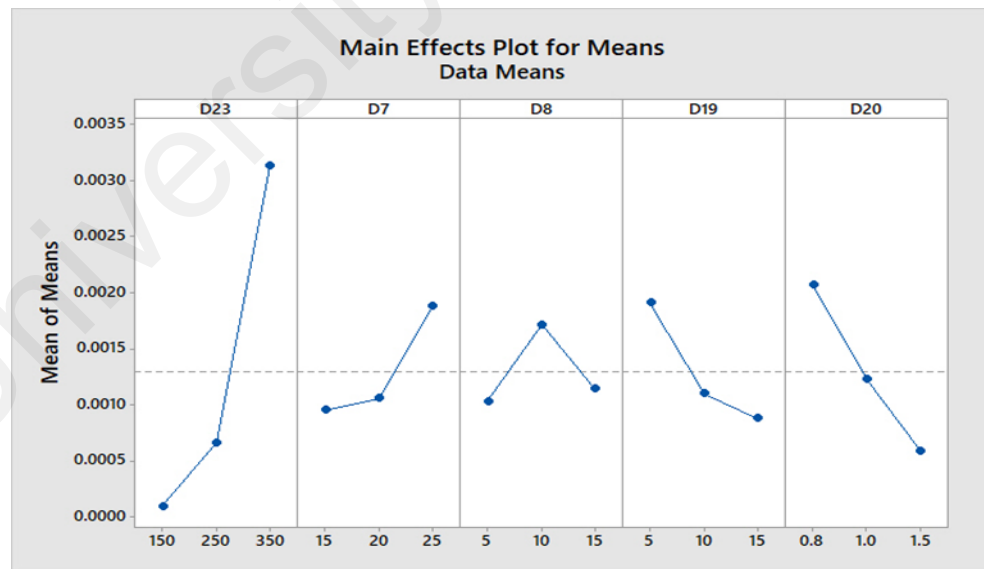


Figure 4. 8 Main effect plot for means of significant parameter of corrugated diaphragm



The graph of mean effect plot show that the deflection of microphone corrugated membranes greatly influences the diameter at 350 $\mu$ m, thickness of 0.8 $\mu$ m, the height of corrugation 5 $\mu$ m and the width of corrugation

The following discussion consists of table and graph shows result of the optimization.

Parameter	Non Optimized	Optimized
D23	500	350
D7	7	25
D8	10	10
D19	3	5
D20	2	0.8

Table 4. 3 Numerical value of Optimized Parameter

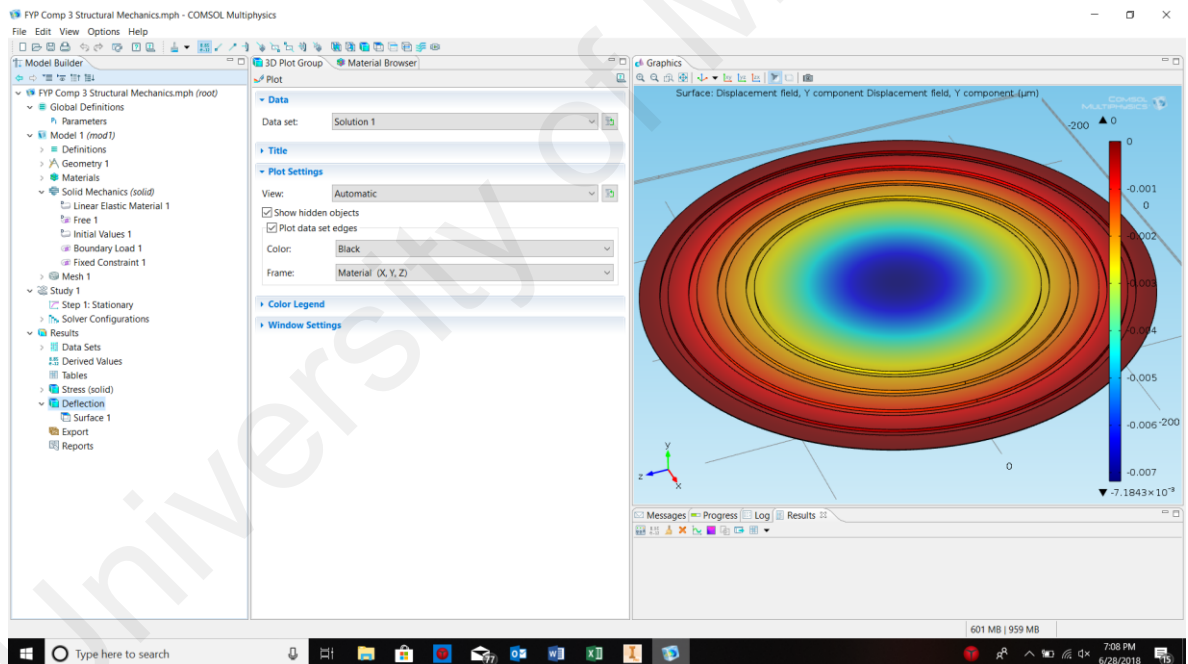


Figure 4. 9 Show the y displacement corrugated membrane

Pressure	Non Optimized	Optimized	Non Optimized	Optimized
	Deflection	Deflection	Sensitivity	Sensitivity
1	0.002	0.01	0.002	0.007
2	0.004	0.01	0.002	0.007
3	0.006	0.02	0.002	0.007
4	0.008	0.03	0.002	0.007
5	0.010	0.04	0.002	0.007
6	0.013	0.04	0.002	0.007
7	0.015	0.05	0.002	0.007
8	0.017	0.06	0.002	0.007
9	0.019	0.06	0.002	0.007
10	0.021	0.07	0.002	0.007

Table 4. 4 Show results of sensitivity of optimized and non-optimized parameter

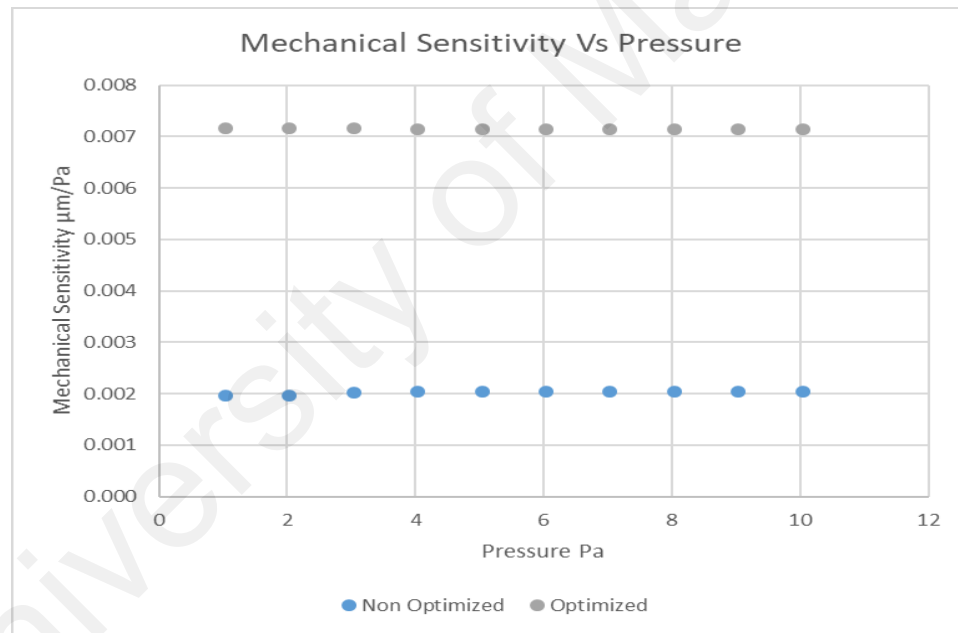


Figure 4. 10 Graph of Mechanical sensitivity vs Pressure

The above the graph shows the sensitivity of structure has been improved by changing the parameter as shown Table 4.3. The mechanical sensitivity has increased to from 0.002  $\mu\text{m}/\text{Pa}$  to 0.007  $\mu\text{m}/\text{Pa}$ . The improvement almost to 3.5 times from the Non-optimized parameter.

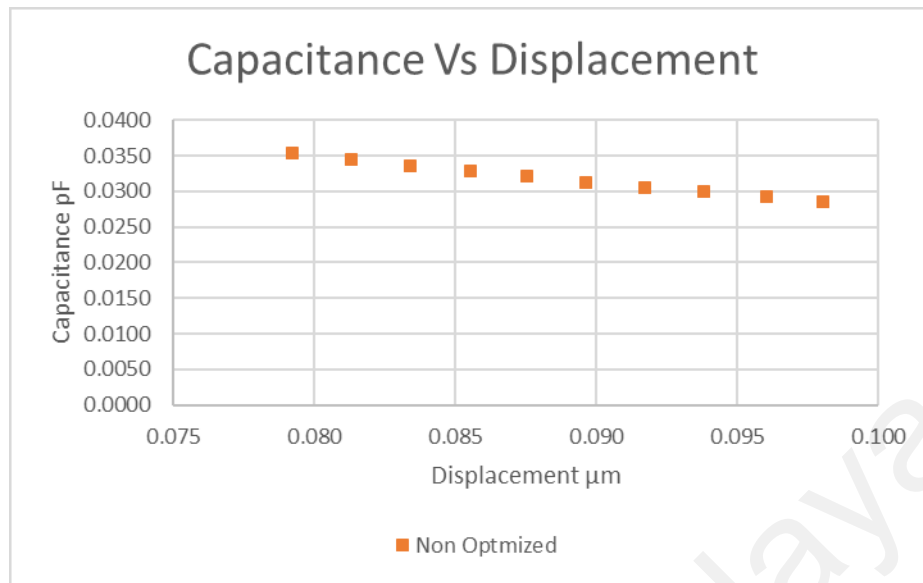


Figure 4. 11 Graph of Capacitance Vs Displacement for Non-Optimized membrane

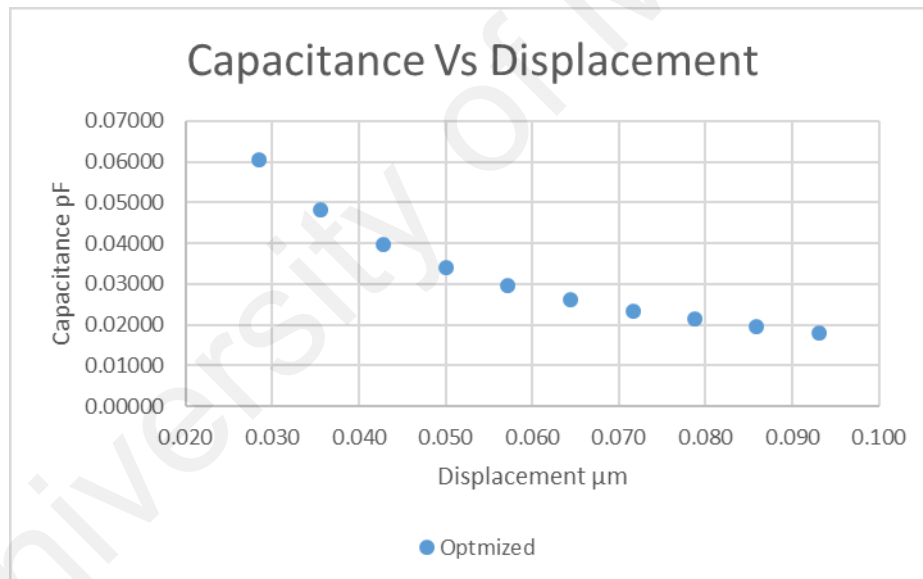


Figure 4. 12 Graph of Capacitance Vs Displacement for Optimized membrane

Based on the above graph the capacitance vs displacement clearly shows the optimized microphone performs nonlinear behavior, while non-optimized membranes exhibit linearity. The linearity achieved from the non-optimized structure is  $0.3 \text{ pF}/\mu\text{m}$ .

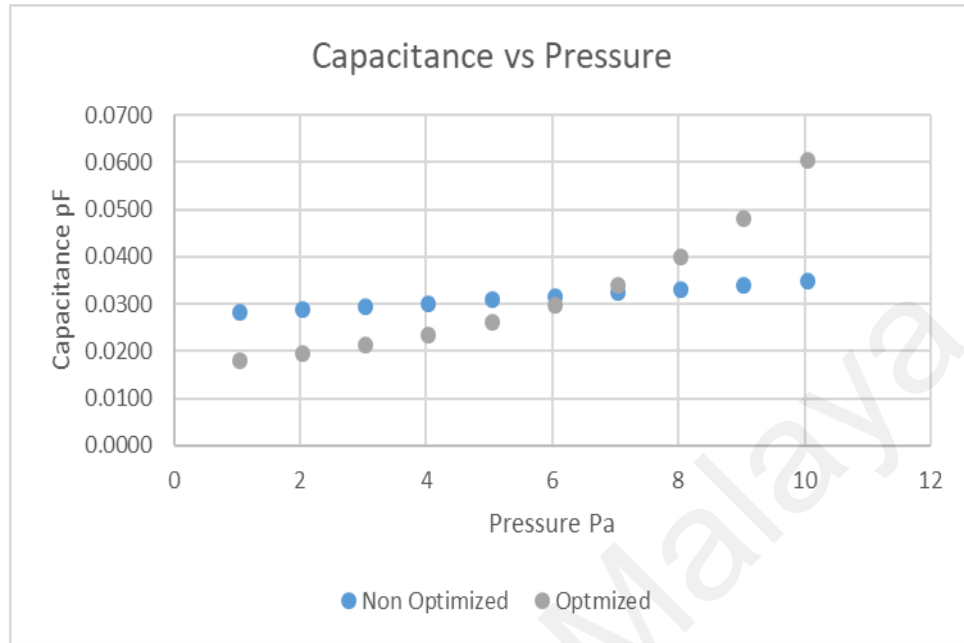


Figure 4. 13 Graph of Capacitance Vs Pressure of Optimized and Non Optimized membrane

Non-optimized membranes its show that the value of capacitance is 0.028pF and the capacitance of the optimized value is 0.018pF at 1pa. However, due to optimized structure performs nonlinear behavior the capacitance of optimized structure is higher at 10 Pa which is 0.061pF and non-optimized structure capacitance at 10 Pa is 0.035 pF.

### 4.1.3 MEMS MICROPHONE STRUCTURE 3

The third comparison structure that will be discussed in this section is from author (Füldner, Dehé, & Lerch, 2005). Its reported mechanical compliance of a spring membrane is inversely proportional to its thickness and its intrinsic stress, spring membranes can be modeled like membranes with full suspension in combination with a design-dependent numerical constant.

Based on the author diaphragm radius of  $100\mu\text{m}$ , diaphragm thickness of  $1\mu\text{m}$  and for corrugated diaphragm. The mechanical sensitivity achieved by the author is for 4 corner supported spring diaphragms is  $0.001\mu\text{m}/\text{Pa}$ .

To improve sensitivity and linearity in this research Taguchi optimization method is used to optimize the parameter such as diameter, thickness, width of support and length of support. The material used for the membranes is polysilicon. In this optimization material property retains the same. Based on the Taguchi optimization Degree of Experiment (DOE) the mean effect plot of graph shows as below.

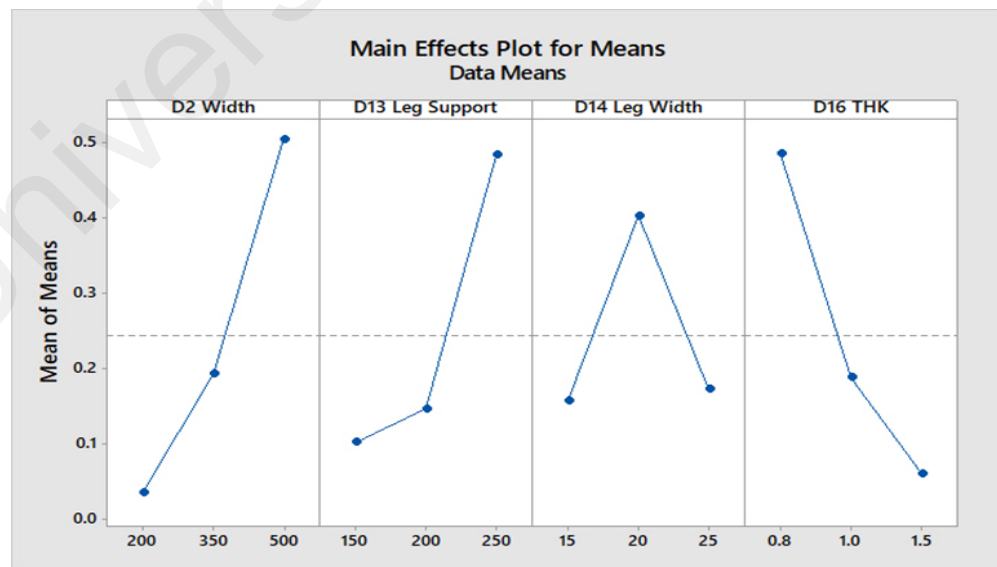


Figure 4. 14 Main effects plot for means for spring supported microphone

The graph of mean effect plot show that the deflection of microphone membranes in Figure 4.3.1 greatly influences the D2 width or diameter at 500 $\mu$ m, thickness of (D16 THK) 0.8 $\mu$ m, D13 Leg support or length of support 250 $\mu$ m and D14 leg width or Spring support width at 20 $\mu$ m. Greatly influences the deflection of the spring diaphragm and noticing that the internal yield stress is are lower than the material yield strength. In this case material which has been used is Polysilicon.

The following discussion are containing of table and graphs for that's shows out come from the optimization process for comparison purpose.

Parameter	Non Optimized	Optimized
D2	100	500
D13	NS 50	250
D14	NS 10	20
D16	1	0.8

Table 4. 5 Numerical value of optimized parameter

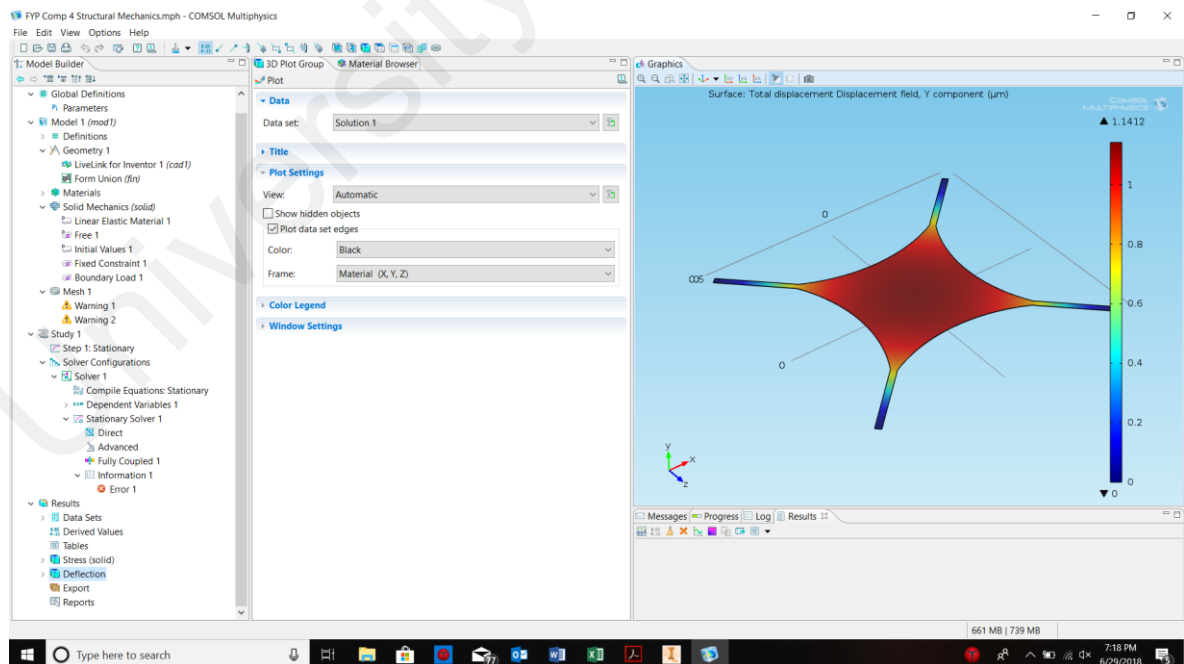


Figure 4. 15 Show the z displacement spring supported membrane

Pressure	Non Optimized	Optimized	Non Optimized	Optimized
	Deflection	Deflection	Sensitivity	Sensitivity
1	0.001	1.14	0.001	1.141
2	0.002	2.28	0.001	1.141
3	0.003	3.42	0.001	1.141
4	0.003	4.56	0.001	1.141
5	0.004	5.71	0.001	1.141
6	0.005	6.85	0.001	1.141
7	0.006	7.99	0.001	1.141
8	0.007	9.13	0.001	1.141
9	0.008	10.27	0.001	1.141
10	0.009	11.41	0.001	1.141

Table 4. 6 Show results of sensitivity of optimized and non-optimized parameter

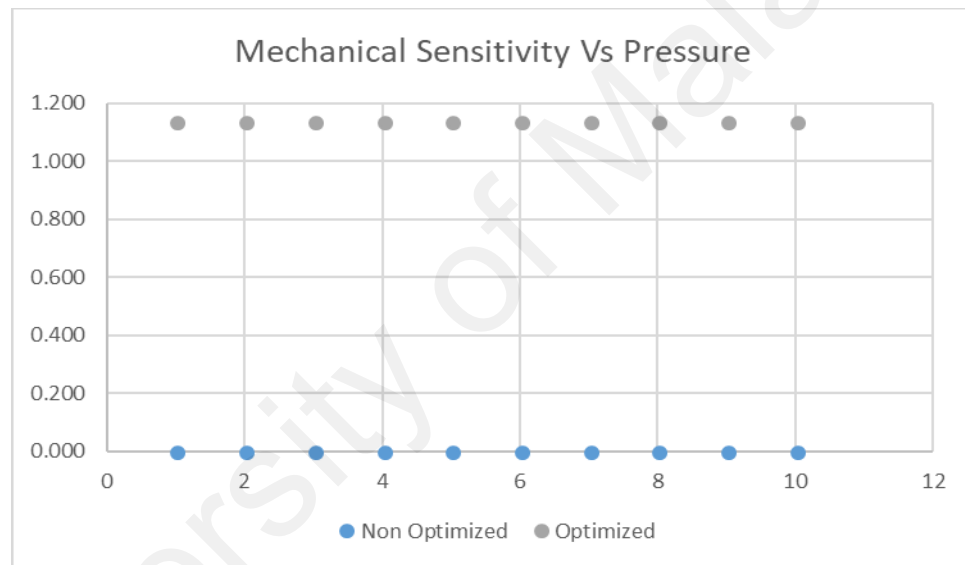


Figure 4. 16 Graph of Mechanical sensitivity vs Pressure

The above the graph in Figure 4.3.3 shows the sensitivity of structure has been improved by changing the diameter 100 $\mu$ m increased to 500 $\mu$ m and thickness from 1 $\mu$ m reduced to 0.8 $\mu$ m, increasing the leg support to 250 $\mu$ m and reducing the support width to 20 $\mu$ m because of the changes the sensitivity has increased to from 0.001  $\mu$ m/Pa to 1.14  $\mu$ m/Pa. The improvement almost to 1140 times from the Non-optimized parameter.

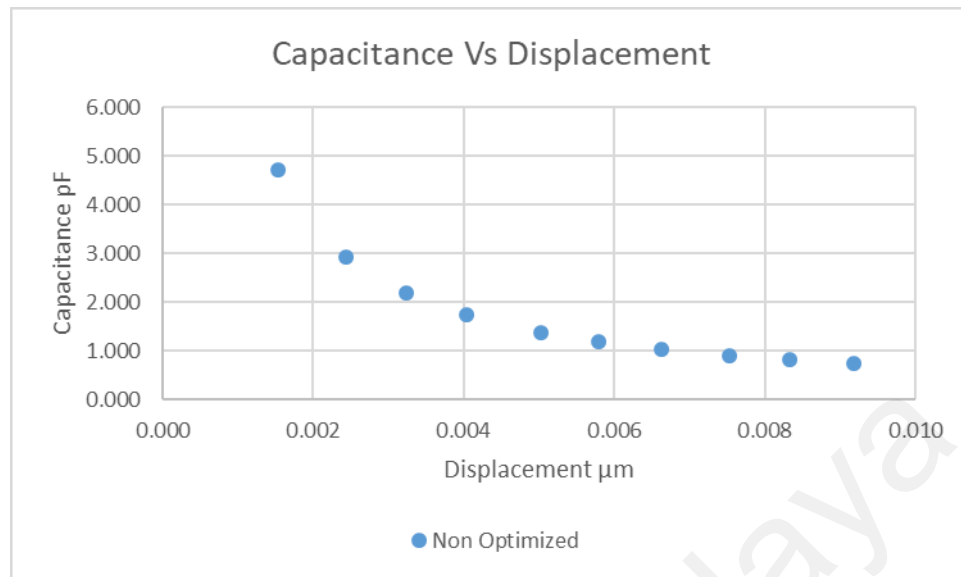


Figure 4. 17 Graph of capacitance vs displacement for non-optimized parameter

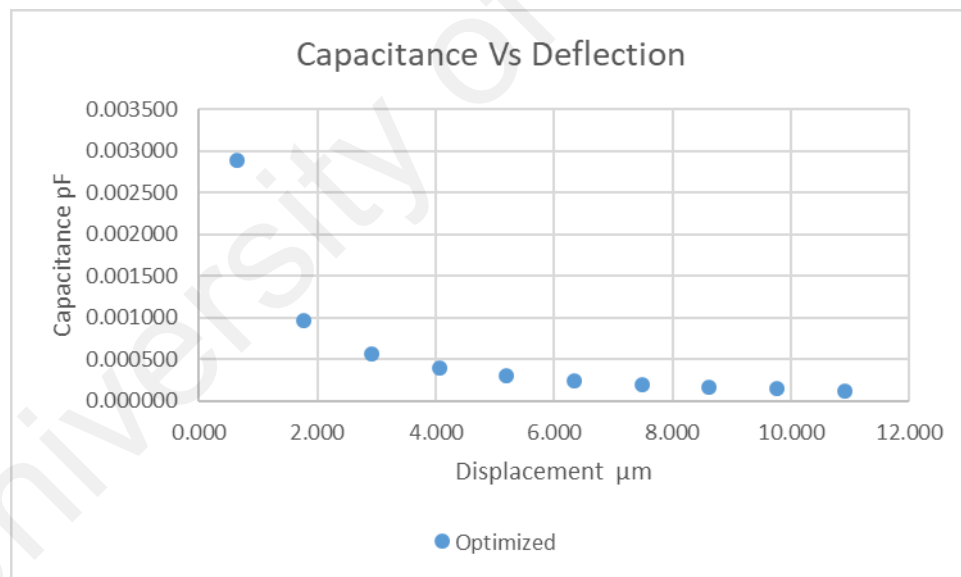


Figure 4. 18 Graph of capacitance vs displacement for optimized parameter

Based on the above graph the capacitance vs displacement of Non-optimized structure and optimized structure show the nonlinear relationship. The linearity of this structure not achieved.



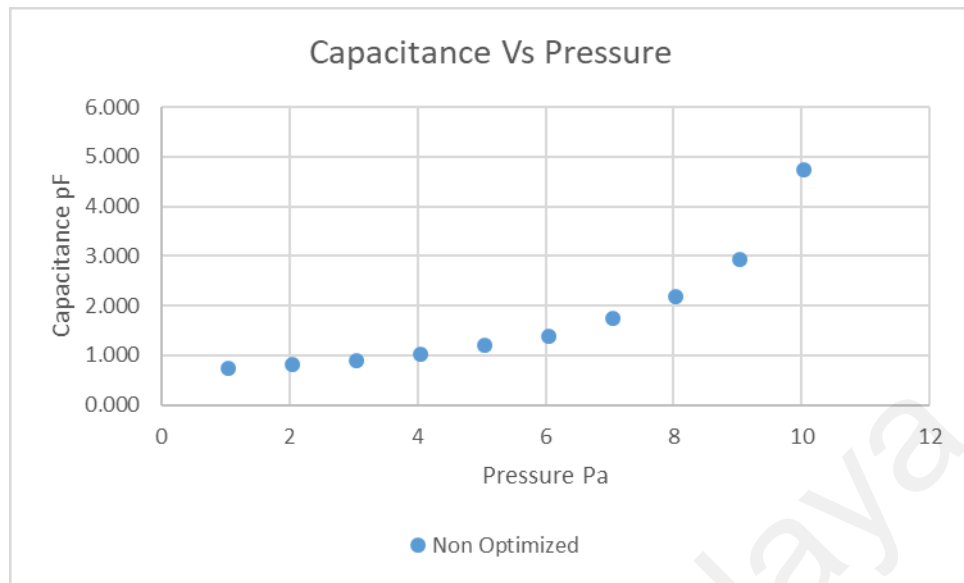


Figure 4. 19 Graph of Capacitance vs Pressure of Non-optimized structure

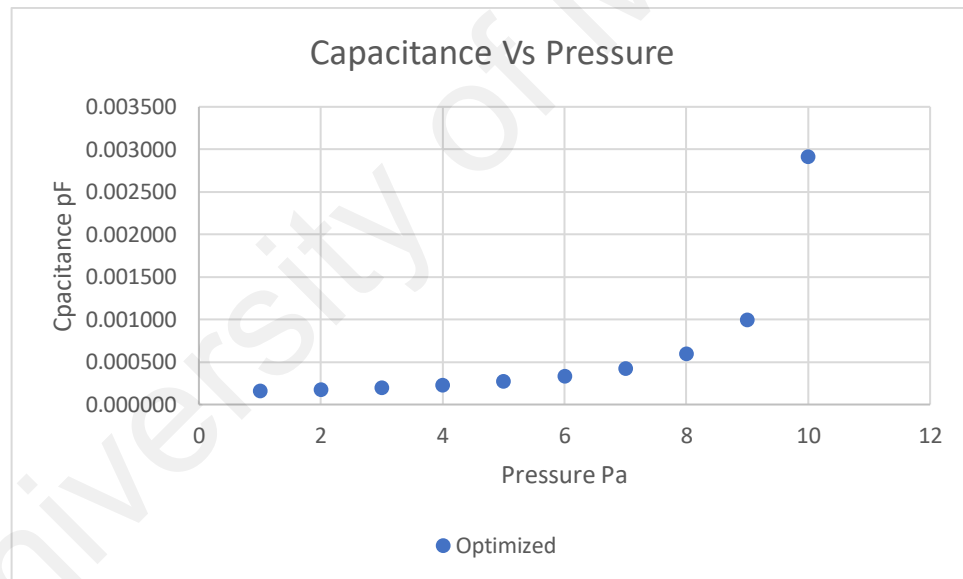


Figure 4. 20 Graph of Capacitance vs Pressure of Non-Optimized structure

Based on the above graph Figure 4.19 and Figure 4.20 clearly shows that non linear relationship between pressure and capacitance for optimized structure and non-optimized structure. However, the capacitance sensitivity has been reduced to from 0.783pF/pa to 0.000158pF/Pa From non-optimized to optimized structure

#### 4.1.4 MEMS MICROPHONE STRUCTURE 4

The fourth optimized structure in this section is from the (Mohamad, Iovenitti, & Vinay, 2007). In his paper it has been clearly analyzed the effect of sensitivity in various diameter and thickness of microphone membranes. The microphone with spring supported diaphragm to further improve condenser microphone performance in terms of sensitivity and frequency response.

It's reported in his work the spring-based condenser microphone design has higher value of mechanical sensitivity compared to the existing edge clamped flat diaphragm condenser MEMS microphone. The spring supported diaphragm is shown to have a flat frequency response up to 7 kHz and more stable under the variations of the diaphragm residual stress.

To improve sensitivity and linearity in this research Taguchi optimization method is used to optimize the parameter such as diameter, thickness, width of support and length of support. The material used for the membranes is polysilicon. In this optimization material property retains the same. Based on the Taguchi optimization Degree of Experiment (DOE) the mean effect plot of graph shows as below.

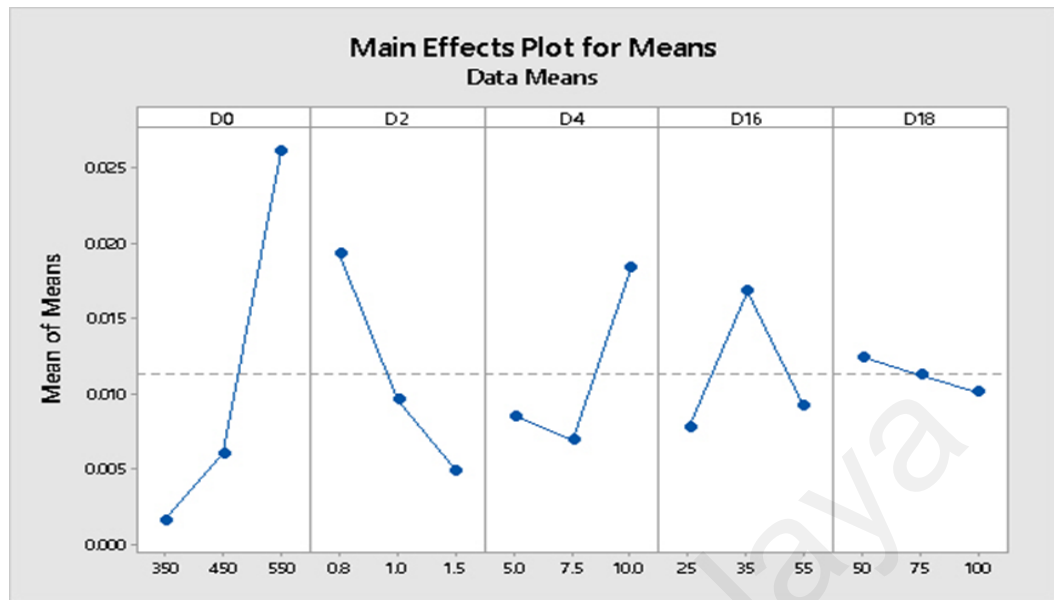


Figure 4. 21 Main effects plot for means for spring condenser microphone

The graph of mean effect plot show that the deflection of condenser spring supported microphone membranes in Figure 4.21. Its influences deflection, the D0 width or diameter at 550 $\mu$ m, thickness of membrane D2 0.8 $\mu$ m, D4 slot hole width 10 $\mu$ m, D16 width of Spring support at 35 $\mu$ m and the space between spring D18 50 $\mu$ m. Its influences the deflection of the spring diaphragm and noticing that the internal yield stress is are lower than the material yield strength. In this case material which has been used is Polysilicon.

The following discussion are containing of table and graphs for that's shows out come from the optimization process for comparison purpose

Parameter	Non Optimized	Optimized
D0	765	550
D2	1.5	0.8
D4	15	10
D16	35	35
D18	100	50

Table 4. 7 Numerical value of optimized parameter

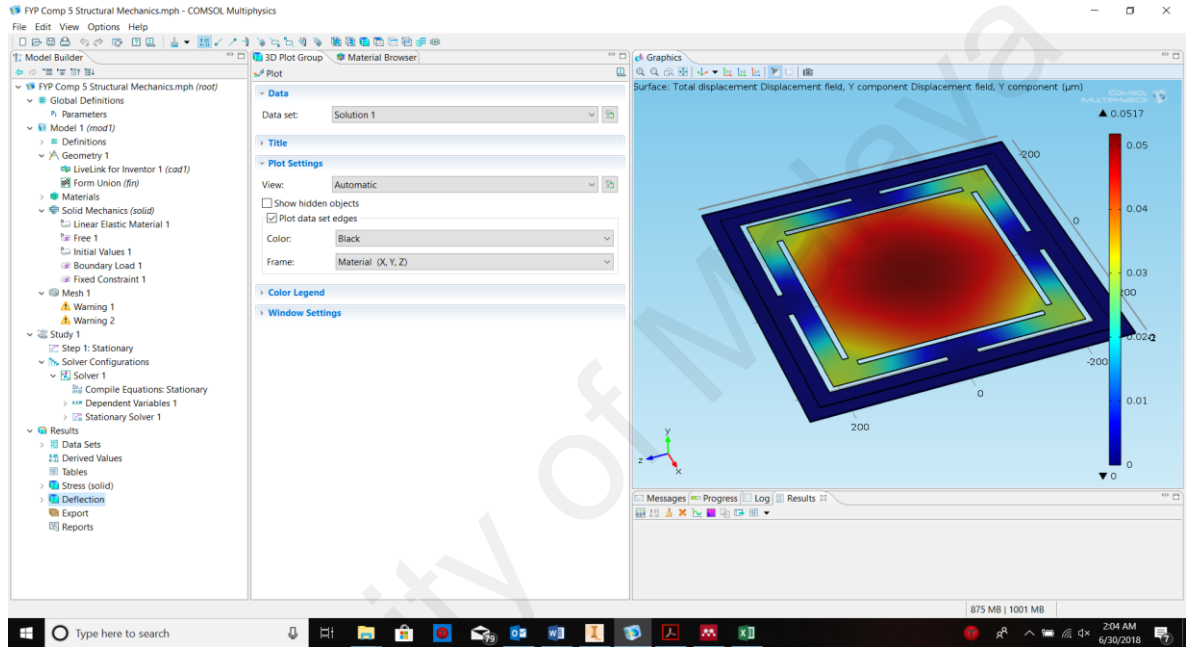


Figure 4. 22 shows y displacement of spring supported membranes

Pressure	Non Optimized	Optimized	Non Optimized	Optimized
	Deflection	Deflection	Sensitivity	Sensitivity
1	0.0509	0.0518	0.0509	0.0518
2	0.1019	0.1036	0.0510	0.0518
3	0.1528	0.1554	0.0509	0.0518
4	0.2037	0.2071	0.0509	0.0518
5	0.2546	0.2589	0.0509	0.0518
6	0.3056	0.3107	0.0509	0.0518
7	0.3565	0.3625	0.0509	0.0518
8	0.4076	0.4143	0.0510	0.0518
9	0.4584	0.4661	0.0509	0.0518
10	0.5093	0.5179	0.0509	0.0518

Table 4. 8 Show results of sensitivity of optimized and non-optimized parameter

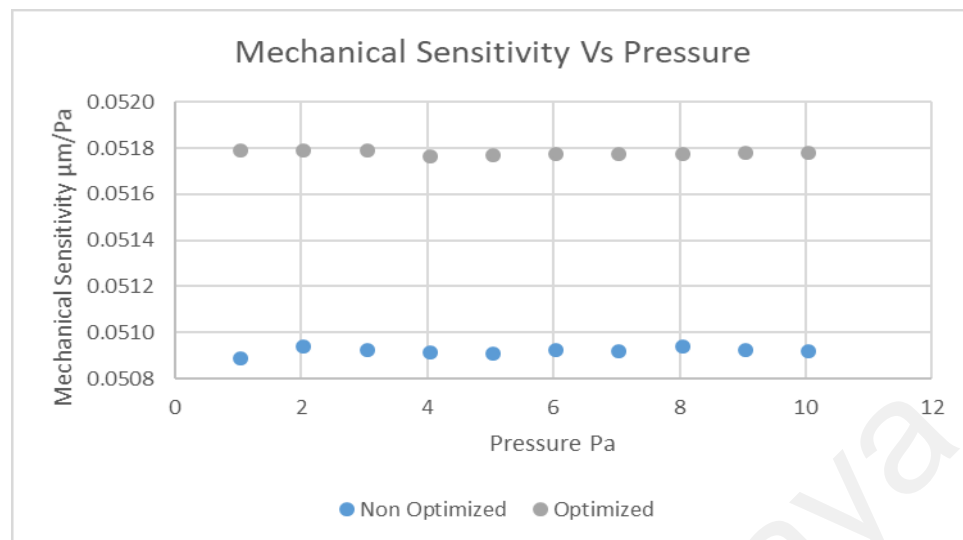


Figure 4. 23 show Graph of Mechanical sensitivity vs Pressure

The above the graph in Figure 4.23 shows the sensitivity of structure has been improved by changing the width of square membrane from 765μm reduced down 550μm and thickness from 1.5 μm reduced to 0.8μm, maintaining the spring width 35μm as a result of the sensitivity has increased to from 0.0508μm/Pa to 0.0518 μm/Pa. Even though the sensitivity only improved slightly but the surface area almost 52.5% has been reduced. The sensitivity improvement almost to 1.02 times from the Non-optimized parameter.

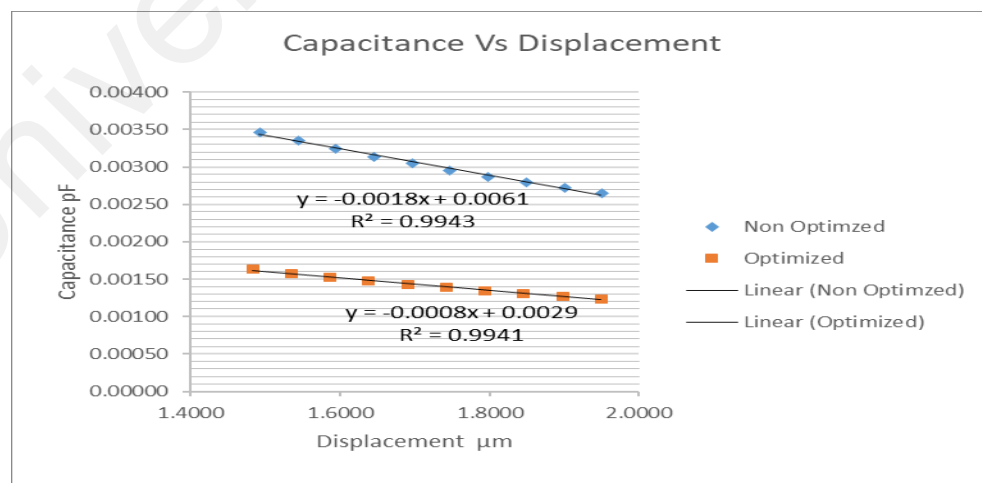


Figure 4. 24 Graph of capacitance vs displacement for non-optimized and optimized structure

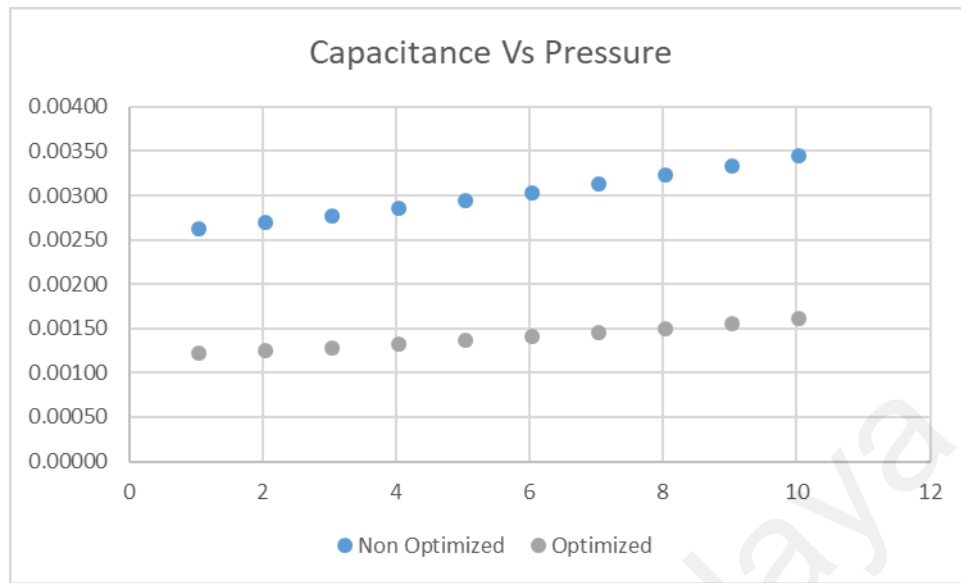


Figure 4. 25 Graph of capacitance vs pressure of non-optimized and optimized structure

The above graph figure 4.25 describes the capacitance vs capacitance of Non-optimized and optimized membranes. Its show that the maximum value of capacitance for non-optimized structure is 0.00266pF and the maximum capacitance of the optimized value is 0.00125pF. The capacitance has successfully reduced almost 2.12 times of Non-optimized parameter.

Figure 4.24 shows the graph of capacitance vs displacement its clearly indicating the linearity of optimized and non-optimized microphone membranes. The linearity of optimized structure is reduced compared to Non-optimized structure this is due to the sized of the structure is been reduced thus gives significant impact in linearity. However the achieved linearity based on optimized structure is 0.0008 pF/ $\mu$ m

#### 4.1.5 MEMS MICROPHONE PROPOSED STRUCTURE

As a last structure to be optimized and analyze before to the comparison table. Proposing a new structure like existing structure. It's a spring-based cantilever support structure. The Figure 4.26 show the structure dimension for the further understanding.

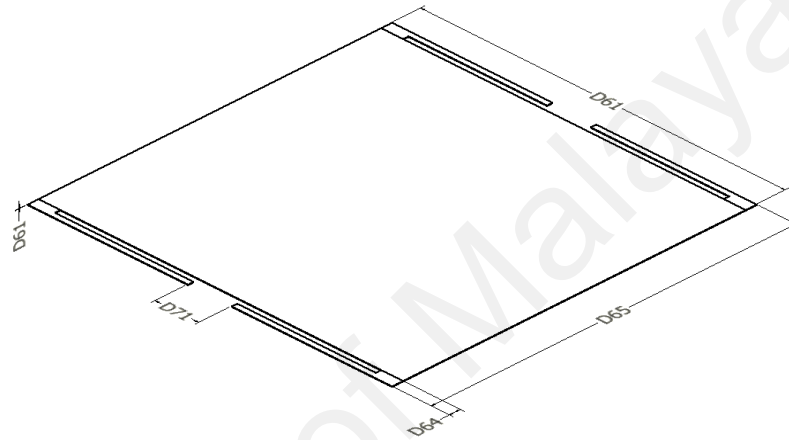


Figure 4. 26 Proposed structure design dimension

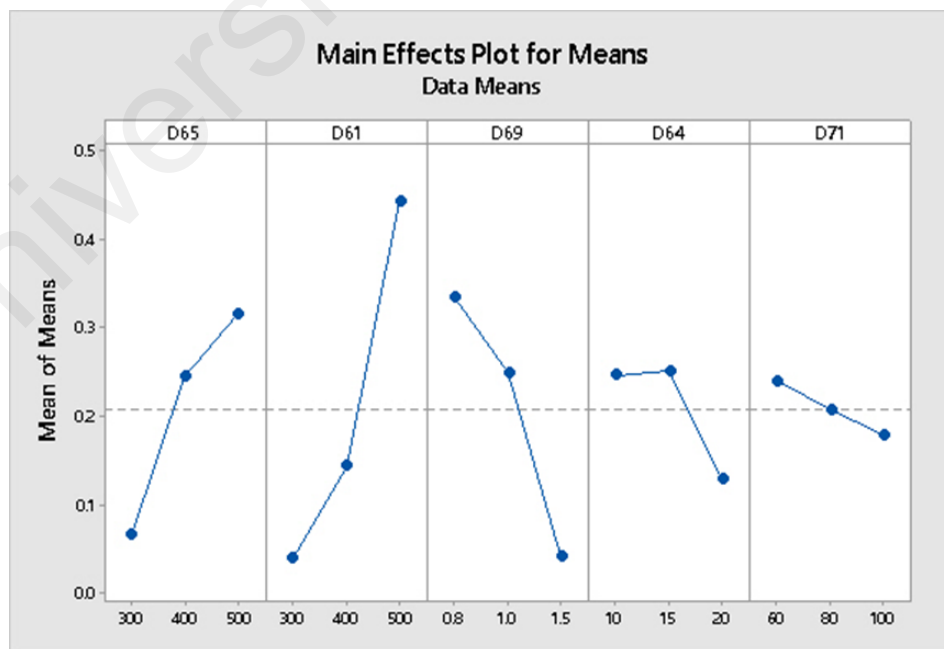


Figure 4. 27 Main effects plot for means for proposed design

The graph of mean effect plot show that the deflection of condenser spring supported microphone membranes in Figure 4.27. Its greatly influences the D65 width at 500 $\mu$ m and D61 the length of diaphragm 500 $\mu$ m, thickness of membrane represents in D69 and its 0.8 $\mu$ m, D64 separation space between support and diaphragm 15 $\mu$ m, D71 distance of between support at 60 $\mu$ m. The parameter selected influences the deflection of the spring diaphragm and noticing that the internal yield stress is are lower than the material yield strength. In this case material which has been used is Polysilicon.

The following discussion are containing of table and graphs for that's shows outcome from the optimization process for comparison purpose

Parameter	Optimized
D65	500
D61	500
D69	0.8
D64	10
D71	60

Table 4. 9 Optimized parameter of the proposed Design

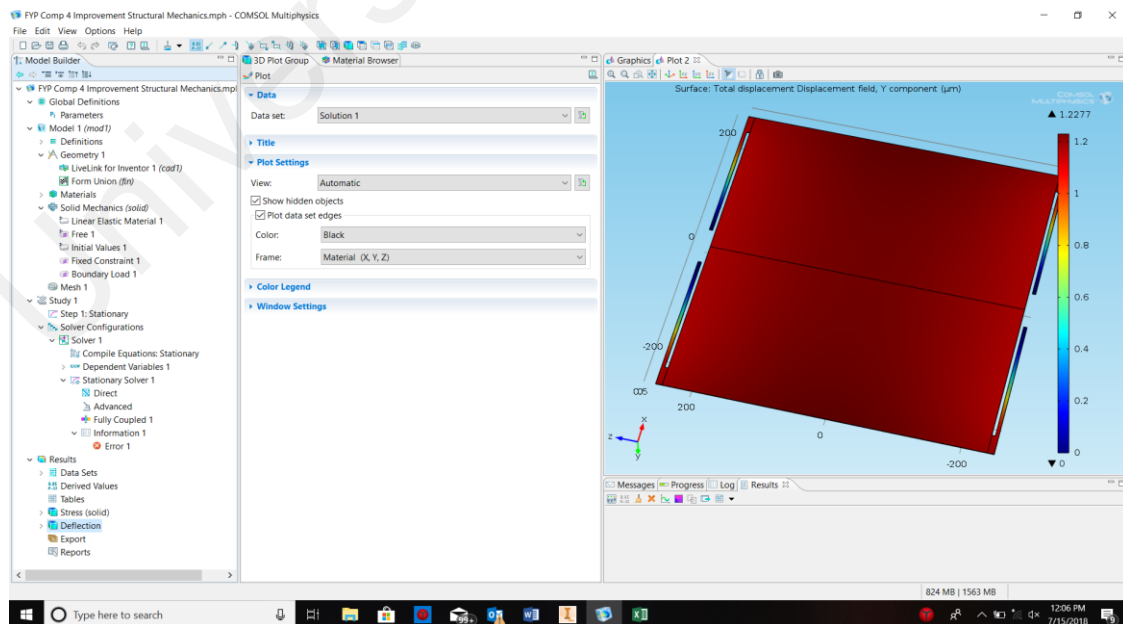


Figure 4. 28 shows y displacement of proposed design



Pressure	Optimized	Optimized	Optimized	Optimized
	Deflection	Sensitivity	Capacitance pF	Linearity
1	1.228	1.228	0.001764	0.001437
2	2.455	1.228	0.000882	0.000359
3	3.683	1.228	0.000588	0.000160
4	4.911	1.228	0.000441	0.000090
5	6.139	1.228	0.000353	0.000057
6	7.366	1.228	0.000294	0.000040
7	8.594	1.228	0.000252	0.000029
8	9.822	1.228	0.000220	0.000022
9	11.049	1.228	0.000196	0.000018
10	12.277	1.228	0.000176	0.000014

Table 4. 10 shows the results of sensitivity, capacitance and linearity

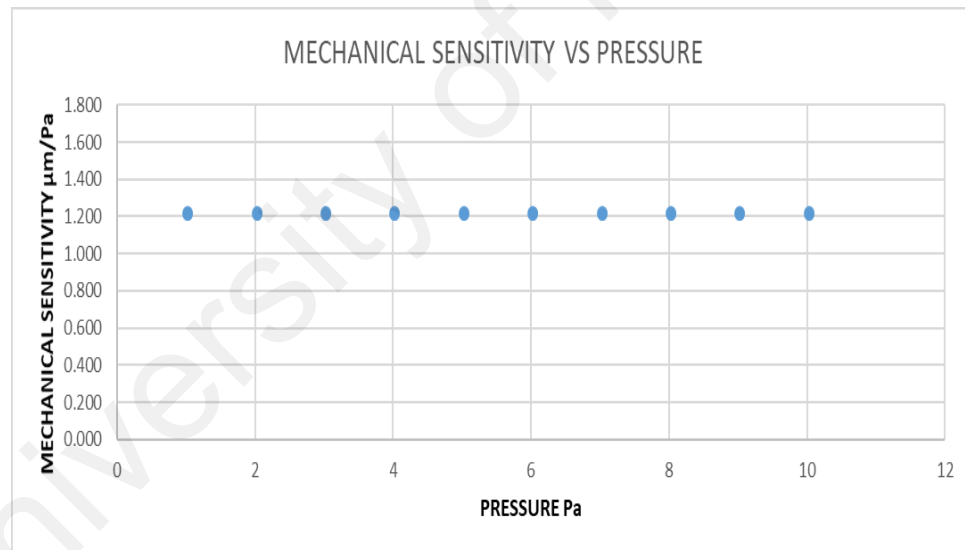


Figure 4. 29 show the graph of mechanical sensitivity vs pressure

The above the graph in Figure 4.29 shows the sensitivity of structure has which is 1.228μm/Pa. The parameter has been optimized to get best outcome from the structure.

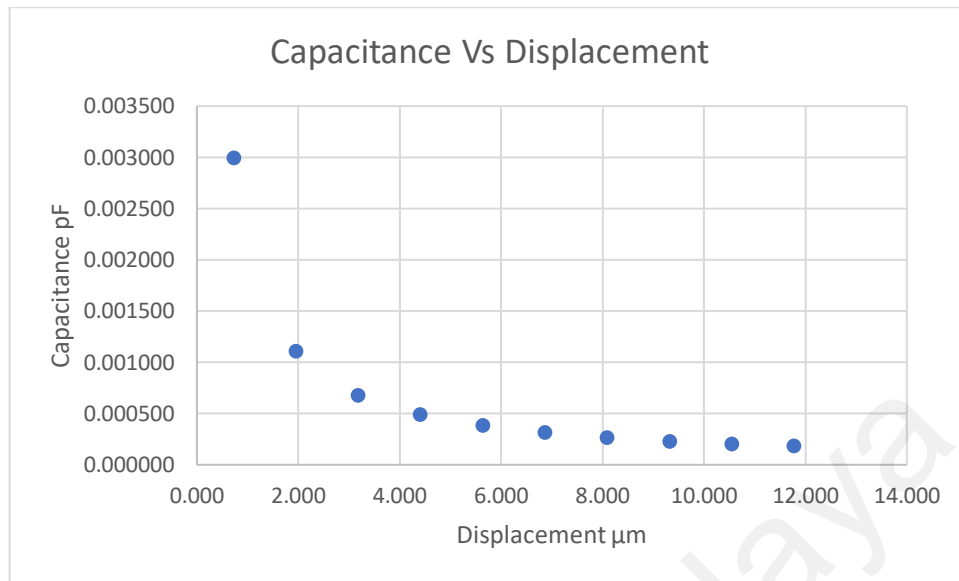


Figure 4. 30 Shows the graph of capacitance vs displacement

The above graph describes the capacitance vs displacement of optimized membranes. Its show that the maximum value of capacitance is 0.003pF. The other fact of graph of capacitance vs displacement its clearly indicating the linearity of its doesn't achieve linearity due to the nonlinear behavior of the structure.

## 4.2 DETERMINATION OF SUITABLE STRUCTURE CI

As a continuation from the above section 4.1 Analysis of Sensitivity and linearity. This section presents tabulation of results from the above section 4.1 as in terms of important parameter to proceed for next phase of analysis which is of eigen frequency and sensitivity and linearity analysis for determination of suitable dimension of each array. Referring to section 3.3.5 its clearly stated the selection criteria is based on the mechanical sensitivity of structure.

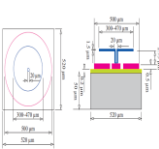
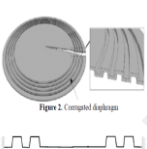

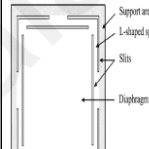
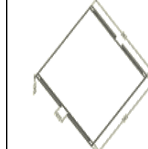
RESULTS OF ANALYSIS OF LINEARITY AND SENSITIVITY						
Structure Figures						
No	Specification	Structure 1	Structure 2	Structure 3	Structure 4	Proposed Design
1	Mechanical Sensitivity $\mu\text{m}/\text{Pa}$	0.06600	0.00700	1.14100	0.05180	1.22770
2	Capacitive Sensitivity $\text{pF}/\text{Pa}$	0.00060	0.01853	0.00016	0.00125	0.00018
3	linearity $\text{pF}/\mu\text{m}$	0.00030	Non Linear	Non Linear	0.00080	Non Linear
4	Capacitance $\text{pF}$	0.00060	0.01850	0.00016	0.00125	0.00018
5	Deflection @ 1 Pa $\mu\text{m}$	0.06600	0.00700	1.14100	0.05180	1.22770

Table 4. 11 Table of Comparison

Table 4.11 shows the Comparison of the results of mechanical sensitivity, capacitive sensitivity, Linearity, Capacitance and deflection of membrane @ 1Pa. The highest mechanical sensitivity and the deflection is from the proposed design.

Even though the four other structure can optimize but proposed design shows good performances in-terms of listed specification in above Figure 4.11 Table of comparison. However, the structure 3 requires large area to resonate at lowest frequency which is 500Hz for about 10 arrays with different frequency unable to achieve with smallest arrays.

In this research our focus is to produce smallest microphone array as well as highest mechanical sensitivity. The suitable structure which can proceed for further analysis is proposed design. As the objective of this research is to improve sensitivity and linearity for cochlear implants. Based on this proposed design can proceed for further Eigen frequency analysis for 10 number of arrays and identifies the geometric dimension suitable for implementation of structures.

University of Malaya

### **4.3 ANALYSIS EIGENFREQUENCY OF EACH ARRAY**

#### **4.3.1 INTRODUCTION**

In this section the proposed structure will go further optimization to get the dimensional relationship with required frequency. As stated in our targeted design specification in Table 3.1 the overall 10 arrays layout required arranged in  $3 \times 3 \text{mm}^2$  or even lesser. This is will lead to reduction in space. Our targeted frequency range to be achieve is from 500Hz to 5000Hz.

Estimated increment of frequency between each array is approximately 500Hz. After this Eigen frequency analysis each structure will go for structural analysis to get sensitivity and linearity of the structure as respect to each structure dimension. The final sensitivity and linearity will be based on analysis of each array.

#### **4.3.2 TAGUCHI METHOD OF ARRAY FOR GEOMETRIC ANALYSIS**

Referring on the section 4.1.5 the proposed design is exhibits highest deflection and lowest capacitance. In this section will again modify the structure accordingly to meets frequency required by the cochlear implant which is targeted from 500Hz to 5000Hz. To obtain and understand structure behavior Taguchi method used to identify the correlation between stated dimensional parameter and frequency.

The Table 4.12 and Figure 4.31 below show the analysis of dimensional parameter and simulated frequency response.

DOE OPTIMIZATION BY TAGUCHI METHOD FOR PROPOSED DESIGN FOR FREQUENCY				
D61	D64	D65	D71	Simulated Frequency Hz
800	15	250	100	2304
800	20	300	250	3502
800	25	350	400	5426
800	30	400	550	6720
1000	15	300	400	2361
1000	20	250	550	4042
1000	25	400	100	1378
1000	30	350	250	2153
1200	15	350	550	1712
1200	20	400	400	1354
1200	25	250	250	1504
1200	30	300	100	1911
1350	15	400	250	679
1350	20	350	100	688
1350	25	300	550	1631
1350	30	250	400	1564

Table 4. 12 Taguchi optimization array matrix for proposed design

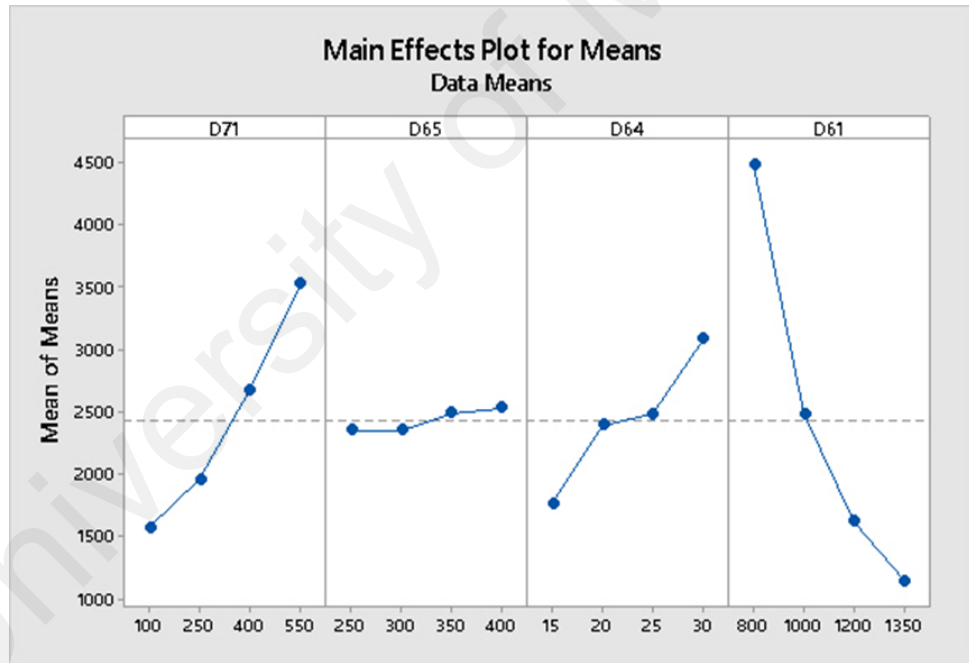


Figure 4. 31 Main effects plot for means of proposed design Eigen frequency

Based on the analysis, D71 is the separation between two cantilever spring type support it's clearly show that, the smaller separation between both support its resulted in lowest frequency and highest separation distance resulted in largest frequency. D65 is the

width of diaphragm as it doesn't make much contribution in resulting the high and low frequency. D64 is the space between the structure and support, its show the greater the space larger the distance, width of spring support is also  $1/2$  D64. To reduce the complication of the analysis the width of spring kept fixed. The length of diaphragm is indicated by the D61. Its resulting in smaller the length diaphragm larger the frequency and vice versa

#### **4.3.3 EIGEN FREQUENCY ANALYSIS OF EACH ARRAYS**

To achieve targeted design specification based on the Table 3.1. There is a limitation on the size of layout arrays in this research our objective is to achieve 10 number of arrays in 3.00mm of layout width. Each microphone diaphragm arrays are equally shared the width of layout. Thus, resulted in 300 $\mu$ m (D65). The other dimensional parameter is adjusted to accordingly for frequency specified.

The following below figures 4.32 to 4.41 show results of Eigen frequency studies of each arrays from COMSOL Multiphysics 4.3a. The frequency analyzed between 500 Hz to 5000Hz.

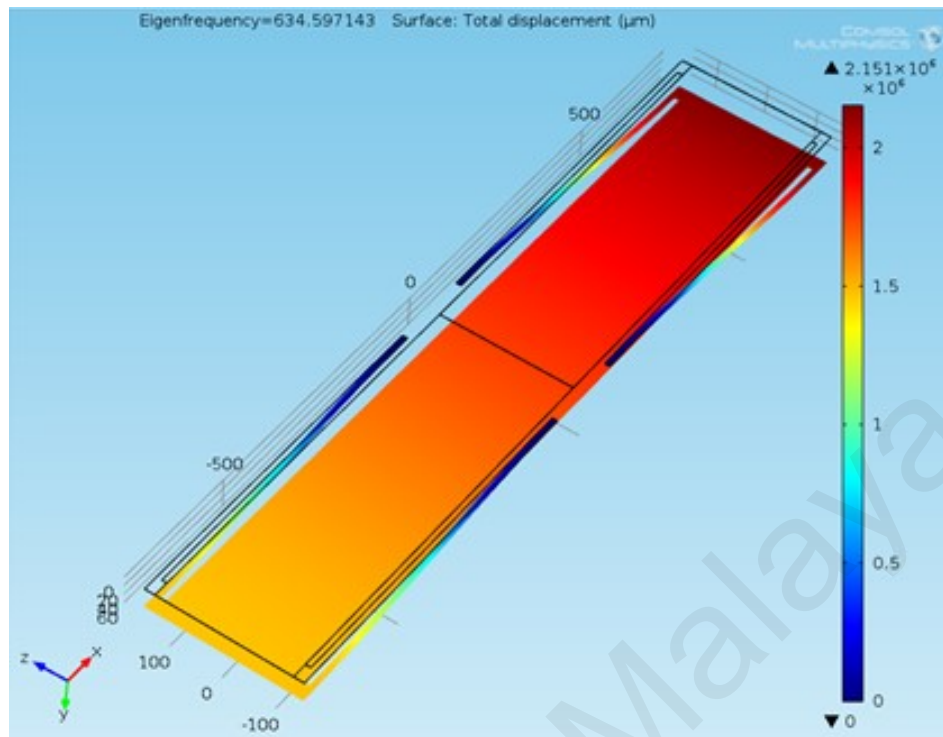


Figure 4. 32 Microphone array 1 Eigenfrequency @635Hz

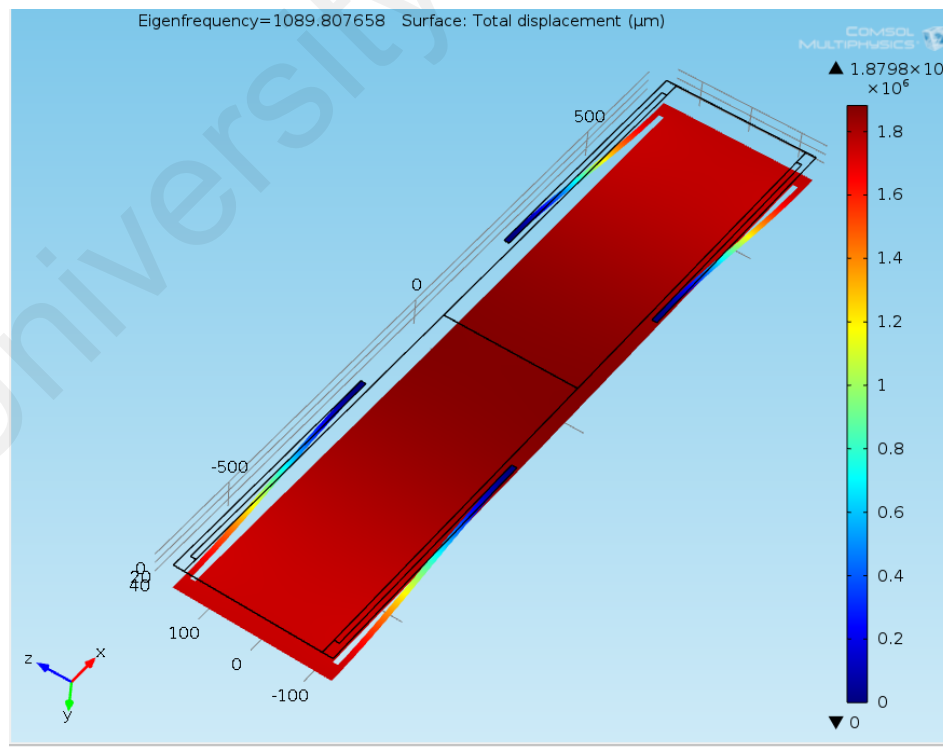


Figure 4. 33 Microphone array 2 eigenfrequency @1000Hz



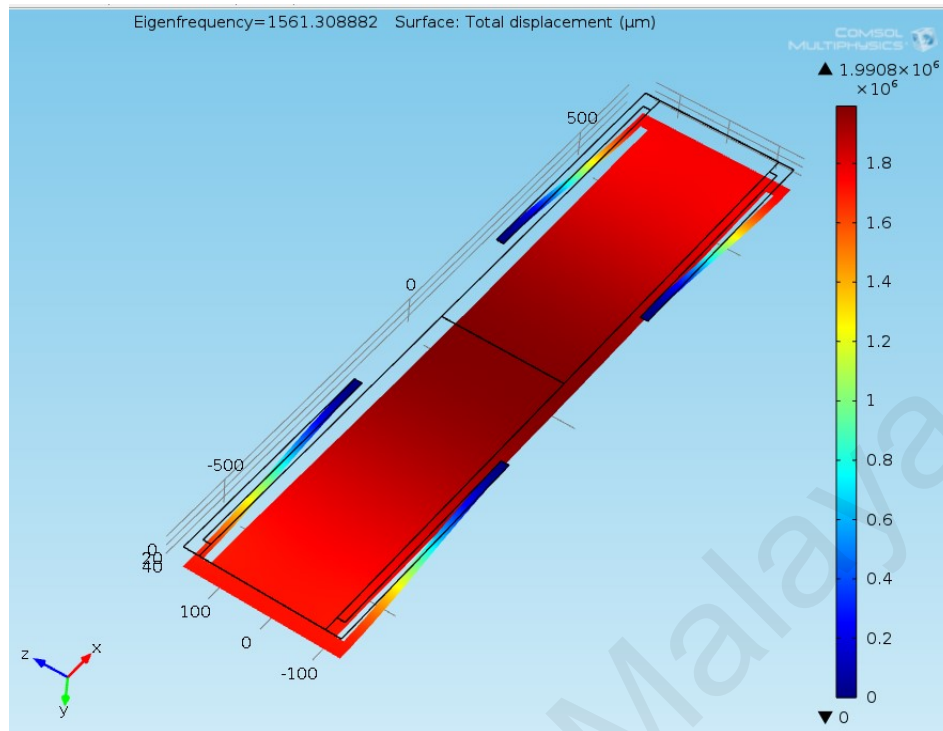


Figure 4. 34 Microphone array 3 eigenfrequency @1500Hz

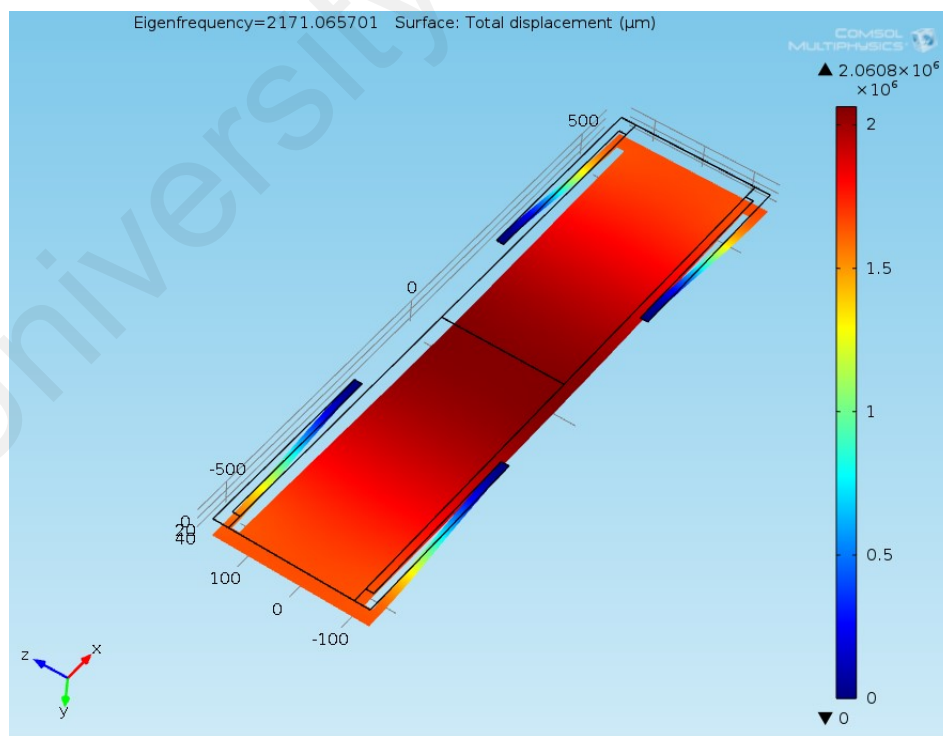


Figure 4. 35 Microphone array 4 eigenfrequency @2000Hz

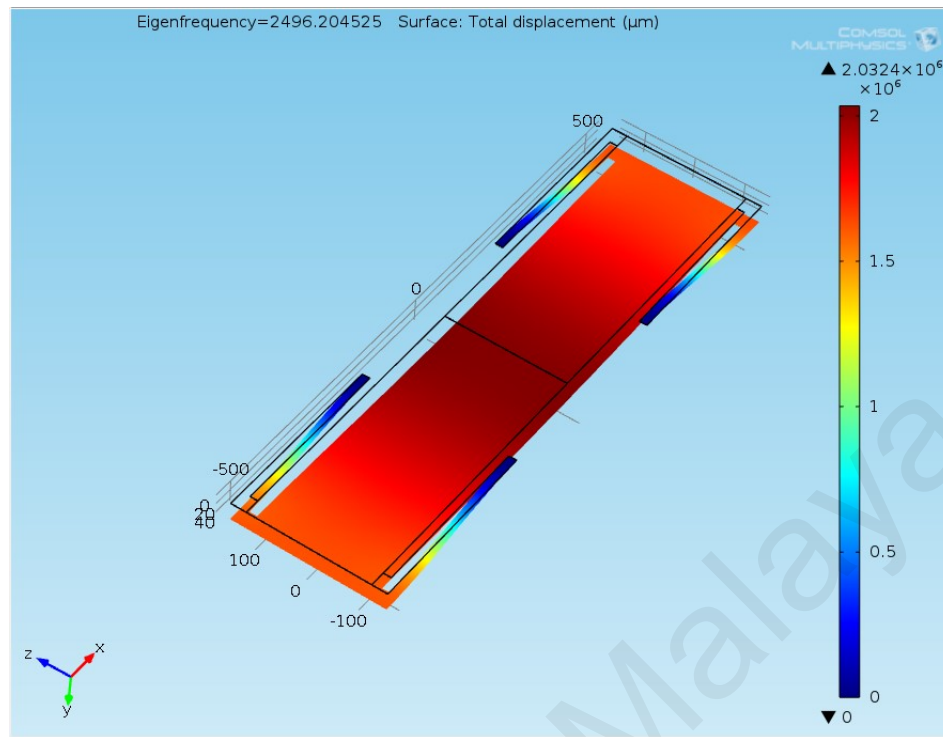


Figure 4. 36 Microphone array 5 eigenfrequency @2500Hz

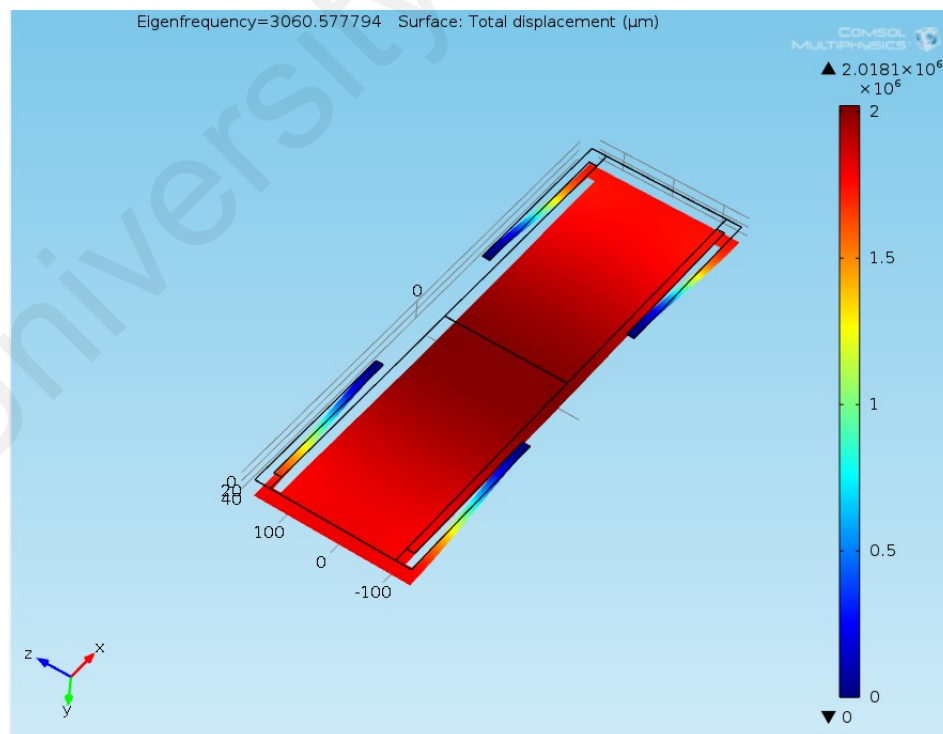


Figure 4. 37 Microphone array 6 eigenfrequency @3000Hz

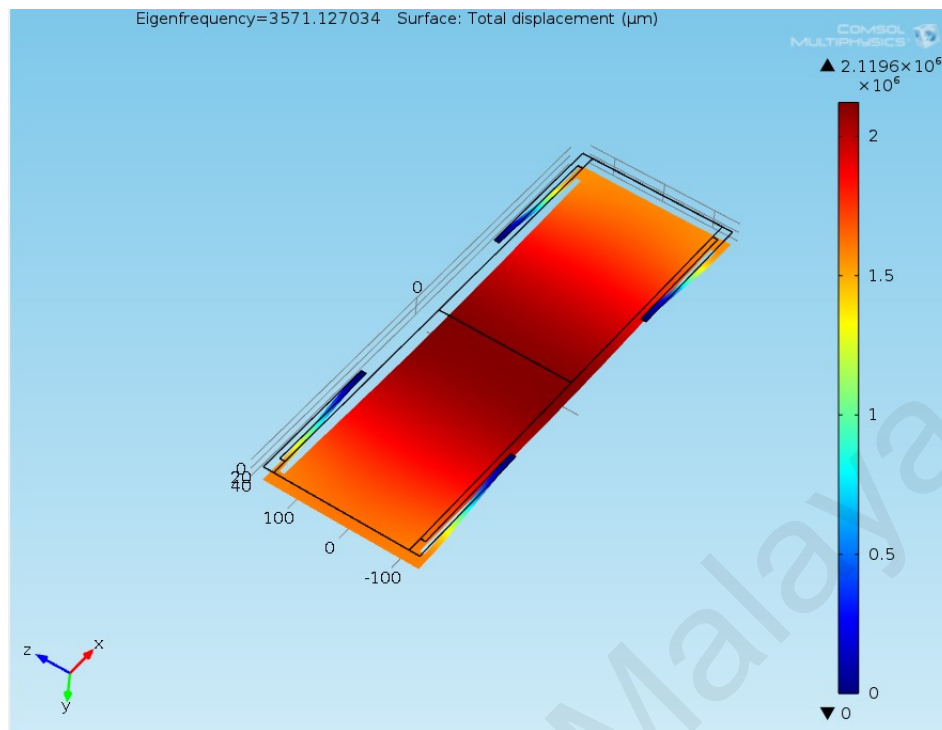


Figure 4. 38 Microphone array 7 eigenfrequency @3500Hz

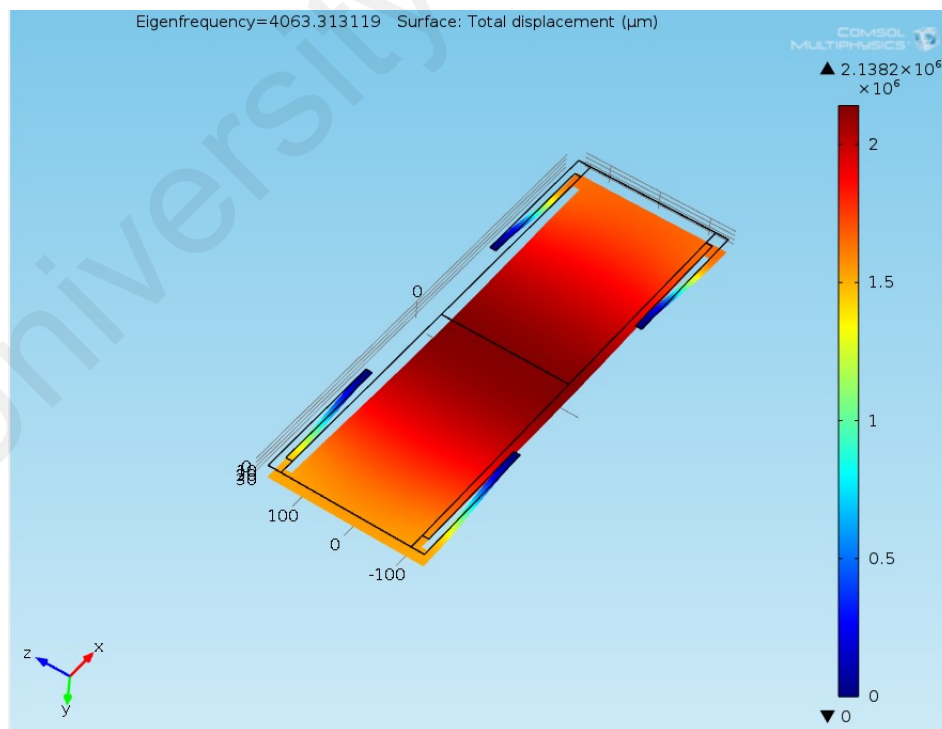


Figure 4. 39 Microphone array 8 eigenfrequency @4000Hz

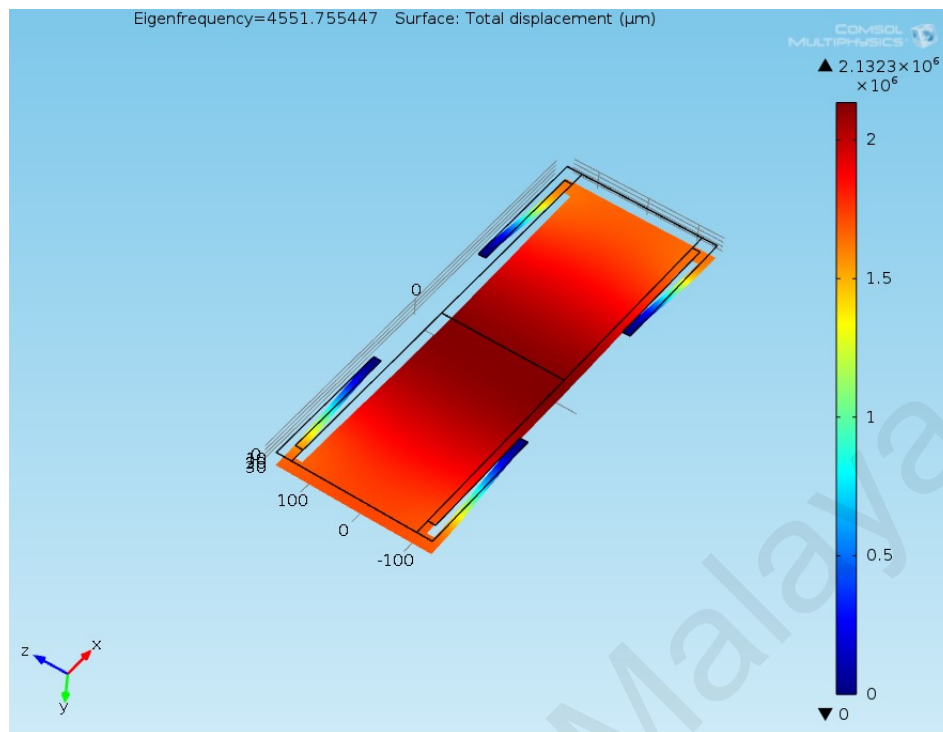


Figure 4. 40 Microphone array 9 eigenfrequency @4500Hz

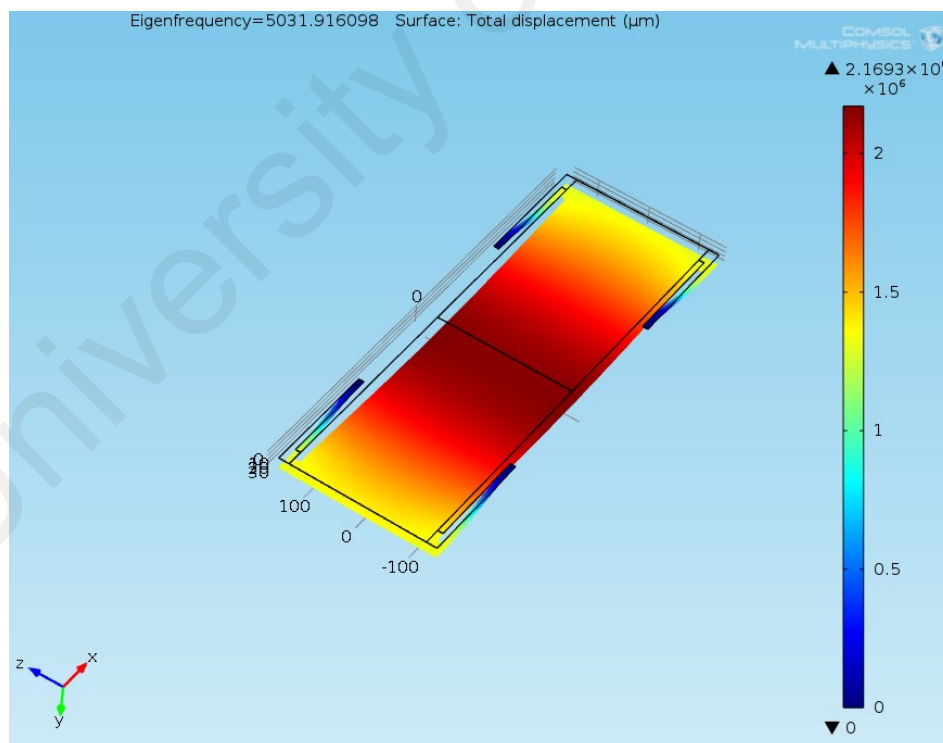


Figure 4. 41 Microphone array 10 eigenfrequency @5030Hz

The internal stress of each arrays is important to analyze due to safety measurement on yield stress of structure. The yield stress of the structure must be lower than yield strength of polysilicon. The Figure 4.42 shows the histogram of internal stress of each array in relation to response frequency. Based on the histogram, it's been shows the structure which has higher internal stress has ability to resonance at lower frequency.

The internal stress of structure is higher in Array 1 @ 635 Hz this is because the separation between the support D71 is smaller and length of structure is D61 is larger compare other arrays this results in spring support length is longer.

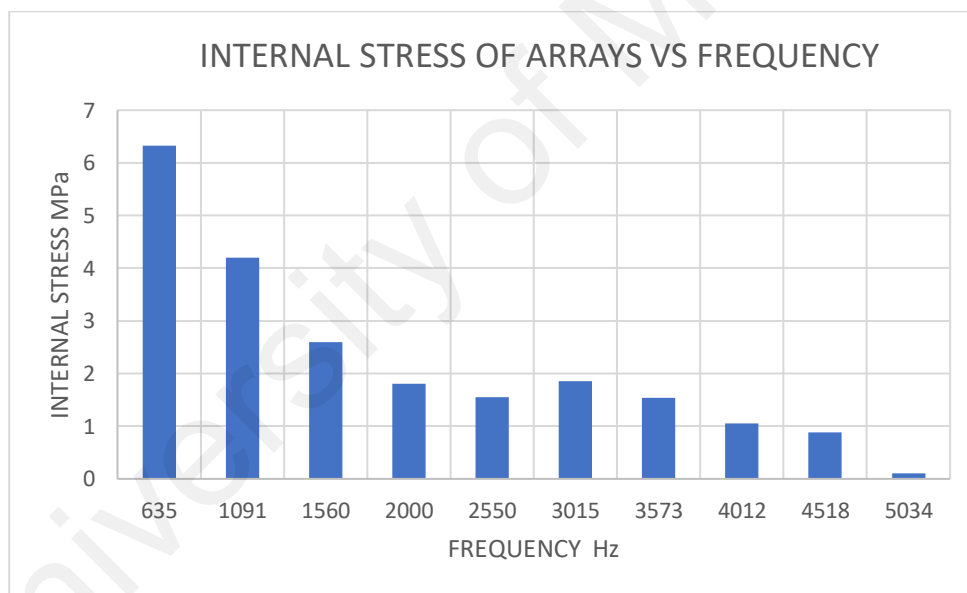


Figure 4. 42 Histogram of internal stress vs frequency

Below the Figure 4.43 The graph of spring constant vs frequency indicating the spring constant relationship between frequency. As a result, its clearly shows that lower spring constant value will able to resonate at lowest frequency. In this research the lowest spring constant (K N/m) achieved at 635Hz about 0.012 N/m. The highest spring constant (K N/m) achieved at 5034Hz about 0.351 N/m

SPRING CONSTANT VALUE OF EACH ARRAY AT RESPECTED FREQUENCY				
ARRAYS	K (N/m)	THEORITICAL FREQUENCY	SIMULATED FREQUENCY	ERROR PERCENTAGE
1	0.012	622	635	2.1
2	0.032	1073	1091	1.6
3	0.057	1515	1560	2.9
4	0.083	1953	2000	2.4
5	0.127	2490	2550	2.3
6	0.152	2837	3015	5.9
7	0.197	3319	3573	7.1
8	0.236	3731	4012	7.0
9	0.281	4234	4518	6.3
10	0.351	4710	5034	6.4

Table 4. 13 Spring constant value and frequency obtained

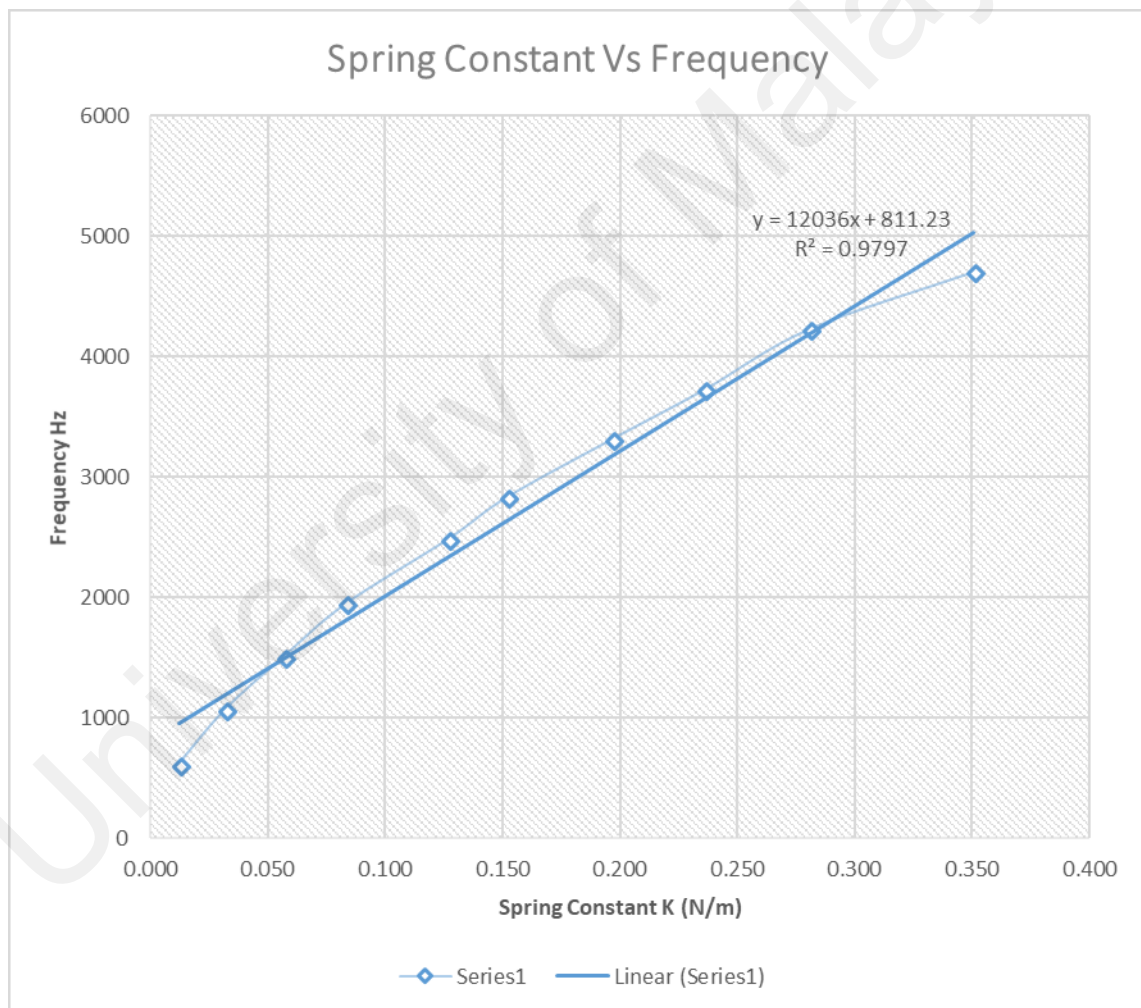


Figure 4. 43 The graph of spring constant vs frequency

#### 4.4 ANALYSIS OF SENSITIVITY AND LINEARITY OF EACH ARRAY

The following below Figures 4.44 to 4.53 show results of structural studies of each array from COMSOL Multiphysics 4.3a. The deflection of membrane analyzed from arrays 1 to array 10. The dimension of each arrays is based on the outcome of the Eigen frequency of each arrays.

Since the Eigen frequency analysis outcome are between the targeted frequencies based on section 3.3.2. The below following figure 4.44 to 4.53 are the result of y axis displacement of each array structure at 60dB which is 0.02Pa based on normal conversion.

Followed by the result of each arrays Y axis displacement. Figure 4.54 to 4.63 will show the graph of Capacitance Vs Displacement of each array for a better understanding of linearity achieved by each array, Figure 4.64 and Figure 4.65 will show the graph of mechanical sensitivity Vs Pressure of all the arrays and the graph of capacitance Vs pressure of all the arrays which has been developed.

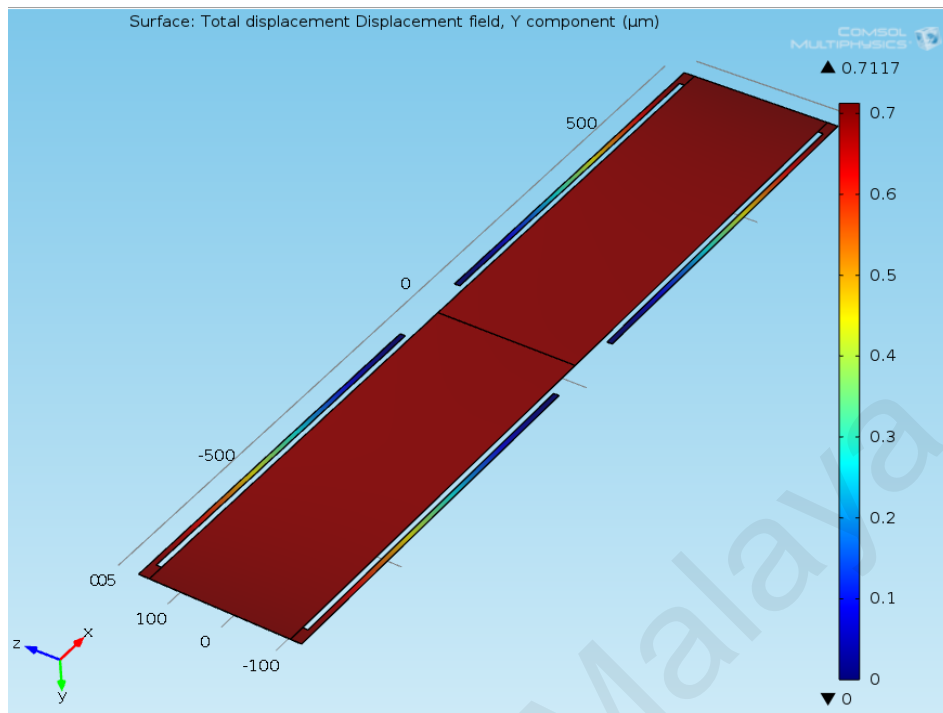


Figure 4. 44 Shows y displacement of Array 1

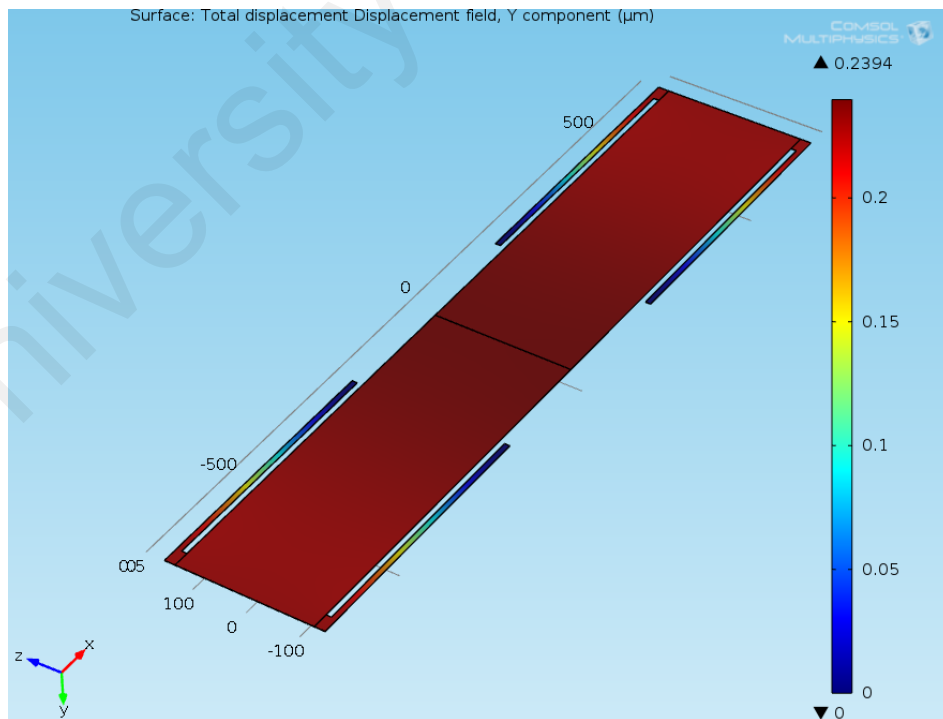


Figure 4. 45 Shows y displacement of Array 2



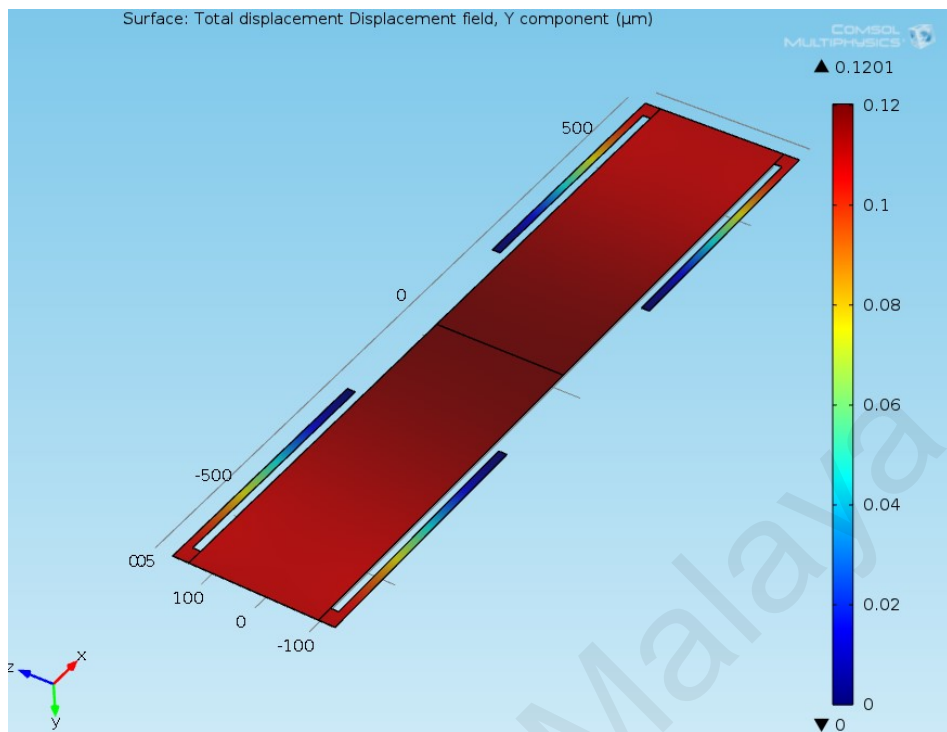


Figure 4. 46 Shows y displacement of Array 3

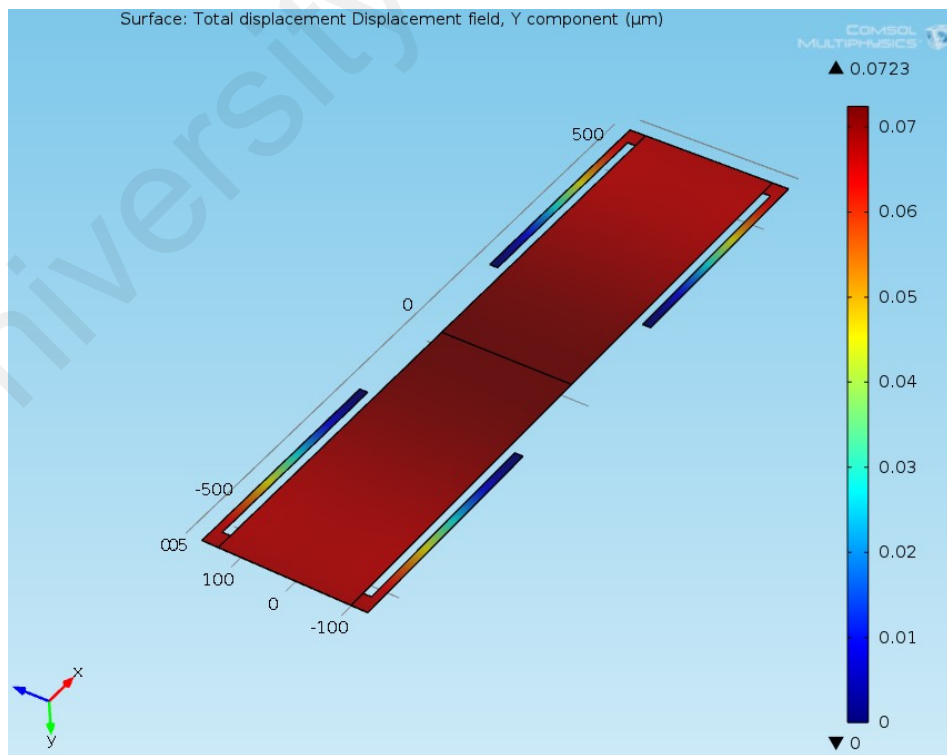


Figure 4. 47 Shows y displacement of Array 4

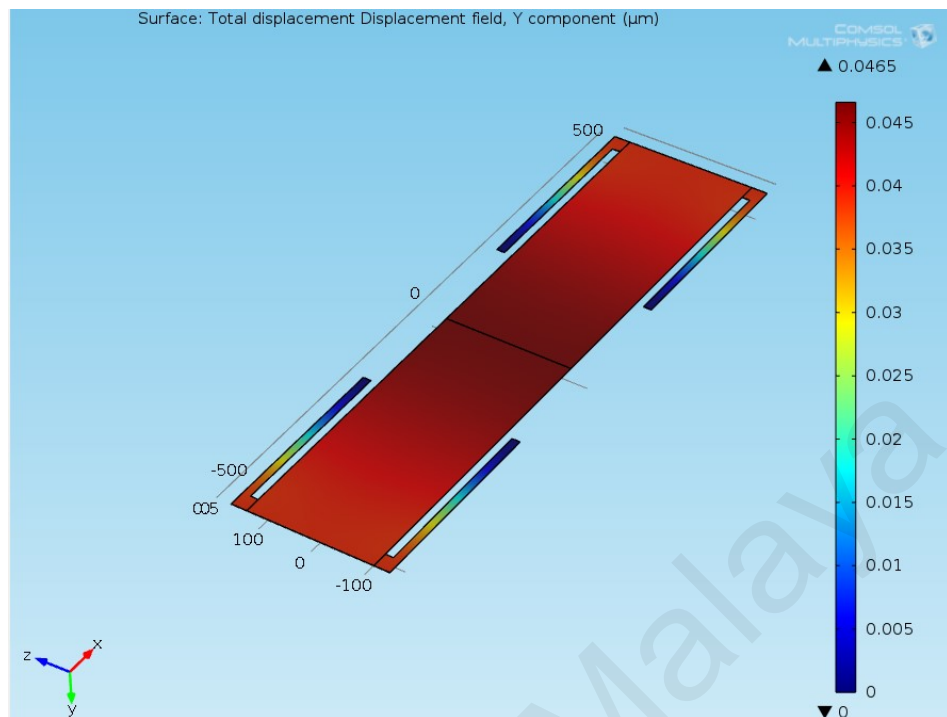


Figure 4. 48 Shows y displacement of Array 5

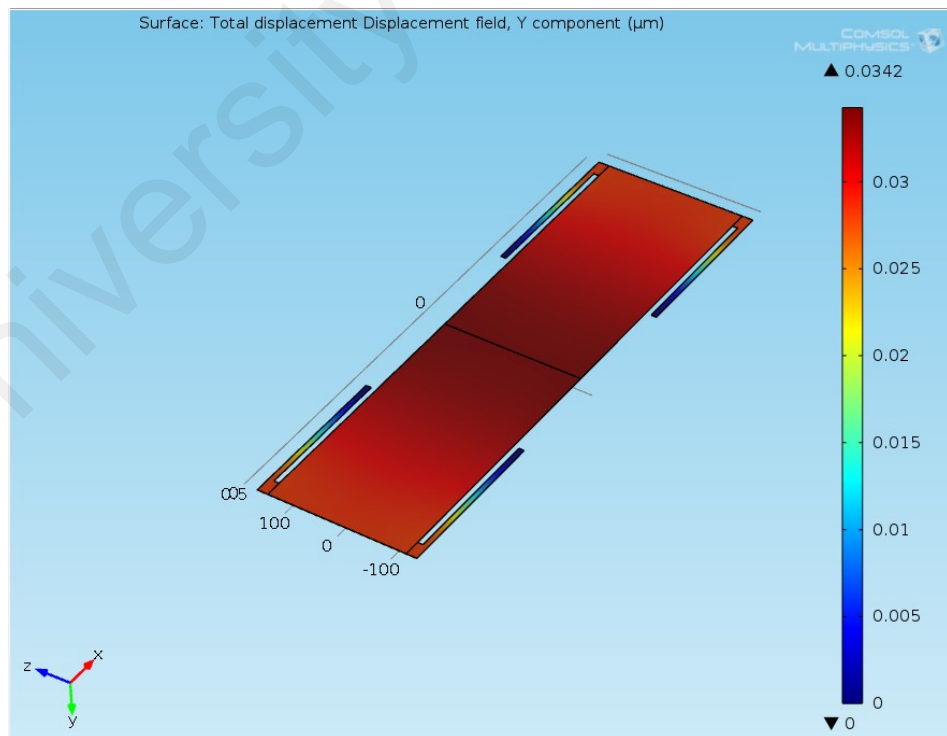


Figure 4. 49 Shows y displacement of Array 6

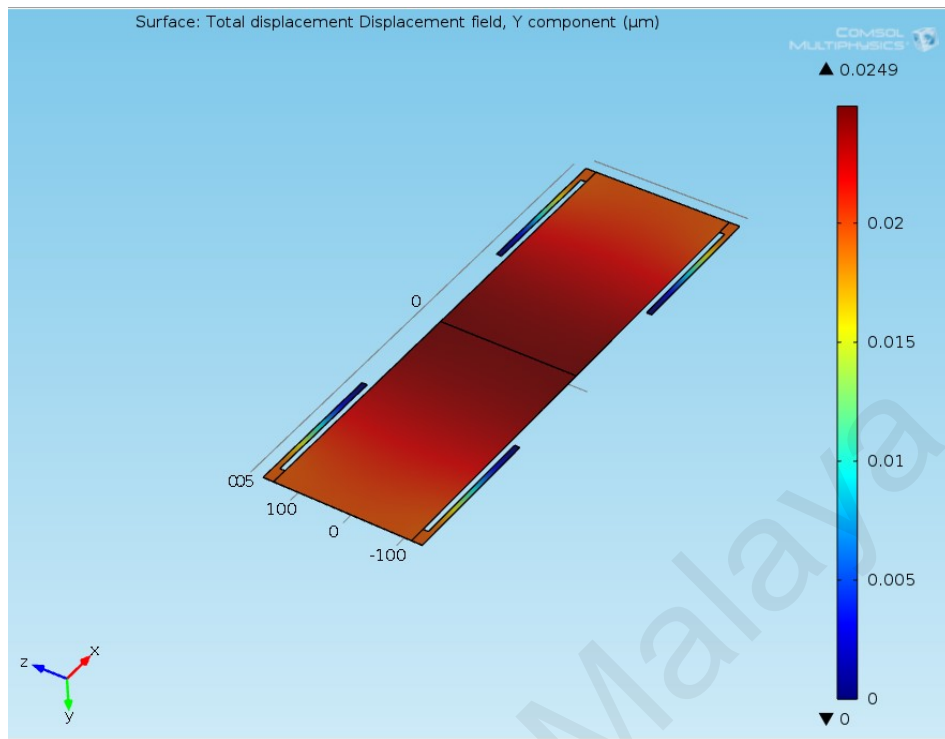


Figure 4. 50 Shows y displacement of Array 7

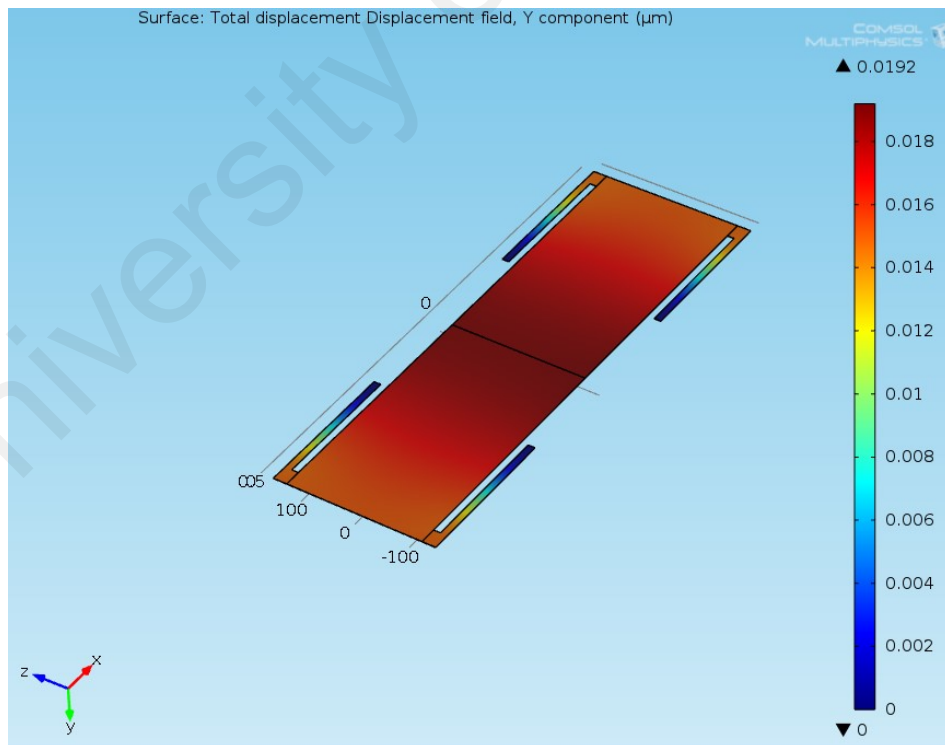


Figure 4. 51 Shows y displacement of Array 8

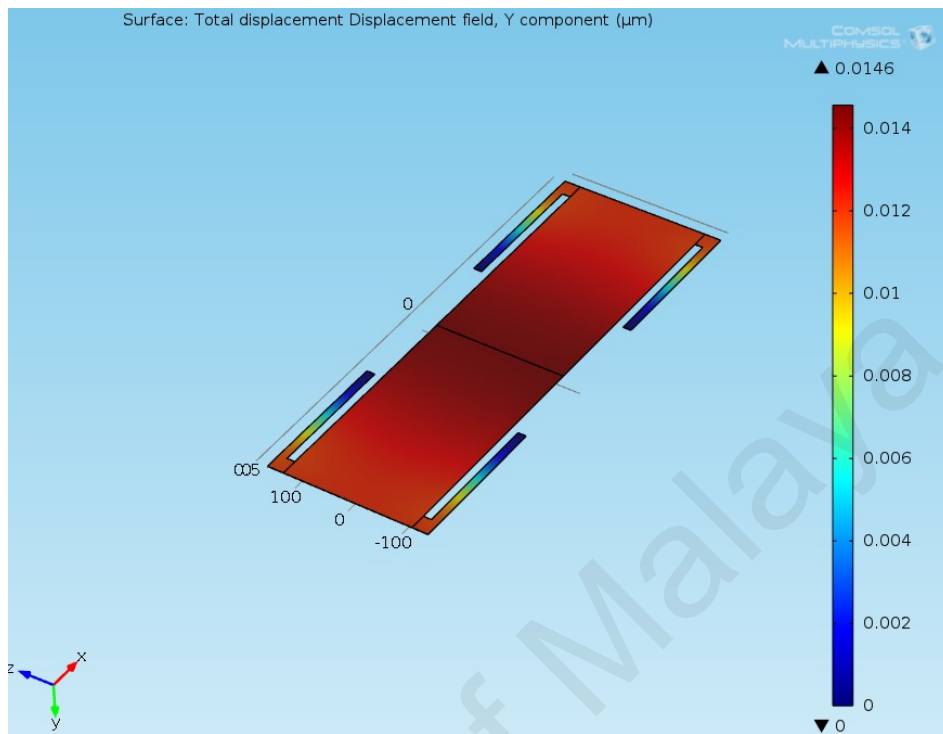


Figure 4. 52 Shows y displacement of Array 9

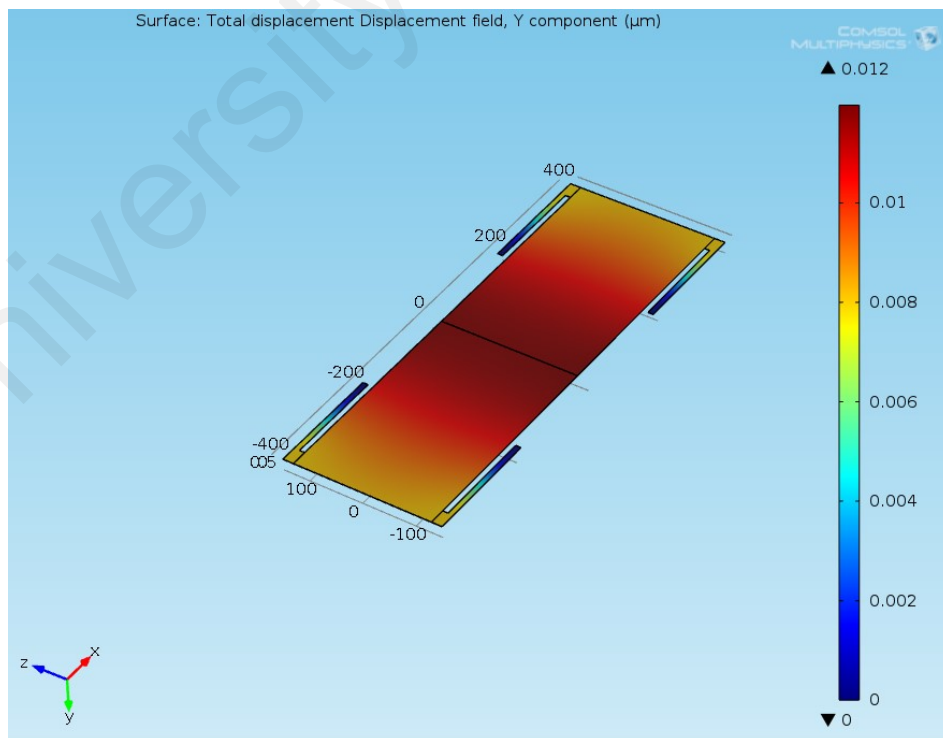


Figure 4. 53 Shows y displacement of Array 10

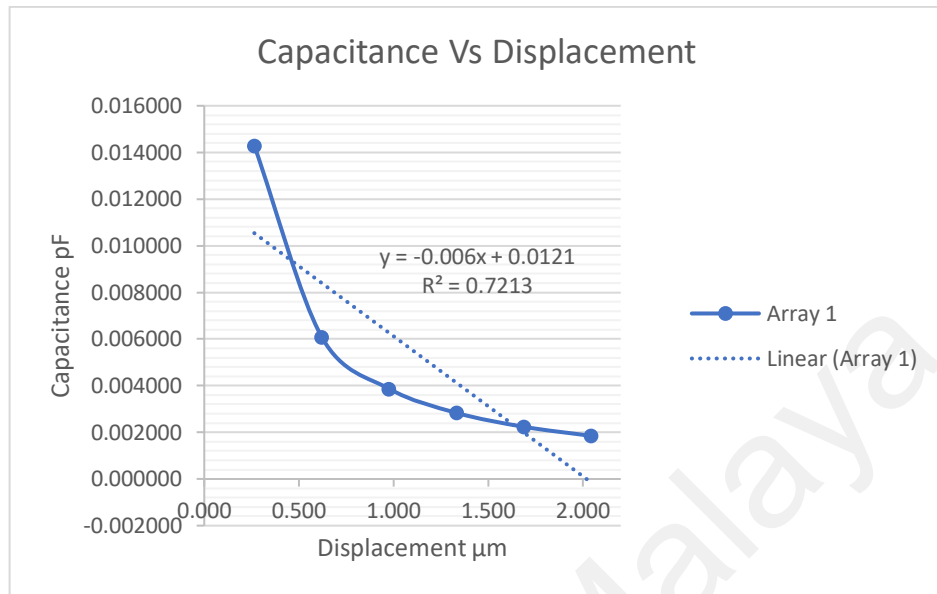


Figure 4. 54 Graph of Capacitance Vs Displacement of Array 1

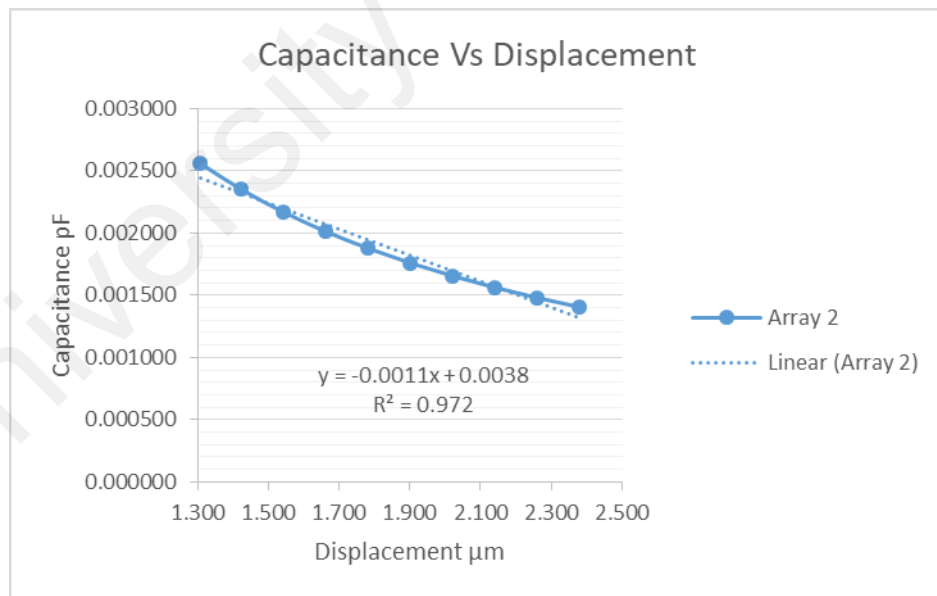


Figure 4. 55 Graph of Capacitance Vs Displacement of Array 2

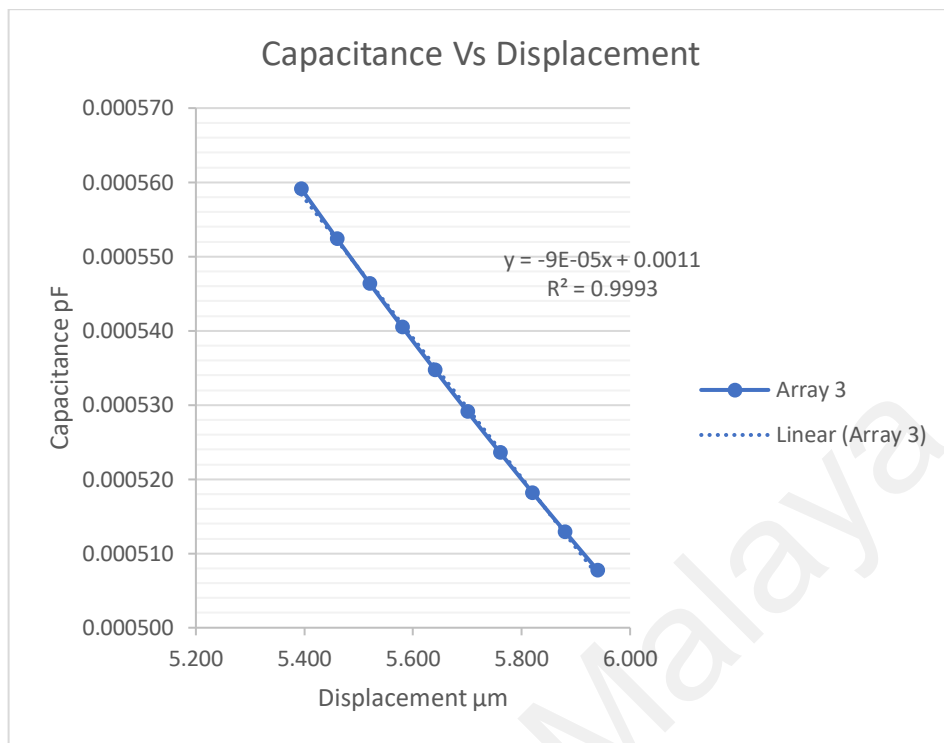


Figure 4. 56 Graph of Capacitance Vs Displacement of Array 3

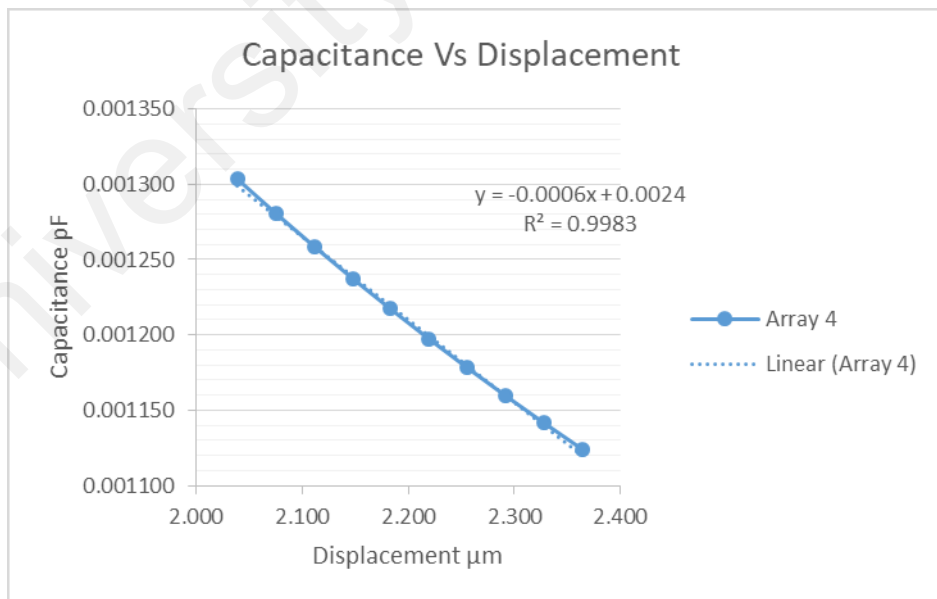


Figure 4. 57 Graph of Capacitance Vs Displacement of Array 4

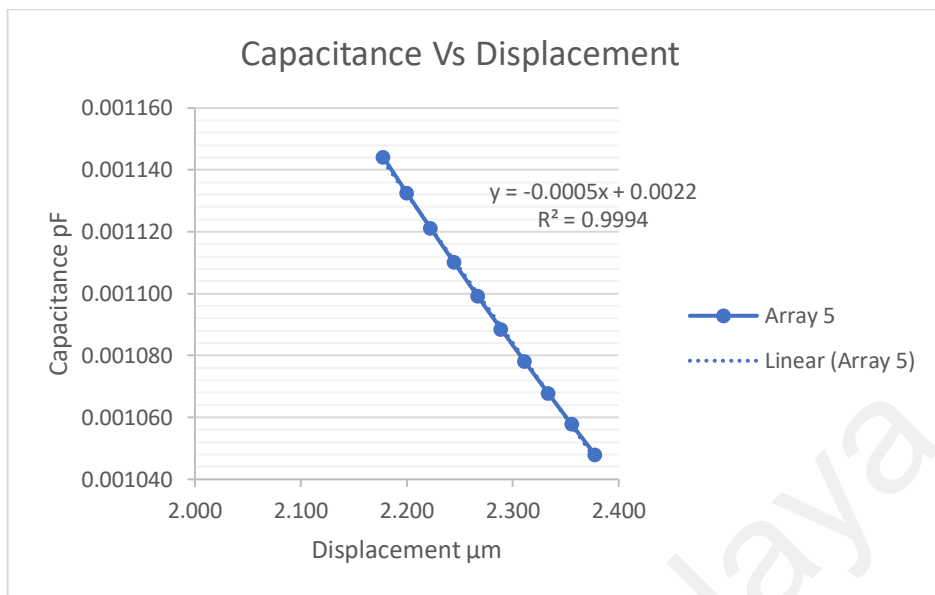


Figure 4. 58 Graph of Capacitance Vs Displacement of Array 5

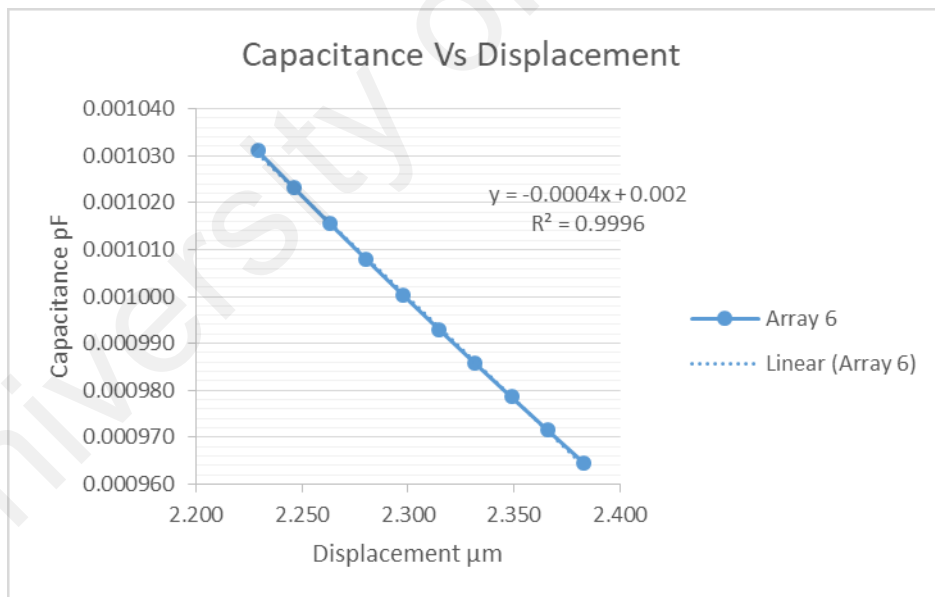


Figure 4. 59 Graph of Capacitance Vs Displacement of Array 6

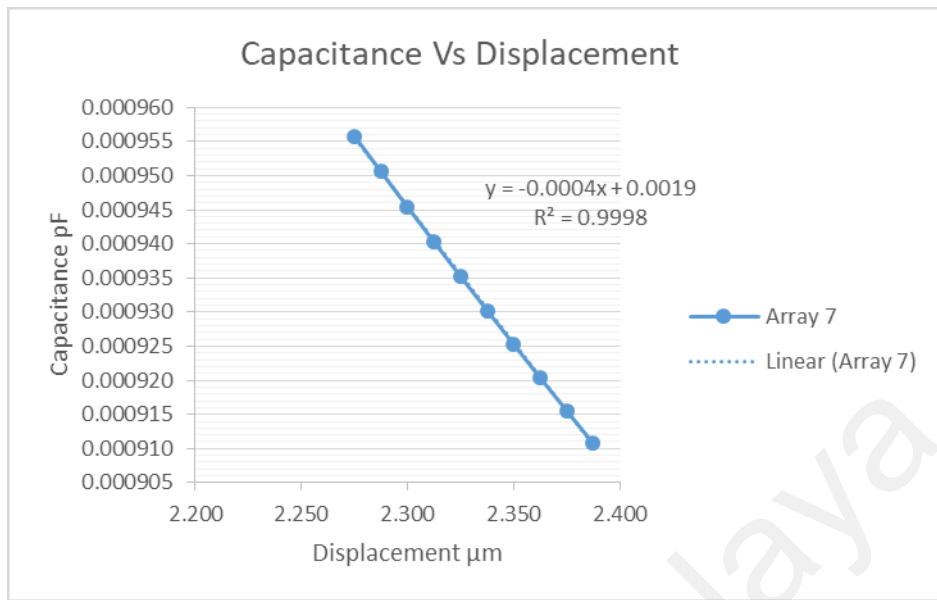


Figure 4. 60 Graph of Capacitance Vs Displacement of Array 7

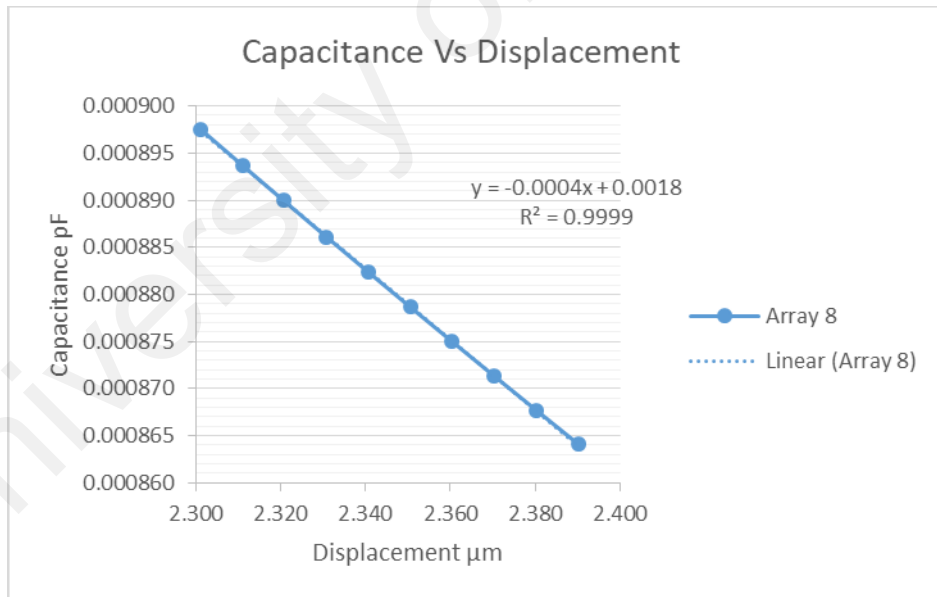


Figure 4. 61 Graph of Capacitance Vs Displacement of Array 8



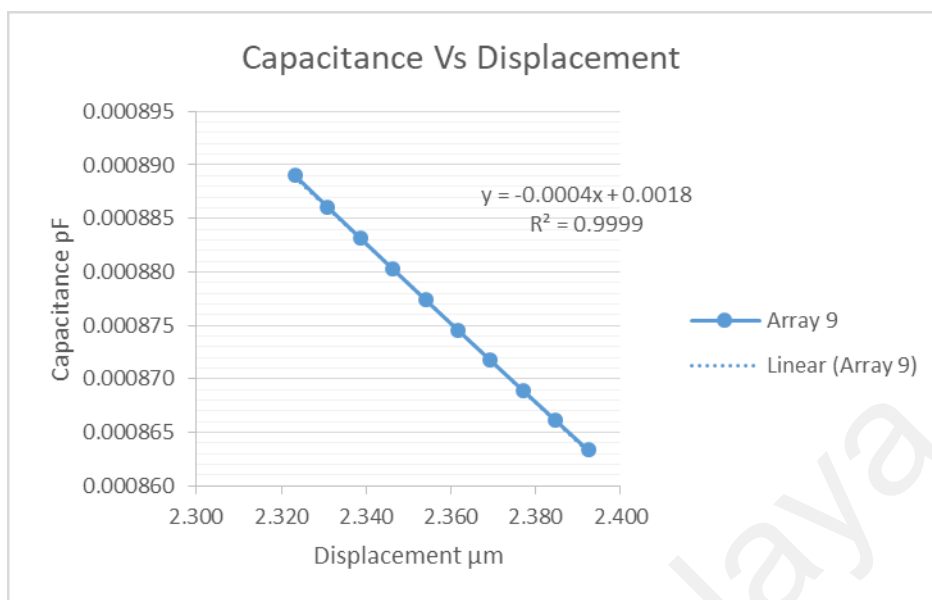


Figure 4. 62 Graph of Capacitance Vs Displacement of Array 9

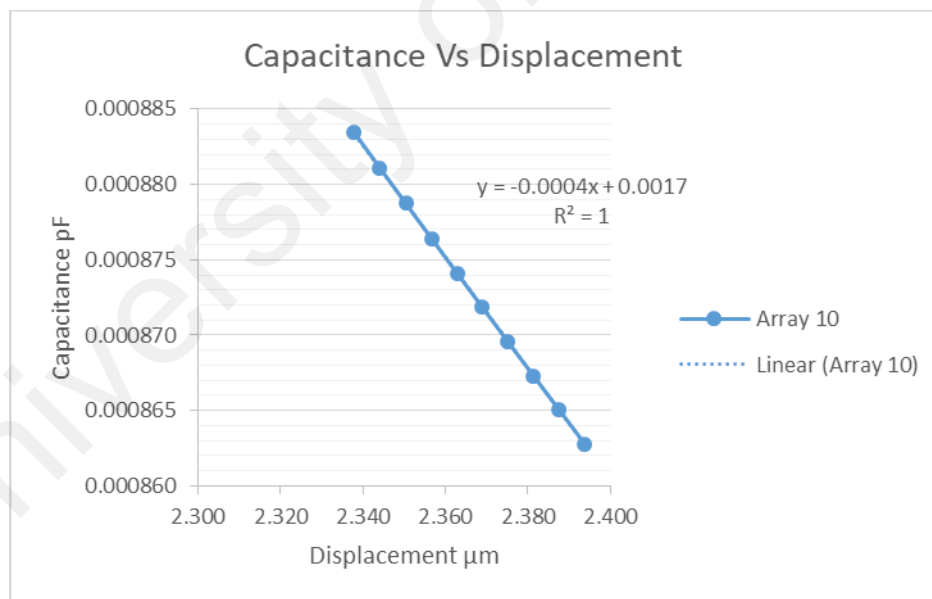


Figure 4. 63 Graph of Capacitance Vs Displacement of Array 10

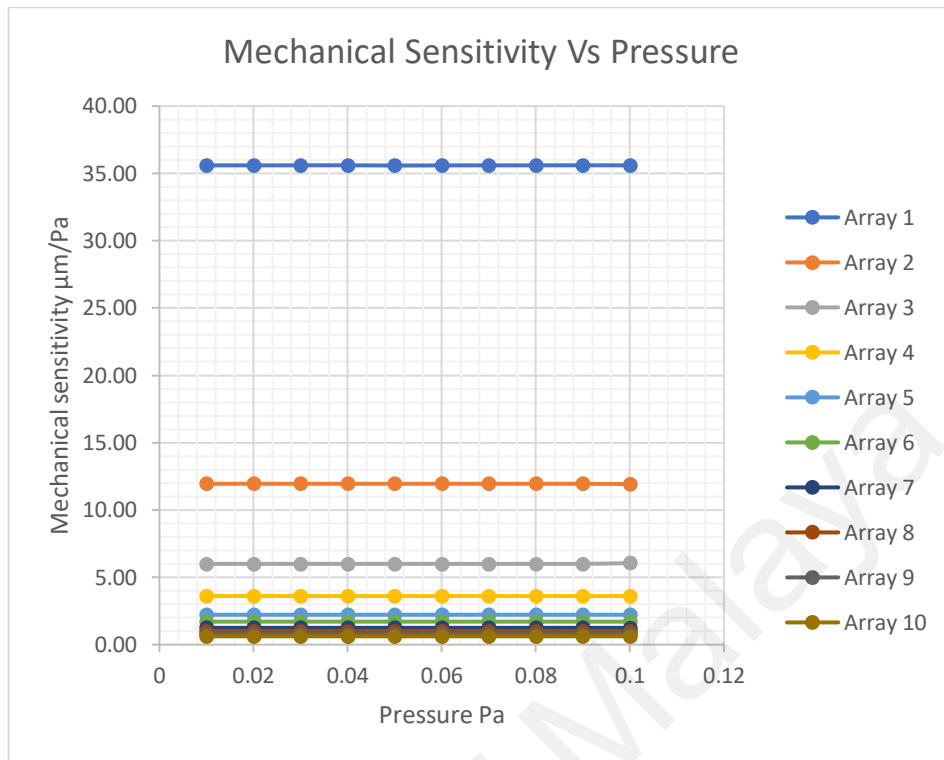


Figure 4. 64 Graph of Mechanical Sensitivity Vs Pressure of all arrays

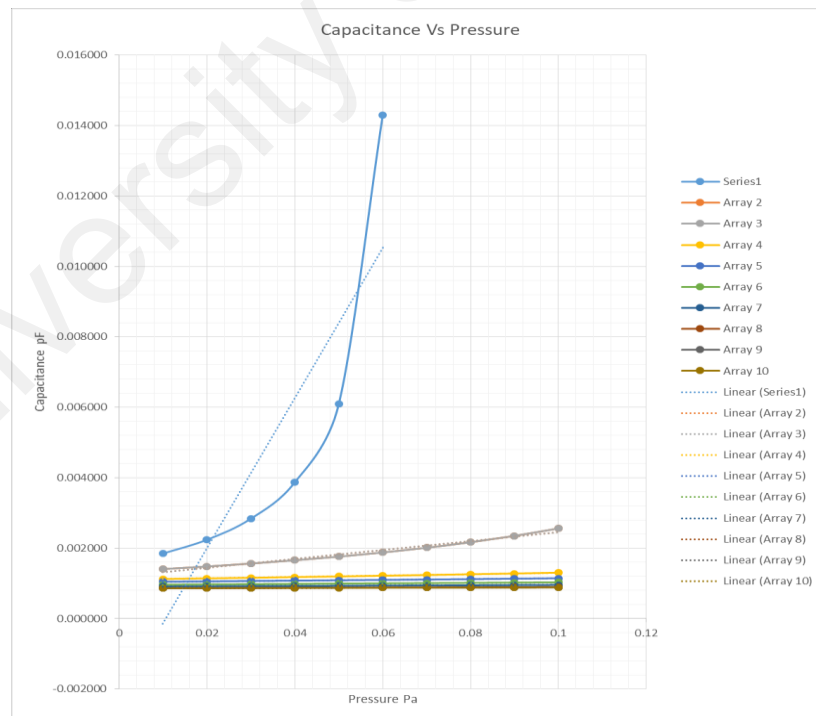


Figure 4. 65 Graph of Capacitance Vs Pressure of all Arrays

The Figure 4.54 to 4.63 shows the graph of capacitance vs displacement of each arrays. Based on the graph capacitance vs displacement linearity of each array can be concluded. Array 2 to 10 are showing a very good linearity from the graph. The slope of the graph is constant in every consecutive points. Array 1 showing a slight nonlinear behavior. This is due nonlinear relationship between gap size and capacitance, however in this research it can be accept due to advantages on higher mechanical sensitivity.

The Figure 4.64 shows the graph of Mechanical sensitivity and Pressure. The mechanical sensitivity shows a good relationship with frequency. The deflection of Array 1 is higher compare to other structure, it is due to the length of supported cantilever spring. The deflection of each structure determined by the length of spring support (Koyuncuoğlu et al., 2017). The mechanical sensitivity directly dependent on the deflection of the structure. This clearly show relationship of Eigen frequency and mechanical sensitivity. Lowest frequency is achieved in highest mechanical sensitivity and the highest frequency is achieved in the lowest mechanical sensitivity (Quiroz, Báez H., Mendoza, Alemán M., , & Villa, 2014). The capacitance of each structure decreases when frequency increases. This because the acoustic pressure wave contact area of each structure decreases as the frequency need to resonate at higher value. The Figure 4.65 show the Graph of Capacitance Vs Pressure of all Arrays. The capacitance and pressure increase linearly based on the graph. The graph also indicates the capacitive sensitivity of each arrays. The capacitive sensitivity decreases as the frequency of the resonance decreases. The following section 4.5 will able show the tabulated results of each arrays.

#### 4.5 DETERMINATION OF SUITABLE DIMENSION OF ARRAYS

After the analysis of Eigen frequency and the analysis of sensitivity and linearity of the proposed design from section 4.3 and 4.4. The final outcome from the both analysis is the dimension of each arrays, spring constant of each array, sensitivity and the linearity of each arrays is shown in Table 4.14. The maxing deflection of each array cannot be more than 2.4 as it will hit back plate electrode and could damage electrode. The yield stress of each structure must need to be lesser than yield strength of polysilicon 3.0 GPa. Based on the structural simulation the maximum yield stress achieved by array is 6.32MPa which is lower than yield strength of polysilicon material. This will avoid the membrane from its plastic deformation. It's compulsory the structure or each array to return to its original state upon releasing the acoustic pressure.

TECHNICAL SPECIFICATION OF COCHLEAR IMPLANT ARRAYS										
PARAMETER	ARRAY 1	ARRAY 2	ARRAY 3	ARRAY 4	ARRAY 5	ARRAY 6	ARRAY 7	ARRAY 8	ARRAY 9	ARRAY 10
D61 $\mu\text{m}$	1500	1375	1300	1150	1075	950	900	875	820	800
D64 $\mu\text{m}$	20	20	30	30	30	20	20	25	30	20
D65 $\mu\text{m}$	300	300	300	300	300	300	300	300	300	300
D69 $\mu\text{m}$	0.8	0.8	0.8	0.8	0.8	0.8	0.8	0.8	0.8	0.8
D71 $\mu\text{m}$	150	400	400	350	375	375	375	350	295	375
Air Gap $\mu\text{m}$	2.4									
Surface Area $\mu\text{m}^2$	426900	378200	340800	300300	281550	259700	245700	233375	215550	217700
Frequency Hz	635	1091	1560	2000	2550	3015	3573	4012	4551	5034
Mechanical Sensitivity $\mu\text{m}/\text{Pa}$	35.6	11.95	6	3.61	2.22	1.71	1.25	0.99	0.77	0.62
Capacitance pF	0.0018	0.0014	0.0013	0.0011	0.0010	0.000965	0.0009	0.0009	0.0009	0.0009
Capacitive Sensitivity pF/Pa	0.18	0.14	0.13	0.11	0.10	0.10	0.09	0.09	0.09	0.09
Deflection $\mu\text{m}$	0.3560	0.1200	0.0600	0.0361	0.0222	0.0171	0.0125	0.0099	0.0077	0.0062
Linearity pF/ $\mu\text{m}$	NA	0.00110	0.00070	0.00060	0.00050	0.00040	0.00040	0.00040	0.00040	0.00040

Table 4. 14 Detail technical specification of proposed design cochlear implants

The overall array dimension of array is attached in Appendix C

#### 4.6 SUMMARY CAPACITIVE MICROPHONE FINAL DESIGN

Final Design Characteristics	
Description	Value
Membrane thickness	0.8 $\mu$ m
Width of membrane	300 $\mu$ m
Length of membrane	800~1500 $\mu$ m
Air Gap	2.4 $\mu$ m
Capacitance	0.0018pF
Capacitive Sensitivity	0.18 pF/Pa
Mechanical Sensitivity	35.6 $\mu$ m/Pa
Linearity	0.0011 pF/ $\mu$ m
Frequency Range	635~5000 Hz
Number of Arrays	10
Material	Polysilicon

Table 4. 15 Summary of final design characteristics

The table 4.15 shows the characteristics of final design as described previously in Section 3.3.4 the Taguchi method is shown good contribution in finding the best quality of my final proposed design.

DESIGN SPECIFICATION				
ITEM	PARAMETERS	EXISTING DESIGN	PROPOSED DESIGN	FINAL DESIGN
1	Number of Array	8 (Koyuncuoğlu et al., 2017)	10	10
2	Overall array Dimension	3.3mm x 3.6mm	3.0mm x 3.0mm	3.01mm x 1.5mm
3	Capacitive Sensitivity	0.17 pF/Pa (Quiroz, Báez H., Mendoza, Alemán M., & Villa, 2014)	>0.17pF/Pa	0.18pF/Pa
4	Linearity	0.0002 pF/ $\mu$ m (Apoorva Dwivedi & Khanna, 2016)	>0.0002pF/ $\mu$ m	0.0011pF/ $\mu$ m
5	Mechanical Sensitivity	0.007 $\mu$ m/Pa (Taybi & Ganji, 2013)	>0.007 $\mu$ m/Pa	35.5 $\mu$ m/Pa
6	Frequency	300Hz - 4800 Hz (Koyuncuoğlu et al., 2017)	300Hz - 5000Hz	635Hz - 5000Hz
7	Material	Polysilicon	Polysilicon	Polysilicon

Table 4. 16 characteristics of microphone final design and existing design

Compared to existing design the number of arrays is increased to 10 arrays and each array has an increment of 500Hz. The range of frequency is from 500~5000Hz within human hearing range. The overall array layout dimension is reduced; thus, the capacitive cochlear implant is smaller. The capacitive sensitivity has improved to 0.18pF/Pa, mechanical sensitivity is 35.5  $\mu\text{m}/\text{Pa}$  and the final linearity is obtained is 0.0011pF/ $\mu\text{m}$ .

University of Malaya

## CHAPTER 5 CONCLUSION AND FUTURE WORKS

### 5.1 CONCLUSION

The objective of this project is successfully achieved, the development capacitive mems microphone for fully implantable of cochlear implants is developed. This innovative design offers a better capacitance, capacitive sensitivity, linearity, mechanical sensitivity and resonance frequency range is between human capabilities hearing range.

The current existing design offer 8 number of arrays with the overall dimension of 3.3mm X 3.6mm. The frequency range developed is 300~5000Hz. In this research it has been improved to 3.01mm X 1.5mm of overall dimension and the frequency range is from 630Hz to 5000Hz with 10 number of arrays. The existing capacitive sensitivity for hearing aids capacitive microphone is 0.17pF/Pa and the linearity is 0.0002 pF/ $\mu$ m. In this research using Taguchi method of optimization the capacitive sensitivity improved to 0.18pF/Pa and the linearity is improved to 0.0011pF/ $\mu$ m for fully implanted cochlear implants. The achievement of high sensitivity and linearity compare to existing design is overcomes the disadvantages of hearing less soft and loud sound. This improvement will also contribute to reduction in preamplifier gain needs less preamplifier gain before the analog-to digital and has ability to capture from far sound source.

## 5.2 FUTURE WORKS

Here some future work for this fully implanted capacitive microphone for cochlear implants are listed below based on the output of this work:

- Extent the study for analyze quality factor
- Extent the study for analyze output voltage of each arrays
- Performs vibrational test to at the fixed acceleration  $9.81\text{m/s}^2$  to verify the response frequency.
- Build up physical model to experiment model response and simulation analysis in terms of output voltage and frequency of response



## REFERENCES

- Bittencourt, A. G., Ikari, L. S., Adelina, A., Della, G., Bento, R. F., Tsuji, R. K., ... Neto, D. B. (2012). Conventional Hearing Aids. *Brazilian Journal of Otorhinolaryngology*, 78(2), 124–127.  
<https://doi.org/10.1590/S1808-86942012000200019>
- Calero, D., Paul, S., Gesing, A., Alves, F., & Cordioli, J. A. (2018). A technical review and evaluation of implantable sensors for hearing devices. *BioMedical Engineering Online*, 17(1), 1–26.  
<https://doi.org/10.1186/s12938-018-0454-z>
- Chaithra, S., Nithya, G., & Nagaraja, V. S. (2017). Design and Simulation of MEMS Microphone for Hearing Aid Application, (1), 12–15.
- Földner, M., Dehé, A., & Lerch, R. (2005). Analytical analysis and finite element simulation of advanced membranes for silicon microphones. *IEEE Sensors Journal*, 5(5), 857–862.  
<https://doi.org/10.1109/JSEN.2004.841449>
- Glucomentor, S. D. (2012). Technical documentation, 1. [https://doi.org/10.1016/0010-4485\(83\)90104-5](https://doi.org/10.1016/0010-4485(83)90104-5)
- Koyuncuoğlu, A., İlik, B., Chamanian, S., Uluşan, H., Ashrafi, P., Işık, D., & Külâh, H. (2017). Bulk PZT Cantilever Based MEMS Acoustic Transducer for Cochlear Implant Applications. *Proceedings*, 1(4), 584. <https://doi.org/10.3390/proceedings1040584>
- Krishnapriya, N. J., & Baiju, M. R. (2014). Design and Multiphysics Analysis of MEMS Capacitive Microphone. *COMSOL Conference*.
- Lima, A. De, Moret, M., & Tabanez, L. (2015). the Implications of the Cochlear Implant for Development of Language Skills :, (2), 1643–1655.
- Mohamad, N. (2010). Modelling and Optimisation of a Spring-Supported Diaphragm Capacitive MEMS Microphone. *Engineering*, 2(10), 762–770. <https://doi.org/10.4236/engineering.2010.210098>
- Mohamad, N., Iovenitti, P., & Vinay, T. (2007). High sensitivity capacitive MEMS microphone with spring supported diaphragm, 6800, 68001T. <https://doi.org/10.1117/12.758987>

Papež, M., & Vlček, K. (2015). Enhanced MVDR Beamforming for MEMS Microphone Array, 2, 42–46.

Quiroz, G., B??ez, H., Mendoza, S., Alem??n, M., & Villa, L. (2014). Design and simulation of a membranes-based acoustic sensors array for cochlear implant applications. *Superficies Y Vacio*, 27(1), 24–29.

Taybi, M., & Ganji, B. A. (2013). International Journal of Engineering The Effect of Corrugations on Mechanical Sensitivity of Diaphragm for MEMS Capacitive Microphone, 26(11), 1323–1330. <https://doi.org/10.5829/idosi.ije.2013.26.11b.07>

Yang, C. T. (2010). The sensitivity analysis of a mems microphone with different membrane diameters. *Journal of Marine Science and Technology*, 18(6), 790–796.

Zwyssig, E., Lincoln, M., & Renals, S. (2010). A digital microphone array for distant speech recognition. *ICASSP, IEEE International Conference on Acoustics, Speech and Signal Processing - Proceedings*, 33812, 5106–5109. <https://doi.org/10.1109/ICASSP.2010.5495040>

U.S Food and Drug Administration

[<https://www.fda.gov/MedicalDevices/ProductsandMedicalProcedures/ImplantsandProsthetics/CochlearImplants/ucm062843.htm>]. Accessed 15 March 2018.

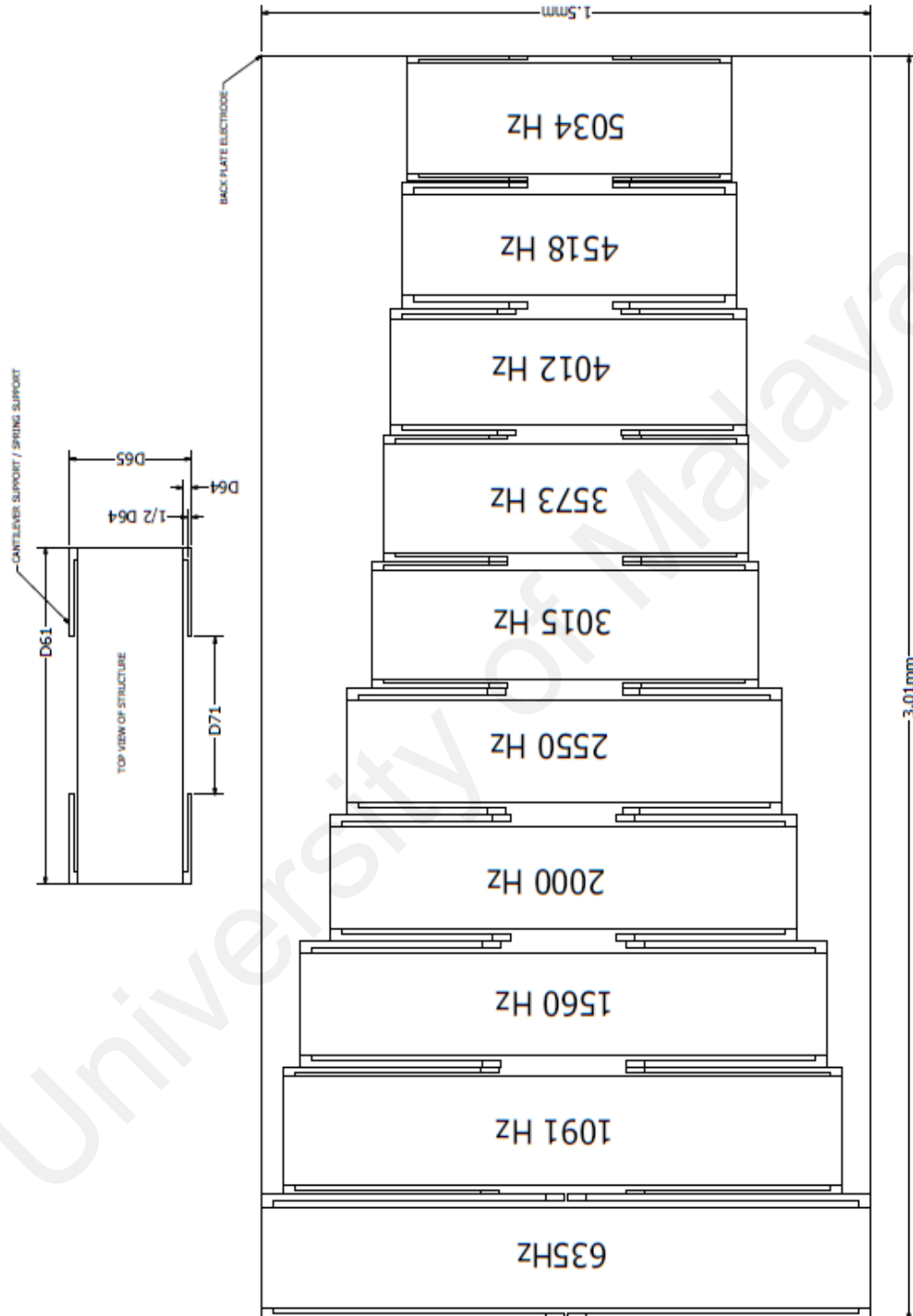
## APPENDIXES

### Appendix A: Table of Calculation

ARRAY 1 @ 635Hz					
Pressure	Deflection	Displacement	Sensitivity	Capacitance pF	Linearity
0.01	0.356	2.044	35.60	0.001848	
0.02	0.712	1.688	35.60	0.002238	-0.0011
0.03	1.068	1.332	35.60	0.002836	-0.0017
0.04	1.424	0.976	35.60	0.003871	-0.0029
0.05	1.779	0.621	35.59	0.006087	-0.0062
0.06	2.136	0.264	35.60	0.014295	-0.0230
0.07	2.492	-0.092	35.60	-0.041111	0.1555
0.08	2.848	-0.448	35.60	-0.008435	-0.0918
0.09	3.205	-0.805	35.61	-0.004696	-0.0105
0.1	3.560	-1.160	35.60	-0.003258	-0.0040
YIELD STRESS OF STRUCTURE 6.32 MPa @ 0.1Pa					
ARRAY 2 @ 1091Hz					
Pressure	Deflection	Displacement	Sensitivity	Capacitance pF	Linearity
0.01	0.120	2.381	11.95	0.001406	
0.02	0.239	2.261	11.95	0.001480	-0.0006
0.03	0.359	2.142	11.95	0.001563	-0.0007
0.04	0.478	2.022	11.95	0.001655	-0.0008
0.05	0.598	1.903	11.95	0.001759	-0.0009
0.06	0.717	1.783	11.95	0.001877	-0.0010
0.07	0.837	1.664	11.95	0.002012	-0.0011
0.08	0.956	1.544	11.95	0.002168	-0.0013
0.09	1.076	1.425	11.95	0.002350	-0.0015
0.1	1.193	1.307	11.93	0.002561	-0.0018
YIELD STRESS OF STRUCTURE 4.2 MPa @ 0.1Pa					
ARRAY 3 @ 1560Hz					
Pressure	Deflection	Displacement	Sensitivity	Capacitance pF	Linearity
0.01	0.060	2.340	6.00	0.001289	
0.02	0.120	2.280	6.00	0.001323	-0.0006
0.03	0.180	2.220	6.00	0.001359	-0.0006
0.04	0.240	2.160	6.00	0.001396	-0.0006
0.05	0.300	2.100	6.00	0.001436	-0.0007
0.06	0.360	2.040	6.00	0.001478	-0.0007
0.07	0.420	1.980	6.00	0.001523	-0.0007
0.08	0.480	1.920	6.00	0.001571	-0.0008
0.09	0.540	1.860	6.00	0.001622	-0.0008
0.1	0.606	1.794	6.06	0.001681	-0.0009
YIELD STRESS OF STRUCTURE 2.6 MPa @ 0.1Pa					
ARRAY 4 @ 2000Hz					
Pressure	Deflection	Displacement	Sensitivity	Capacitance pF	Linearity
0.01	0.036	2.364	3.61	0.001124	
0.02	0.072	2.328	3.61	0.001142	-0.00048
0.03	0.108	2.292	3.61	0.001160	-0.00050
0.04	0.144	2.256	3.61	0.001178	-0.00051
0.05	0.181	2.220	3.61	0.001197	-0.00053
0.06	0.217	2.183	3.61	0.001217	-0.00055
0.07	0.253	2.147	3.61	0.001238	-0.00057
0.08	0.289	2.111	3.61	0.001259	-0.00059
0.09	0.325	2.075	3.61	0.001281	-0.00061
0.1	0.361	2.039	3.61	0.001303	-0.00063
YIELD STRESS OF STRUCTURE 1.8 MPa @ 0.1Pa					
ARRAY 5 @ 2550Hz					
Pressure	Deflection	Displacement	Sensitivity	Capacitance pF	Linearity
0.01	0.022	2.378	2.22	0.001048	
0.02	0.044	2.356	2.22	0.001058	-0.00044
0.03	0.067	2.333	2.22	0.001068	-0.00045
0.04	0.089	2.311	2.22	0.001078	-0.00046
0.05	0.111	2.289	2.22	0.001089	-0.00047
0.06	0.133	2.267	2.22	0.001099	-0.00048
0.07	0.156	2.244	2.22	0.001110	-0.00049
0.08	0.178	2.222	2.22	0.001121	-0.00050
0.09	0.200	2.200	2.22	0.001132	-0.00051
0.1	0.222	2.178	2.22	0.001144	-0.00052
YIELD STRESS OF STRUCTURE 1.55 MPa @ 0.1Pa					

ARRAY 6 @ 3015Hz					
Pressure	Deflection	displacement	Sensitivity	Capacitance pF	Linearity
0.01	0.017	2.383	1.71	0.000965	
0.02	0.034	2.366	1.71	0.000971	-0.00041
0.03	0.051	2.349	1.71	0.000979	-0.00041
0.04	0.068	2.332	1.71	0.000986	-0.00042
0.05	0.085	2.315	1.71	0.000993	-0.00043
0.06	0.103	2.297	1.71	0.001000	-0.00043
0.07	0.120	2.280	1.71	0.001008	-0.00044
0.08	0.137	2.263	1.71	0.001016	-0.00045
0.09	0.154	2.246	1.71	0.001023	-0.00045
0.1	0.171	2.229	1.71	0.001031	-0.00046
YIELD STRESS OF STRUCTURE 1.85 MPa @ 0.1Pa					
ARRAY 7 @ 3573Hz					
Pressure	Deflection	Displacement	Sensitivity	Capacitance pF	Linearity
0.01	0.013	2.388	1.25	0.000911	
0.02	0.025	2.375	1.25	0.000916	-0.00038
0.03	0.038	2.363	1.25	0.000920	-0.00039
0.04	0.050	2.350	1.25	0.000925	-0.00039
0.05	0.063	2.338	1.25	0.000930	-0.00040
0.06	0.075	2.325	1.25	0.000935	-0.00040
0.07	0.088	2.313	1.25	0.000940	-0.00040
0.08	0.100	2.300	1.25	0.000945	-0.00041
0.09	0.113	2.288	1.25	0.000951	-0.00041
0.1	0.125	2.275	1.25	0.000956	-0.00042
YIELD STRESS OF STRUCTURE 1.54 MPa @ 0.1Pa					
ARRAY 8 @ 4012Hz					
Pressure	Deflection	displacement	Sensitivity	Capacitance pF	Linearity
0.01	0.010	2.390	0.99	0.000864	
0.02	0.020	2.380	0.99	0.000868	-0.00036
0.03	0.030	2.370	0.99	0.000871	-0.00037
0.04	0.040	2.360	0.99	0.000875	-0.00037
0.05	0.049	2.351	0.99	0.000879	-0.00037
0.06	0.059	2.341	0.99	0.000882	-0.00038
0.07	0.069	2.331	0.99	0.000886	-0.00038
0.08	0.079	2.321	0.99	0.000890	-0.00038
0.09	0.089	2.311	0.99	0.000894	-0.00039
0.1	0.099	2.301	0.99	0.000898	-0.00039
YIELD STRESS OF STRUCTURE 1.05 MPa @ 0.1Pa					
ARRAY 9 @ 4518Hz					
Pressure	Deflection	displacement	Sensitivity	Capacitance pF	Linearity
0.01	0.008	2.392	0.77	0.000863	
0.02	0.015	2.385	0.77	0.000866	-0.00036
0.03	0.023	2.377	0.77	0.000869	-0.00036
0.04	0.031	2.369	0.77	0.000872	-0.00037
0.05	0.038	2.362	0.77	0.000875	-0.00037
0.06	0.046	2.354	0.77	0.000877	-0.00037
0.07	0.054	2.346	0.77	0.000880	-0.00037
0.08	0.061	2.339	0.77	0.000883	-0.00038
0.09	0.069	2.331	0.77	0.000886	-0.00038
0.1	0.077	2.323	0.77	0.000889	-0.00038
YIELD STRESS OF STRUCTURE 0.885 MPa @ 0.1Pa					
ARRAY 10 @ 5034Hz					
Pressure	Deflection	displacement	Sensitivity	Capacitance pF	Linearity
0.01	0.006	2.394	0.62	0.000863	
0.02	0.012	2.388	0.62	0.000865	-0.00036
0.03	0.019	2.381	0.62	0.000867	-0.00036
0.04	0.025	2.375	0.62	0.000870	-0.00037
0.05	0.031	2.369	0.62	0.000872	-0.00037
0.06	0.037	2.363	0.62	0.000874	-0.00037
0.07	0.043	2.357	0.62	0.000876	-0.00037
0.08	0.050	2.350	0.62	0.000879	-0.00037
0.09	0.056	2.344	0.62	0.000881	-0.00037
0.1	0.062	2.338	0.62	0.000883	-0.00038
YIELD STRESS OF STRUCTURE 0.105 MPa @ 0.1Pa					

## Appendix B: Overall dimension of Array



# Analytical Analysis and Finite Element Simulation of Advanced Membranes for Silicon Microphones

Marc Földner, Alfons Dehé, and Reinhard Lerch, *Member, IEEE*

**Abstract**—In this paper, advanced membrane designs are simulated in order to improve the sensitivity of micromachined silicon condenser microphones. Analytical analyses and finite element simulations have been carried out to derive algebraic expressions for the mechanical compliance of corrugated membranes and membranes supported at spring elements. It is shown that the compliance of both types of membranes can be modeled with the help of an enhanced theory of circular membranes. For spring membranes, a numerically derived and design dependent constant takes into account the reduced suspension. The mechanical stress in corrugated membranes is calculated using a geometrical model and is confirmed by finite element simulations. A very good agreement between theory and experimental results is demonstrated for spring membranes of different shape and for membranes with varying number of corrugations. In a silicon microphone application, a high electro-acoustical sensitivity up to 8.2 mV/Pa/V is achieved with a membrane diameter of only 1 mm.

**Index Terms**—Corrugated membrane, finite element method (FEM), modeling, silicon microphone, spring membrane.

## I. INTRODUCTION

TODAY, in most microphone applications like mobile phones, camcorders, or personal digital assistants, mass-produced electret condenser microphones (ECMs) are installed. In a condenser microphone, sound causes the capacitance built of a flexible membrane and a rigid backplate separated by a small air gap to vary. Recent ECMs use fluorinated ethylene-propylene (FEP) as material for the electret foil, which is applied to the back electrode. Because of the limited temperature resistance of FEP foils, ECMs are soldered by hand [1].

In contrast to standard ECMs, silicon microphones fabricated with techniques from IC processing fulfil the temperature requirements of automated assembly lines. Therefore, the costs of placing a silicon microphone packaged as surface mounted device on a printed circuit board are strongly reduced compared to the assembling costs of standard ECMs.

Most silicon microphones also base on capacitive sensing because of its superior performance compared to piezoelectric or piezoresistive detection principles [2]. Due to the complexity of

coupled acoustical, mechanical, and electrical components, simplifications have to be introduced to describe the microphone behavior. A common approach is the reduced-order network modeling with linear lumped elements [3]. In this technique, mass, stiffness, and damping are represented by electric inductors, capacitors, and resistors. In the field of microphones, network modeling has been extensively used [4]–[7]. Defining the mechanical compliance  $C$  (in meters per Pascal) of a membrane by the ratio of average deflection to the applied sound pressure, as a first approximation, the electro-acoustical sensitivity  $S$  (in volts per Pascal) of a condenser microphone is given by

$$S \approx \frac{U_0}{x_0} \cdot C \quad (1)$$

where  $U_0$  is the bias voltage and  $x_0$  the air gap height of the microphone capacitor. Thus, a precise description of the membrane compliance depending on the geometrical design and state of stress is essential for the optimization of condenser microphones. In the case of a circular membrane, the mechanical compliance  $C_{\text{circular}}$  is well known and can be approximately calculated by the theory of plates and shells [8]

$$C_{\text{circular}} \approx \frac{R^2}{8 \cdot t \cdot \sigma_0} \cdot \left( \frac{2 \cdot E \cdot t^2}{(1 - \nu^2) \cdot \sigma_0 \cdot R^2} + 1 \right)^{-1} \quad (2)$$

where  $R$  is the radius and  $t$  the thickness of the membrane.  $\sigma_0$ ,  $E$ , and  $\nu$  are the intrinsic stress, modulus of elasticity, and Poisson's ratio of the membrane material.

However, the application of novel membrane structures for improved microphone sensitivity presented in Section II of this paper requires more complex analytical and numerical analyses. Besides the conventional circular design, membranes clamped at narrow spring structures with reduced restoring force, and corrugated membranes for stress relaxation have been fabricated. So far, only little effort has been spent on the simulation of these type of microphone membranes.

Kovács and Stoffel [9], [10] have presented the fabrication and finite element simulation of membranes with free-standing structures (mechanical springs) realized by slots in the membranes. Unfortunately, results from numerical simulations are only applicable to specific designs. To keep the advantages of the network modeling technique with fast analyses and optimization of the microphone system, in Section III, an expression for the mechanical compliance of spring membranes is derived from detailed finite element simulations.

Extensive parameter studies of membranes with corrugations have been performed by Ying *et al.* [11]. As mentioned here, an algebraic description which is valid over a large range of design parameters is desirable for network modeling. An expression

Manuscript received November 5, 2003; revised July 1, 2004. This work was supported by BMBF under Grant 16SV1273. The associate editor coordinating the review of this paper and approving it for publication was Prof. Fahrettin Degerciyan.

M. Földner and A. Dehé are with the Infineon Technologies AG, 81730 Munich, Germany (e-mail: marc.fueldner@infineon.com; alfons.dehe@infineon.com).

R. Lerch is with the Department of Sensor Technology, University of Erlangen, 91052 Erlangen, Germany (e-mail: reinhard.lerch@lsc.oci.uni-erlangen.de).

Digital Object Identifier 10.1109/JSEN.2004.841449

## Modelling and Optimisation of a Spring-Supported Diaphragm Capacitive MEMS Microphone

Norizan Mohamad<sup>1</sup>, Pio Iovenitti<sup>1</sup>, Thurai Vinay<sup>2</sup>

<sup>1</sup>Faculty of Engineering and Industrial Sciences, Swinburne University of Technology, Hawthorn, Australia

<sup>2</sup>School of Electrical and Computer Engineering, RMIT University, Melbourne, Australia

E-mail: [norizan@utem.edu.my](mailto:norizan@utem.edu.my)

Received June 9, 2010; revised September 6, 2010; accepted September 21, 2010

### Abstract

Audio applications such as mobile communication and hearing aid devices demand a small size but high performance, stable and low cost microphone to reproduce a high quality sound. Capacitive microphone can be designed to fulfill such requirements with some trade-offs between sensitivity, operating frequency range, and noise level mainly due to the effect of device structure dimensions and viscous damping. Smaller microphone size and air gap will gradually decrease its sensitivity and increase the viscous damping. The aim of this research was to develop a mathematical model of a spring-supported diaphragm capacitive MEMS microphone as well as an approach to optimize a microphone's performance. Because of the complex shapes in this latest type of diaphragm design trend, analytical modelling has not been previously attempted. A novel diaphragm design is proposed that offers increased mechanical sensitivity of a capacitive microphone by reducing its diaphragm stiffness. A lumped element model of the spring-supported diaphragm microphone is developed to analyze the complex relations between the microphone performance factors and to find the optimum dimensions based on the design requirements. It is shown analytically that the spring dimensions of the spring-supported diaphragm do not have large effects on the microphone performance compared to the diaphragm and backplate size, diaphragm thickness, and air-gap distance. A 1 mm<sup>2</sup> spring-supported diaphragm microphone is designed using several optimized performance parameters to give a -3 dB operating bandwidth of 10.2 kHz, a sensitivity of 4.67 mV/Pa (-46.5 dB ref. 1 V/Pa at 1 kHz using a bias voltage of 3 V), a pull-in voltage of 13 V, and a thermal noise of -22 dBA SPL.

**Keywords:** Capacitive Microphone, Spring-Supported Diaphragm, Microphone Modelling

### 1. Introduction

The silicon capacitive microphone has been studied and shown to potentially replace the existing and widely used piezoelectric microphone due to its high sensitivity, long term stability and ability to withstand a high temperature soldering process [1,2]. This type of microphone has been designed to use various diaphragm materials including silicon nitride, polysilicon, aluminum, and polyimide [3-6]. A different diaphragm material was chosen to suit the intended application based on the required dimension, sensitivity, and operating frequency range. Open-circuit sensitivity of a capacitive microphone can be increased by applying a higher bias voltage or reducing the diaphragm stiffness. Since many small size audio applications prefer a low voltage operation, the microphone sensitivity needs to be increased by reducing the

diaphragm stiffness alone. The diaphragm stiffness can be reduced by using a low stress material, perforated diaphragm or as a combination with corrugated or spring type diaphragm [4,6-12]. However, the reduction in diaphragm stiffness will cause the reduction in its operating frequency range and pull-in voltage. Moreover, the desired smaller device size and capacitor air-gap thickness will increase the thin film air damping effect which will decrease its open-circuit sensitivity further. Due to the trade-offs relation between these performance factors, the optimization of the microphone parameters is always required depending on the design requirements.

Previous research has been carried out using various spring type diaphragm to increase the sensitivity of a capacitive MEMS microphone. Kim *et al.* [11] has demonstrated the use of a flexure hinge diaphragm to achieve 0.2 m diaphragm centre deflection with a flat frequency





## The Effect of Corrugations on Mechanical Sensitivity of Diaphragm for MEMS Capacitive Microphone

M. Taybi, B. A. Ganji\*

Electrical & Computer Engineering Department, Babol University of Technology, Babol, Iran

### PAPER INFO

#### Paper history:

Received 11 June 2012

Received in revised form 12 February 2013

Accepted 28 February 2013

#### Keywords:

Corrugated Diaphragm

Residual Stress

Mechanical Sensitivity

Diaphragm Displacement

### ABSTRACT

In this paper the effect of corrugations on mechanical sensitivity of diaphragm for MEMS capacitive microphone is investigated. Analytical analyses have been carried out to derive mathematic expression for mechanical sensitivity and displacement of corrugated diaphragm with residual stress. It is shown that the mechanical sensitivity and displacement of diaphragm can be modeled using thin plate theory. The mechanical stress of corrugated diaphragm is calculated using mathematical model and its relationship with residual stress is expressed. The analytical results show that the mechanical sensitivity of diaphragm can be increased using corrugations, because of reducing the effect of residual stress in corrugated diaphragm.

doi: 10.5829/idosi.ije.2013.26.11b.07

### 1. INTRODUCTION

Microphone is a transducer that converts acoustic energy to electrical energy. It is widely used in voice communications, hearing aids, noise and vibration control and biomedical application [1-3]. During the past years, the capacitive microphone has been the most attractive research topic in micro-electromechanical systems (MEMS), because it has superior characteristics such as high sensitivity and low noise level compared with piezoelectric and piezoresistive microphones [4, 5]. Till now, most of MEMS capacitive microphones were developed using flat diaphragm to sense acoustic wave, because it is easy to fabricate [6].

The capacitive microphones generally consist of a diaphragm which vibrates by impinging of acoustic wave pressure, a back plate and air gap. In its simplest form, a flat diaphragm is stretched over a conductive back plate and supported by post so that there is a gap between the diaphragm and the back plate. The high residual stress diaphragm may give undesirable effects such as higher actuation voltage, film buckling and diaphragm cracking. The mechanical sensitivity of diaphragm is limited by residual stress of deposited layer. The residual stress can be controlled by the parameters of the deposition process [7].

Since the control of thin film stress during the fabrication process is rather difficult, therefore making shallow corrugations in diaphragm can reduce the effect of residual stress and subsequently increase the mechanical sensitivity of diaphragm. In this paper, we investigate the effect of corrugations on mechanical sensitivity and diaphragm deflection for using it for the first time in MEMS capacitive microphone.

### 2. MODELING OF MECHANICAL SENSITIVITY

The center deflection ( $y$ ) of a flat circular diaphragm with clamped edges and without residual stress, due to a homogeneous pressure ( $P$ ) can be calculated from [8]:

$$\frac{PR^4}{Eh^4} = \frac{5.33}{1-\nu^2} \left(\frac{y}{h}\right) + \frac{2.83}{1-\nu^2} \left(\frac{y}{h}\right)^3 \quad (1)$$

where  $E$ ,  $\nu$ ,  $R$  and  $h$  are Young's modulus, Poisson's ratio, radius and thickness of diaphragm, respectively. It is illustrated from Equation (1) that if  $(y/h) \ll 1$  the cubic term of displacement can be neglected, thus the relation between center deflection and applied pressure is linear. For large values of  $(y/h)$  the relation is nonlinear. For large value of initial tension, the deflection of a flat circular diaphragm can be represented by [8]:

\*Corresponding Author Email: [baganji@nit.ac.ir](mailto:baganji@nit.ac.ir) (B. A. Ganji)



# THE SENSITIVITY ANALYSIS OF A MEMS MICROPHONE WITH DIFFERENT MEMBRANE DIAMETERS

Cheng-Ta Yang\*

Key words: MEMS microphone, sensitivity, diameter, coupling.

## ABSTRACT

In MEMS capacitive microphone design, it is very critical to get highest yielding rate and sensitivity as the two major factors dominate structure design of microphone. The central-post MEMS microphone is introduced in this paper to differentiate from traditional fixed membrane boundary microphone since the construction is simple and only few masks are required in the process so that the yielding can be greatly enhanced. Thus, it is necessary to find the relationship between the sensitivity and dimension of the diameter of the membrane. The main research steps described in this paper include using CoventorWare to develop one analysis model of MEMS microphone with coupled electro-mechanic system and analyzing the relationship between the sensitivity and the dimension of the diameter of the membrane.

## I. INTRODUCTION

In recent years, micro electro mechanical systems (MEMS) technology is widely applied to design MEMS microphones. In 1992, Scheeper *et al.* [10] developed a novel capacitive microphone as shown in Fig. 1 and this design has been becoming a classical structure however larger residual stress was often introduced by fixed boundary. In 2000, Torkkeli *et al.* [11] developed a higher sensitivity microphone using low stress polysilicon fixed boundary membrane with  $1 \mu\text{m}^2$  area but still have larger residual stress introduced by fixed boundary. In sensing mechanism, a capacitive microphone has higher sensitivity, stability and signal to noise ratio than piezoresistor and piezoelectric types [2]. For membrane material on MEMS capacitive microphone, metal, polysilicon, and  $\text{Si}_3\text{N}_4$  etc. are all applicable [8]. The successful application is to use polysilicon as membrane material on MEMS capacitive microphone due to lower coefficient of thermal expansion on polysilicon.

Paper submitted 07/30/09; revised 01/25/10; accepted 02/02/10. Author for correspondence: Cheng-Ta Yang (e-mail: albert.yang@mail.ncku.edu.tw).

\*Department of Marine Engineering, National Kaohsiung Marine University, Kaohsiung, Taiwan, R.O.C.

In 2008, Ganjia *et al.* [6] developed a new microphone by reducing acoustical resistance with perforated Al (aluminum) diaphragm to improve the sensitivity of microphone as shown in Fig. 2.

CoventorWare based on the finite element method is a well known software tool for efficient development in MEMS fields [4]. The capacitance of relative humidity (RH) sensor [7] as well as calibration data of the pressure sensor [5] is simulated by this software. Besides, the torsional varactor and capacitive ultrasonic transducers are simulated by this software [9, 12].

## II. SIMULATION METHOD

### 1. Comparison between the CoventorWare and Theoretical Models of Cantilever Beam with Rectangular Section

A theoretical model of a cantilever beam with rectangular section is expressed as

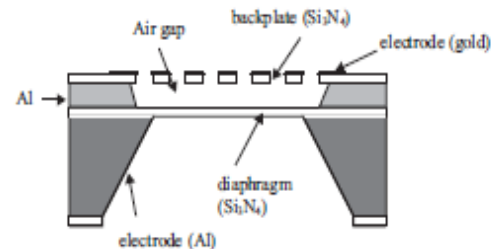


Fig. 1. Capacitive silicon microphone designed by Scheeper *et al.* [10].

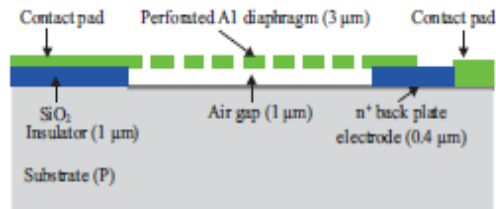


Fig. 2. Cross-sectional view of the microphone using a perforated aluminum diaphragm [6].



# Thin Film PZT Acoustic Sensor for Fully Implantable Cochlear Implants <sup>†</sup>

Bedirhan İlik <sup>1,2</sup>, Aziz Koyuncuoğlu <sup>2</sup>, Hasan Uluşan <sup>1</sup>, Salar Chamanian <sup>1</sup>, Dilek Işık <sup>2</sup>,  
Özlem Şardan-Sukas <sup>2</sup> and Haluk Külâh <sup>1,2,\*</sup>

<sup>1</sup> Department of Electrical and Electronics Engineering, Middle East Technical University, Ankara, Turkey; bedirhan@metu.edu.tr (B.İ.); hulusan@mems.metu.edu.tr (H.U.); schamanian@mems.metu.edu.tr (S.C.)

<sup>2</sup> MEMS Research and Application Center, Middle East Technical University, Ankara, Turkey; akoyuncuoglu@mems.metu.edu.tr (A.K.); disik@mems.metu.edu.tr (D.I.); osukas@mems.metu.edu.tr (Ö.Ş.-S.)

\* Correspondence: kulah@metu.edu.tr; Tel.: +90-312-210-2345

<sup>†</sup> Presented at the Eurosensors 2017 Conference, Paris, France, 3–6 September 2017.

Published: 22 August 2017

**Abstract:** This paper presents design and fabrication of a MEMS-based thin film piezoelectric transducer to be placed on an eardrum for fully-implantable cochlear implant (FICI) applications. Resonating at a specific frequency within the hearing band, the transducer senses eardrum vibration and generates the required voltage output for the stimulating circuitry. Moreover, high sensitivity of the sensor, 391.9 mV/Pa @900 Hz, decreases the required power for neural stimulation. The transducer provides highest voltage output in the literature (200 mVpp @100 dB SPL) to our knowledge. A multi-frequency piezoelectric sensor, covering the daily acoustic band, is designed based on the test results and validated through FEA. The implemented system provides mechanical filtering, and mimics the natural operation of the cochlea. Herewith, the proposed sensor overcomes the challenges in FICI operations and demonstrates proof-of-concept for next generation FICIs.

**Keywords:** cochlear implant; acoustic sensor; MEMS vibration-based transducers; thin film PZT

## 1. Introduction

The cochlea, the eardrum, and the ossicles together form one of the most elaborated structures in mammals. They provide frequency selectivity and sound perception, which makes ear the best acoustic sensor in the nature. According to the World Health Organization (WHO), approximately 15% of the world's adult population has some degree of hearing loss. In total, there are 360 million people living with disabling hearing loss greater than 40 dB SPL as of 2015, 32 million of which are children [1]. Amount of hearing loss can be classified as mild, moderate, severe or profound. For mild-to-moderate damage a hearing aid can be used to restore the hearing loss by sound amplification. Whereas, Cochlear Implants (CIs) can be utilized for treatment of severe-to-profound hearing loss. CIs recover hearing to a certain extend by directly stimulating the auditory nerves via electrodes. However, current state of the commercial CIs has some drawbacks such as high cost and the need for frequent battery charging/replacement preventing patients' continuous access to sound. Another disadvantage of CIs is that wearing external components causes patients to feel stigmatized. Also, there is a risk of damage especially when exposed to water (shower, pool). In this study, we present a novel method utilizing a multi-frequency thin film piezoelectric transducer that eliminates main bottlenecks of CIs. The transducer consists of several cantilever beams each of which resonates at a specific frequency within the hearing band that covers the daily acoustic band. The design of the transducer is accomplished considering volume and mass limitations. Finally, achieved results, generated signals on the piezoelectric transducers, will be shaped by interface electronics to stimulate the auditory neurons at cochlea.